Western Graduate&PostdoctoralStudies

Western University
Scholarship@Western

Electronic Thesis and Dissertation Repository

2-1-2022 11:00 AM

Spatiotemporal characterization of the prr12 paralogues in zebrafish

Renee Jeannine Resendes, *The University of Western Ontario*

Supervisor: Kelly, Gregory M., *The University of Western Ontario*
Co-Supervisor: Bulakbasi Balci, Tugce, *The University of Western Ontario*
A thesis submitted in partial fulfillment of the requirements for the Master of Science degree in Biology
© Renee Jeannine Resendes 2022

Follow this and additional works at: https://ir.lib.uwo.ca/etd

Part of the Biology Commons, and the Developmental Biology Commons

Recommended Citation

Resendes, Renee Jeannine, "Spatiotemporal characterization of the prr12 paralogues in zebrafish" (2022). *Electronic Thesis and Dissertation Repository*. 8375.
https://ir.lib.uwo.ca/etd/8375

This Dissertation/Thesis is brought to you for free and open access by Scholarship@Western. It has been accepted for inclusion in Electronic Thesis and Dissertation Repository by an authorized administrator of Scholarship@Western. For more information, please contact wlswadmin@uwo.ca.

Abstract

Pathogenic variants in the human *PRR12* (*Proline Rich 12*) gene are associated with *PRR12*-related Neuroocular Syndrome. However, little is known about the gene/protein function. The zebrafish was utilized to address this, as its attributes place it as a premier model to study genes involved in human development and disease. *In situ* hybridization and RT-PCR of embryos and larvae, and qRT-PCR of adult tissues revealed the spatial and temporal distributions of the *prr12* paralogues: *prr12a* and *prr12b*. Both paralogues were detected from the maternal and zygotic transcriptomes in a global and diffuse expression pattern, and there was enrichment of *prr12a* in the ovary and *prr12b* in the male mesencephalon of adult zebrafish. Overall, research into the *PRR12* zebrafish orthologues, provides new information to help elucidate its function in humans; and more importantly, it sets the stage for using zebrafish as a model to study this and other rare human disorders.

Keywords

Proline Rich 12, proline rich 12a, proline rich 12b, *PRR12*-realated Neuroocular Syndrome, Rare disorder, Zebrafish, Development, Embryonic development, Larval development, Spatiotemporal expression

Summary for Lay Audience

Rare diseases are individually rare but collectively common, and they impact the life of approximately 1 in 12 Canadians. Majority of rare diseases are seen in children, who face debilitating disorders that affect many organ systems. Almost all individuals will wait on average 5 years to receive a diagnosis. Getting a diagnosis opens the way for treatment options, which is paramount for the wellbeing of patients and their families. However, a genetic diagnosis is only possible based on the available knowledge connecting genes to diseases.

Animal systems may be used to investigate gene function and model human genetic disorders. In this thesis, the human gene *Proline Rich 12* (*PRR12)* was the target of interest. Disease causing changes in the *PRR12* gene have been recently associated with the *PRR12*-related Neuroocular Syndrome. Individuals with this syndrome present primarily with developmental impairment and eye abnormalities. Currently, there is little known about the *PRR12* gene or protein it encodes in normal or abnormal development. Therefore, I sought to investigate its expression in zebrafish, an established developmental and disease animal system. Zebrafish have two gene copies of *PRR12*, known as *prr12a* and *prr12b* (paralogues). I hypothesized the *prr12* paralogues would act similarly in zebrafish development like those in humans. Furthermore, when turned off using a genetic approach, the zebrafish would present phenotypes reminiscent of patients with Neuroocular Syndrome. In a first step, I found that both *prr12a* and *prr12b* are expressed throughout early zebrafish development and in various embryonic and larval tissues. In adults, *prr12a* is predominately expressed in the ovary and *prr12b* is expressed in specific neural structures in the brain and eyes.

These patterns suggest *prr12a* and *prr12b* are required in early development, similar to reports of human *PRR12*, and have more restricted roles in adult zebrafish. Taken together, these results provide a rationale for using zebrafish to investigate *PRR12* and the *PRR12*-related Neuroocular Syndrome. The next steps, beyond the scope of my work, will be to study the effects of mutations of these paralogues, which may ultimately help to understand their functions and lead to the development of targeted therapies in humans.

Co-Authorship Statement

All studies in this thesis were performed by Renée J. Resendes under the supervision of Dr. Gregory M. Kelly and co-supervision of Dr. Tugce B. Balci, who both aided in project and experimental design, interpretation of data/findings, and provided financial support.

Acknowledgments

To my supervisor, Dr. Gregory Kelly, thank you for welcoming me into the Kelly Lab and providing me the opportunity to explore my research interests in developmental biology and zebrafish disease modelling. Thank you for the guidance, teaching(s) on how to think and ask questions like a scientist, and all the experiences that grew my critical thinking skills, curiosity, and resiliency. To my co-supervisor, Dr. Tugce Balci, thank you for giving me the opportunity to integrate into the realm of clinical genetics. Thank you for the support and encouragement throughout my degree and for being a leader, I hope to emulate one day.

To my advisory committee, Dr. Anne Simon and Dr. Stephen Renaud, for your support and time invested into my development as a student and researcher, I thank you.

To all past and current members of the Kelly Lab, I would like to thank you for contributing to my graduate experience. To Danielle Spice, thank you for your support, advice, lab chats, and continued friendship. To Mohamed Gatie, for your mentorship, continued friendship, and all you have done for me in and out of the lab. Not only did you inspire me every day to become a great researcher but more importantly, a better person.

To the incredible lifelong friends, I've made along the way: Breanna Craig, Michelle O'Donnell, Becky Poisson, Jessica Sinka, Naomi Mishan, and Andrew Bell. Thank you all for your continued support, laughter, and encouragement throughout all our graduate experiences.

To my family, there is simply not enough space on this page to thank you for all you have done and continue to do for me. To my brother Ryan Resendes, thank you for always supporting me throughout all the highs and lows, and for being my best friend throughout our life experiences. To my mother Caroline Resendes, for your unconditional love and support, willingness to always listen, and for whole-heartedly believing in me when I failed to do so myself. To my father Francis Resendes, my biggest role model, thank you for your unconditional love and guidance, for encouraging me to always see the *big picture*, and for modelling to me every day that with hard work and dedication anything is possible.

Dedication

To all the patients and families with the PRR12-related Neuroocular Syndrome.

To have had the opportunity to study this rare disorder, has brought incredible meaning and purpose, to me as a researcher. I hope with continuing efforts we (scientists and clinicians) can develop potential therapeutics to better the lives of those impacted by this rare disorder.

Table of Contents

Abstract ii

Summary for Lay Audience iii

Co-Authorship Statement iv

Acknowledgments v

Dedication vi

Table of Contents vii

List of Tables x

List of Figures xi

List of Abbreviations xiii

Chapter 1 1

1 Introduction 1

1.1 *PRR12*-related neuroocular syndrome 2

1.1.1 Genetic and molecular characteristics of *PRR12* 6

1.1.2 *PRR12* from bedside to bench 7

1.2 Zebrafish 9

1.2.1 Zebrafish development: from zygote to adult 10

1.3 Zebrafish, a model organism in development 15

1.4 Molecular toolbox to manipulate the zebrafish genome 17

1.5 Intersection between rare genetic diseases and zebrafish modelling 19

1.6 *PRR12* and zebrafish 20

1.7 Rationale, hypothesis, and objectives 22

Chapter 2 23

2 Materials and Methods 23

2.1 Zebrafish husbandry: maintenance and embryo collection 23

2.2 Embryo, larval, and adult mRNA expression analysis 24

2.2.1 Embryo and larval mRNA isolation 24

2.2.2 Adult tissue dissection and mRNA isolation 24

2.3 Qualitative (endpoint, RT-PCR) and quantitative reverse-transcription (qRT-PCR) polymerase chain reaction 25

2.4 Spatiotemporal expression analysis 26

2.4.1 Plasmid preparation and *in vitro* transcription for *in situ* hybridization 26

2.4.2 Whole-mount *in situ* hybridization (WMISH) 28

2.5 *In silico* analysis 29

2.5.1 Analysis of proline rich 12 sequences 29

2.5.2 Whole zebrafish RNA-sequencing 29

2.6 Statistical analysis 29

Chapter 3 31

3 Results 31

3.1 Exonic structure arrangement of human *PRR12*, zebrafish *prr12a*, and zebrafish *prr12b* 31

3.2 Schematic representation of the AT-hook domain regions within human PRR12, zebrafish Prr12a, and zebrafish Prr12b 33

3.3 Transcriptome profiling of *prr12a* and *prr12b* in zebrafish development 35

3.4 Representative temporal expression profile of *prr12a* and *prr12b* in zebrafish development 37

3.5 Whole-mount *in situ* hybridization assay of *prr12a* expression in zebrafish development 39

3.6 Whole-mount *in situ* hybridization assay of *prr12b* expression in zebrafish development 42

3.7 *prr12a* expression in male and female adult zebrafish tissues 45

3.8 *prr12b* expression in male and female adult zebrafish tissues 47

3.9 *prr12a* and *prr12b* expression in the brain and eye of male and female adult zebrafish 49

Chapter 4 52

4 Discussion 52

4.1 Summary of findings 52

4.2 Limitations and future directions 58

4.3 Conclusion 61

References 62

Appendices 89

Curriculum Vitae 101

List of Tables

Table 1. Summary of the *proline rich* genes in development and associated human disease . 8

Table 2. RT-PCR primer sequences for zebrafish target genes 26

Table 3. qRT-PCR primer sequences for zebrafish target genes 26

Table 4. Primer sequences for zebrafish *in situ* hybridization probes 27

Table 5. Restriction enzyme and RNA polymerases for *in vitro* transcription 28

List of Figures

Figure 1. Images of facial features from selected individuals with *PRR12* variants. 5

Figure 2. Overview of zebrafish development. 11

Figure 3. Zebrafish gastrula onset (50%-epiboly) fate map. 13

Figure 4. Exonic structure arrangement of human *PRR12* isoforms and zebrafish *prr12a*, and zebrafish *prr12b*. 32

Figure 5. Schematic representation of the AT-hook domain regions within human PRR12, zebrafish Prr12a, and zebrafish Prr12b. 34

Figure 6. Transcriptome profiling of *prr12a* and *prr12b* in zebrafish development 36

Figure 7. Representative temporal expression of *prr12a* and *prr12b* in zebrafish development. 38

Figure 8. Whole-mount *in situ* hybridization (WMISH) showing *prr12a* expression in zebrafish development. 41

Figure 9. Whole-mount *in situ* hybridization (WMISH) showing *prr12b* expression in zebrafish development. 44

Figure 10. Tissue distribution of *prr12a* expression in male and female zebrafish..... 46

Figure 11. Tissue distribution of *prr12b* expression in male and female zebrafish..... 48

Figure 12. Expression of *prr12a* and *prr12b* in the brain and eye of male and female adult zebrafish 51

List of Appendices

Appendix 1. Animal use protocol 89

Appendix 2. Phylogenetic relationship of *proline rich 12* amongst vertebrates..... 90

Appendix 3. Schematic representation of DUF4122 region within human PRR12, zebrafish Prr12a, and zebrafish Prr12b..... 92

Appendix 4. Zebrafish *prr12a* and *prr12b* single cell RNA-sequencing analysis..... 93

Appendix 5. Generation of knockout zebrafish lines..... 96

Appendix 6. Preliminary analysis of *prr12a* genetic disruption..... 99

List of Abbreviations

°C	Degrees Celsius
µL	Microliter
nM	Nanomolar
5' UTR	5 prime untranslated region
3' UTR	3 prime untranslated region
AB	Star-AB zebrafish strain
AHDC1	Human AT-Hook DNA Binding Motif Containing Protein 1
ALDH7A1	Human gene encoding Aldehyde Dehydrogenase 7 Family Member A1 protein
aldh7a1	Zebrafish gene encoding aldehyde dehydrogenase 7 family member a1 protein
BCIP	5-bromo-4-choloro-3'-indolyphosphate
bp	Base pair
CCR2	Human gene encoding C-C chemokine receptor type 2 protein
CCR5	Human gene encoding C-C chemokine receptor type 5 protein
CNS	Central nervous system
CRISPR	Clustered regularly interspaced short palindromic repeats
DIG	Digoxigenin
dlx3	Zebrafish gene encoding distal-less homeobox 3 protein
DNA	Deoxyribonucleic acid
Dpf	Days post fertilization
DSB	DNA double stranded breaks
DUF4211	Domain of Unknown Function 4211
F_0	Founder fish
foxP2	forkhead box protein P2
gapdh	Zebrafish gene encoding glyceraldehyde-3-phosphate dehydrogenase protein
HDR	Homology directed repair
Hpf	Hours post fertilization
ID	Intellectual disability
kars1	Zebrafish gene encoding lysyl-tRNA synthetase 1 protein
kb	Kilobase

kDa	Kilodalton
kdra	Zebrafish gene encoding vascular endothelial growth factor-2 receptor protein
krox-20	Zebrafish gene encoding early growth response 2b protein
LOF	Loss-of-function
lsm12b	Zebrafish gene encoding like-sm protein 12 homolog b protein
MBT	Midblastula transition
MeCP2	Human Methyl-CpG Binding Protein 2
mRNA	Messenger RNA
NBT	Nitroblue tetrazolium
NCBI	National Center for Biotechnology Information
NHEJ	Non-homologous end joining
NOC	Neuroocular Syndrome
OMIM	Online Mendelian Inheritance in Man
PBST	Phosphate Buffered Saline, Tween-20
PCR	Polymerase chain reaction
PDE	Pyridoxine-Dependent Epilepsy
PRR12	Human gene encoding Proline Rich 12 protein
Prr12	Mouse gene encoding Proline rich 12 protein
prr12a	Zebrafish gene encoding Proline rich 12a protein
prr12b	Zebrafish gene encoding Proline rich 12b protein
PRR12	Human Proline Rich 12 protein
Prr12a	Zebrafish Proline rich 12a protein
Prr12b	Zebrafish Proline rich 12b protein
ptk7	Zebrafish gene encoding for protein tyrosine kinase 7
qRT-PCR	Quantitative reverse-transcription polymerase chain reaction
RNA	Ribonucleic acid
RT-PCR	Qualitative (end-point) reverse-transcription polymerase chain reaction
sgRNA	Single guide RNA
SYBR	N',N'-dimethyl-N-[4-[(E)-(3-methyl-1,3-benzothiazol-2-ylidene) methyl]- 1-phenylquinolin-1-ium-2-yl]-N-propylpropane-1,3-diamine
T3	Bacteriophage T3 RNA polymerase
T7	Bacteriophage T7 RNA polymerase

TAE	Tris-acetate-EDTA
TALENs	Transcription activator-like effector nucleases
TPM	Transcripts per Million
TU	Tübingen zebrafish strain
tyr	Zebrafish gene encoding tyrosinase
UMI	Unique molecular identifier
WIK	Wild India Kolkata zebrafish strain
WMISH	Whole-mount *in situ* hybridization
WT	Wildtype zebrafish strain
ZFIN	The Zebrafish Information Network
ZFN	Zinc finger nucleases

Chapter 1

1 Introduction

Rare diseases are individually rare but collectively common[1] and affect the life of approximately 1 in 12 Canadians[2]. It is estimated that 80% of rare diseases are caused by genetic disorders[3], and to date, there are approximately 7000 known rare diseases[4]. Many rare diseases are severe and multisystemic, presenting with a wide spectrum of phenotypes[5]; and even though the scientific landscape is rapidly evolving with efforts in discovery and diagnostic technologies, rare disease patients continue to face a diagnostic odyssey[6]. Indeed, the average wait time from disease onset to receiving a clinical diagnosis is almost 5 years[6–8]. Throughout this waiting period patients undergo a variety of diagnostic tests in succession, including single-gene or multi-gene panel tests, whole exome sequencing and/or whole genome sequencing[6], yet approximately 50%[9] of patients will not receive a timely diagnosis, or one at all[10,11]. In addition, even if a diagnosis can be made less than 5% of rare diseases have a beneficial therapy for patients[12]. Early diagnosis and therapeutic intervention in these patients is paramount, as 83% of rare diseases affect children[13] and cause 30% fatality to children before five years of age[14]. Ultimately, lack of diagnosis and an uncertainty of disease progression leaves patients and their families emotionally and psychologically burdened[15]. Therefore, highlighting the increasing demands for initiative and collaborative efforts on the forefront of rare genetic diseases.

While animal systems cannot fully recapitulate the human disease phenotype, they provide strong means to explore the causality of diseases and in particular, help expedite research into the continuously growing pool of candidate rare disease variants[16].

Since the early 1980s, the zebrafish has emerged as an important organism in elucidating normal and pathological conditions during vertebrate development[17] and available molecular techniques poise the zebrafish as a platform to recapitulate rare genetic diseases[18]. In particular, established genetic and transgenic zebrafish disease models are advantageous in drug discovery and pre-clinical trials[19]; as many compounds can penetrate zebrafish embryos via passive diffusion through the water or can be easily administered

orally through a gavage needle[19,20]. From a physiological perspective, zebrafish are also advantageous in studying drug metabolism[21], as the kidney and liver function develops early in zebrafish[22]. Furthermore, from an ethical perspective zebrafish are well suited model organisms for drug discovery as animal welfare regulation considers zebrafish an animal only after 5 days post fertilization (dpf)[21]. Since major organs in the zebrafish form by 5 dpf and are functioning[18], if experimentation is completed within this timeframe, substantial information and data can be gathered without comprising the principals of replacement, reduction, and refinement in animal research[23].

In this chapter, I will first present a specific rare disease and its underlying genetic cause: the *PRR12*-related Neuroocular Syndrome. Then, I will focus on zebrafish as an animal model, including its role in understanding rare diseases, to finally focus on the hypothesis underlying my thesis objectives.

1.1 *PRR12*-related neuroocular syndrome

The first *Proline Rich 12* (*PRR12*, OMIM #616633) variant associated with disease was reported by Córdova-Fletes and colleagues, in 2015, where an 11 year old individual with a *de novo* t(10;19)(q22.3;q13.33) reciprocal chromosomal translocation disrupting the *PRR12* and *ZMIZ1* (Zinc Finger MIZ-Type Containing 1) genes was documented[24]. Specifically, this individual presented with a wide range of clinical features such as intellectual disability (ID), neuropsychiatric alterations, and strabismus[24]. Subsequently, a report in 2018 revealed 3 unrelated individuals who were found to have heterozygous, *de novo* truncating variants, who presented with ID, global developmental delay, neuropsychiatric problems, vision, and iris abnormalities[25]. More recently, Reis and colleagues reported 4 additional individuals with truncating *PRR12* variants, from a cohort of individuals with eye anomalies[26]. This study identified for the first time, familial dominant transmission of eye anomalies segregating with the pathogenic *PRR12* variant[26]; solidifying the autosomal dominant inheritance pattern originally proposed[24,25]. Most recently, Chowdhury and colleagues reported the largest *PRR12* cohort to date, with 21 additional individuals, all with *de novo* heterozygous apparent loss-of-function (LOF) sequence variants and one individual with a gross chromosomal deletion including the

PRR12 gene[27]. Within this large cohort, all individuals present with developmental impairment and some individuals present with additional variable clinical features such as structural eye defects, kidney and heart anomalies, hypotonia, and growth delay[27]. Hence the condition is now named *PRR12*-related Neuroocular Syndrome (NOC) in Online Mendelian Inheritance in Man (OMIM #619539) and to date, the cohort encompasses 29 individuals, reported in the literature. Notably, within the larger cohort there is an almost equal male to female ratio (15:14), showing this rare syndrome can affect both sexes equally[24–27].

Reported individuals with deleterious disruptions in *PRR12* contain either distinct sequence variants, gross deletions, or chromosomal translocations. Of the identified *PRR12* sequence variants, 16 are frameshift mutations, 7 are nonsense mutations, 2 are missense changes and 2 affect splice sites[25–27]. The predicted result of the frameshift, nonsense, and splice site mutation variants is the introduction of a premature stop codon inducing nonsense-mediated decay of *PRR12* mRNA[25–27]. *PRR12* has two known isoforms, with mutations occurring in both the long and short isoform[24–27]. Of note, there did not appear to be significant differences in clinical features among those with variants that affect both isoforms compared to variants that exclusively affect the long isoform. Altogether, it seems that alteration of the long isoform specifically underlies pathogenesis[25,27].

As mentioned previously, the clinical features of the *PRR12*-related Neuroocular Syndrome comprise developmental impairment, ocular defects, hypotonia, growth delays, and systemic defects affecting cardiovascular and renal systems[24–27]. Specifically, reported pathogenic variants of *PRR12* result in: 97% of individuals having developmental impairments, 56% having structural eye defects, including microphthalmia and anophthalmia (bilateral or unilateral), coloboma (bilateral or unilateral), optic nerve and iris defects, 48% having hypotonia, 52% having growth failure, 41% having heart defects, and 28% having minor kidney defects[24–27]. Indeed, the *PRR12* cohort reveals a broad spectrum of features, with the most associated phenotype being developmental impairment, presented in the form of global developmental delay, intellectual disability or isolated delays in motor and speech-language[24–27]. Further, the more severe structural ocular defects reported include bilateral anophthalmia described as no eye globe within the orbit[28],

(**Figure 1A**)[27] and microphthalmia (**Figure 1B**)[26] described as small eye(s) in comparison to average eye size in the orbit[28]. Milder forms of structural eye defects were also reported, such as stellate iris (**Figure 1C**)[25], where the iris appears to have a star-like pattern[29] and iris coloboma (**Figure 1D**)[25] a "keyhole-like" pupil feature (not a typical rounded pupil) which can involve the pigment epithelium and stroma[30]. Mild visual impairment such as myopia (nearsightedness) and strabismus, when the visual axis of the eye are misaligned[31] were also documented[24–27]. It is important to note that not all patients with *PRR12* variants present with structural ocular abnormalities[24,27], adding to the complexity of phenotypes seen in *PRR12* LOF mutations. The cardiac phenotypes reported included atrial and ventricular defects, or pulmonary stenosis[27]. Several dysmorphic features were commonly observed, however, these were variable and nonspecific[24–27]. The clinical phenotypes of the *PRR12*-related Neuroocular Syndrome are exclusive to this rather small cohort, thus the addition of other patients harboring *PRR12* variants is paramount in identifying an associated signature phenotype(s). In conclusion, this rare syndrome is believed to be caused by heterozygous apparent LOF variants, with strong evidence to suggest that haploinsufficiency is the causative genetic mechanism[24–27]. However, there is very little known about the function and dysfunction of this gene in mammals, hence a better understanding of the molecular mechanisms of PRR12 in normal and aberrant conditions is crucial for providing an accurate diagnosis.

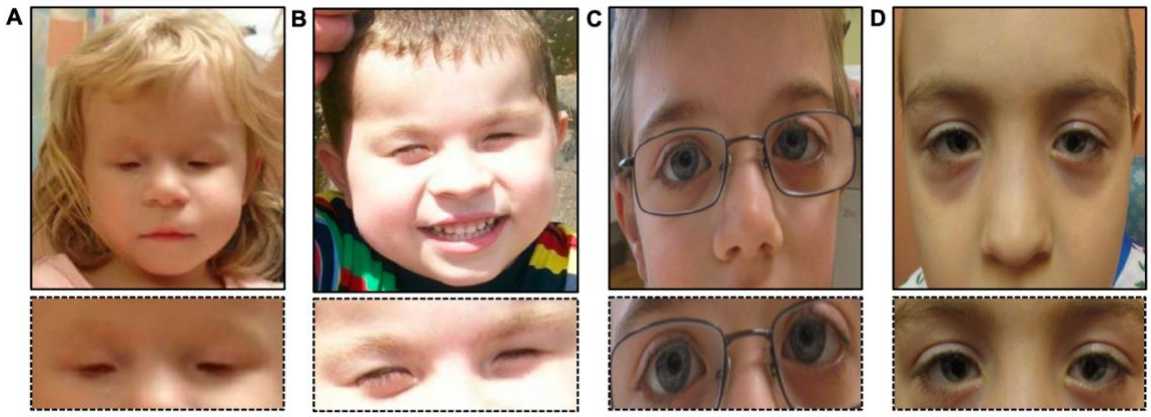

Figure 1. Images of facial features from select individuals with *PRR12* variants. Individual A. bilateral anophthalmia[27]; **Individual B.** unilateral microphthalmia[26]; **Individual C.** stellate iris[25]; **Individual D.** bilateral coloboma[25]. Adapted and modified from Chowdhury *et al.*, 2021[27], Reis *et al.*, 2020[26], and Leduc *et al.*, 2018[25].

1.1.1 Genetic and molecular characteristics of *PRR12*

Human *PRR12* is located on chromosome 19 (19q13.33)[24] and produces 2 functional isoforms via alternative splicing: one long and one short transcript[24]. The long transcript (ENST00000418929.7) contains 14 exons encoding a 2036 amino acid protein[24,32] and is well conserved amongst vertebrate species[24,33]. The short transcript (ENST00000615927.1), encoding a 1215 amino acid protein, contains 12 exons, does not contain exon 1-3, and lacks a large portion of exon 4 of the large transcript[24,32]. *PRR12* mRNA is widely expressed amongst many human adult tissues, however, there is enriched expression in the cerebellum, pituitary and thyroid gland, and the female reproductive tract (GTEx)[27,34]. Also, it has been reported that *PRR12* appears to be expressed more in fetal brain in comparison to adult brain[27,35], suggesting a role in fetal brain development[27]. The majority of promoter/enhancer regions in *PRR12* are also present with a bivalent state in induced pluripotent stem cell lines and human embryonic stem cell lines[27,32,36]. This chromatin state allows for embryonic cell differentiation and is linked to developmental genes[37], thus further supporting that *PRR12* may play a role in embryonic neurogenesis[27].

In vitro studies have revealed a similar fetal-adult expression profile with mouse Prr12 isoforms, where the longer Prr12 (~212-kDa) is abundantly expressed in embryonic (E15) brain cells in comparison to postnatal (P1) and adult mouse brain cells[24]. Further, this *in vitro* study revealed distinct subcellular localization of the two Prr12 isoforms with the longer Prr12 confined to the nucleus and the shorter Prr12 detected both in and outside of the nucleus[24]. Therefore, it is speculated that PRR12/Prr12 may participate as a nuclear cofactor during transcriptional regulation[24,25].

The human *PRR12* gene encodes a protein with two predicted AT-hook domains[24,25,27], which are DNA-binding peptide motifs that enable the protein to bind to the minor grove of adenine and thymine-rich sequences[38]. These motifs are present in high mobility group proteins[38], which have been associated with chromatin and DNA-binding proteins[39]. Together, these AT-hook domains and observed nuclear localization are also indicative of a role for PRR12 in transcriptional regulation[24]. In support of this role, PRR12 contains post-translational phosphorylation (phosphoserine and phosphothreonine)[40] and

acetylation sites[41], which are speculated to cause its epigenetic regulation[25]. Moreover, Lysine-402 is acetylated[41] and since bromodomain-containing proteins (bind and recognize lysine residues that are acetylated)[42] were found to be co-expressed with *PRR12*[27,43–45], it is further speculated that PRR12 may be modulated via epigenetic regulation[27].

Although the mechanism of *PRR12* function is poorly understood, new insight into its regulation was discovered by Mao and colleagues in glioblastoma cells lines[46]. This group discovered that *PRR12* is a downstream target gene of miR-766-5p, an upregulated microRNA in gliomas, where overexpressing *PRR12* in these cells decreased proliferation and increased apoptosis[46]. While this study sheds light on the role of *PRR12* in tumorigenesis, there remains a huge gap in the literature describing the role of *PRR12* in development and disease.

In summary, based on the clinical features of *PRR12* LOF[24–27], and in reported expression patterns, human *PRR12* mRNA seems to be differentially expressed in various adult human tissues, with abundant expression in the brain and female reproductive system (GTEx)[27,34]. Specifically, *PRR12* expression is elevated in fetal brain, compared to the adult brain[27,35], but while the spatiotemporal expression of *PRR12* is currently inferred, further functional studies are needed to elucidate the expression profile of this target in human development.

1.1.2 *PRR12* from bedside to bench

In further investigating orthologous human disease-associated genes in zebrafish, databases such as OMIM[47] impart information regarding genetic disease. Specifically, OMIM is a repository consisting of human genes and genetic phenotypes linked to disease, which can be used as a diagnostic tool and reference for clinicians and researchers[48,49]. When investigating candidate genes, OMIM provides a platform to cross reference and identify if there are known genotype-phenotype correlations of target genes. The *Proline Rich* gene family contains 22 members in humans, with 9 of the 22 having an identifiable zebrafish counterpart (**Table 1**, verified through Ensemble Genome Browser[32] and OMIM database searches[47]).

Table 1. Summary of the *proline rich* genes in development and associated human disease

Gene Symbol	OMIM Ref.	Role in Human Development	Human Tissue Expression (GTEx)	Associated Human Disease(s)	References
PRR5 *(Proline Rich 5)*	609406	Regulates platelet-derived growth factor	Spleen, breast, and pituitary	Breast and colorectal tumorigenesis	34,47,50–57
PRR7 *(Proline Rich 7)*	618306	Brain and blood lymphocytes development	Brain, pituitary, and lymphocytes cells	Not identified	34,47,58–62
PRR11 *(Proline Rich 11)*	615920	Cell-cycle progression	Fibroblast cells, lymphocyte cells, and esophagus (mucosa)	Breast, esophageal, gastric, pancreatic, colorectal, ovarian, and hilar cholangiocarcinoma tumorigenesis	34,47,63–81
PRR12 *(Proline Rich 12)*	616633	Neural development	Brain, thyroid, and female productive tract	Neuroocular syndrome: intellectual impairment, eye abnormalities, heart anomalies, kidney anomalies, growth delay, and tumorigenesis	24–27,34,46,47
PRR13 *(Proline Rich 13)*	610459	Not identified	Whole blood, small intestine, and kidney	Ovarian cancer and ulcerative colitis	34,47,82–84
PRR14 *(Proline Rich 14)*	617423	Promotes cell proliferation, skeletal myogenesis and MyoD activity	Brain, uterus, and spleen	Not identified	34,47,85–91
PRR16 *(Proline Rich 16)*	615931	Promotes cell size, mitochondrial mass, and respiration	Fibroblast cells, aorta artery, and uterus	Carotid paragangliomas	34,47,92–95
PRR18 *(Proline Rich 18)*	Not found.	Not identified	Brain, lymphocyte cells, and liver	Not identified	34,47
PRR33 *(Proline Rich 33)*	Not found.	Not identified	Spleen, whole blood, and adrenal gland	Not identified	34,47

Collectively, the *Proline Rich* genes have some overlap in neural expression (*PRR7*, *PRR12*, *PRR14*, and *PRR18*) and varying types of tumorigenesis as the most common associated disease (*PRR5*, *PRR11*, *PRR13,* and *PRR16*). However, due to limited literature, identifying a definitive role of the *Proline Rich* genes in development and disease cannot be ascertained at this time. Within the *Proline Rich* gene family, as previously discussed is *PRR12*, a current candidate gene associated with Neuroocular Syndrome (OMIM #619539) and the target of this thesis. As mentioned above, there is relatively little literature describing the molecular function and pathogenic mechanisms of *PRR12*, and the protein it encodes, which has unknown function(s)[24–27]. PRR12 contains proline-rich regions, which have been described to consist of repetitive prolines, consisting of approximately 5-8 residues in length[96]. While the proline-rich regions of PRR12 have not been characterized, a shared element of proline-rich regions is their involvement in binding processes (*e.g.*, protein-protein binding and transcription)[96]. Furthermore, proteins with proline-rich regions have been linked to synaptic vesicle-associated neuronal proteins[96], and curiously, the short Prr12 isoform in mouse was also identified in the perisynapse, postsynaptic density, and synaptosomes[24]. While one can speculate on the function of PRR12, further *in vivo* modelling efforts are critical in elucidating the biological function of *PRR12*/PRR12 in development.

1.2 Zebrafish

The zebrafish (*Danio rerio*) is a small tropical fish[18] and named due to its signature horizontal stripes[97]. Geographically, zebrafish are native to areas of India, Nepal, and Pakistan, where they can be found in rivers and slow moving streams at fluctuating temperatures (12.3ºC – 38ºC)[98–100] and elevations (39m – 63m above sea level)[98]. In the wild, zebrafish form shoals, a social behavior needed for optimal survival, which allows for increased foraging and escaping predation[101]. Wild zebrafish primarily spawn during the rainy season, where females oviposit their clutch of eggs into substrate, in preparation for male fertilization[99]. After successful fertilization, clutches will develop and mature without parental care[99]. On average, wild zebrafish live up to 3 years of age[102], and since their use as a model to study embryogenesis in the 1930s[103], captive bred zebrafish have been documented to live up to 5 years of age[102].

1.2.1 Zebrafish development: from zygote to adult

Optimal zebrafish embryogenesis occurs over the course of 3 days at 28.5ºC as described by Kimmel *et al*[22], however, increasing the temperature to 32ºC can accelerate this process[104]. Embryogenesis is initiated with the egg and sperm fusing to form a zygote[22,105], in which, embryogenesis is comprised of 7 periods: zygote, cleavage, blastula, gastrula, segmentation, pharyngula, and hatching (**Figure 2**)[22]. The transition from the short-lived zygotic stage is signaled by the first cleavage event, ~40 minutes after fertilization[22]. These blastomeres undergo synchronous division every 15 minutes until reaching the 64-cell stage. Cells undergo incomplete cytokinesis during the 2-16 cell stage due to their connection to the underlying yolk. Subsequent stages, 16-64-cell stages, undergo both complete cytokinesis of inner blastomeres and incomplete cytokinesis of outer blastomeres, as the latter are still in contact with the yolk[22]. During these early stages of embryogenesis, the animal-vegetal axis is visible, with cytoplasmic streaming forming the blastodisc at the animal pole, and the yolk at the vegetal pole[22]. These early cell division events are defined as meroblastic cleavage, as each cleavage furrow divides through the blastodisc but not the yolk[22].

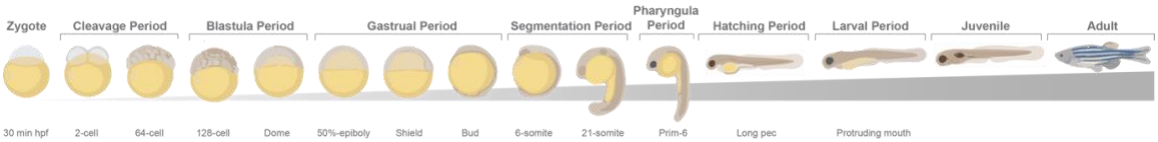

Figure 2. Overview of zebrafish development. There are seven developmental periods from the zygote stage through the larval period, corresponding to key embryonic (and larval) structures (on bottom). Adapted and modified from S. Lepage, using BioRender[106], not drawn to scale.

Progression through the 128-cell stage marks the onset of the blastula period and near the 10th cell division event (512-cell stage) the initiation of the midblastula transition (MBT) occurs[22]. The MBT is characterized by the lengthening of the cell cycle, metasynchronous cell divisions[22], and activation of the zygotic genome[107,108]. This blastula now contains 4 main layers: deep cells that give rise to the embryo proper; the yolk cell, which is an uncleaved cell-like structure containing yolk; the yolk syncytial layer between the deep cells and the yolk; and the enveloping layer of external cells of the blastoderm. The blastula period ends and gastrulation begins following epiboly, a process causing the migration of the blastoderm and cells of the yolk syncytial layer to spread over the yolk[22].

Gastrulation, whereby morphogenetic movements including epiboly, involution, convergence, and extension, is initiated by the involution of the deep blastoderm cells migrating outwards[22]. These and subsequent coordinated cell movements determine which cells become specific tissue and organ structures (**Figure 3**). Following involution, the germ ring forms around 5.75 hours post fertilization (hpf), and convergent movements cause a thickening along the margin of the blastoderm, creating two layers: epiblast (outer layer) and hypoblast (inner layer). Around 6 hpf, the accumulation of these cell layers transition and form the embryonic shield, a structure also referred to as the organizer that marks the future dorsal side of the embryo[22,109]. By 8 hpf (75%-epiboly), the epiblast and hypoblast are more visually distinctive with cells residing in the epiblast fated towards ectoderm lineages, while cells within the hypoblast comprising the mesoderm or endoderm lineages. The end of epiboly, where convergence and extension movements cause the blastoderm to nearly cover the entire yolk, signals the completion of gastrulation around 10 hpf (Bud stage)[22].

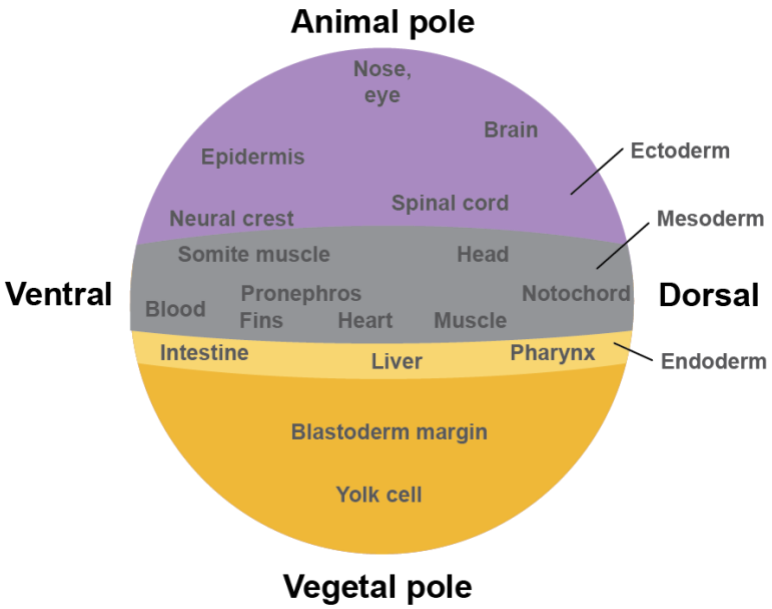

Figure 3. Zebrafish gastrula onset (50%-epiboly) fate map. Adapted and modified from Gilbert, 2000[110] and Kimmel *et al.*, 1995[22].

During the segmentation period (10 hpf - 24 hpf), the embryo lengthens, and many morphological processes occur. The tail bud becomes distinguishable, and the first somite furrow (1-somite stage) and primary embryonic organs are seen. Somites, which give rise to the skeletal muscle in the trunk region and axial skeleton, develop anterior to posterior in a process referred to as somitogenesis (1 - 26-somite stage). At later stages, the primordia of the brain and optic vesicles are seen at 11.75 hpf (5-somite stage) and by 16 hpf (14-somite stage) the telencephalon, diencephalon, mesencephalon, and rhombencephalon clearly demarcate the divisions of the brain. By 19 hpf, organ systems have developed, including the pronephric (embryonic) kidney and side-to-side movements of the embryo are frequently observed at the end of segmentation[22].

The pharyngula period (24 hpf - 48 hpf), referred to as the phylotypic stage, is characterized as embryos having a hollow nervous system, brain regions delineated into 5 lobes, a notochord, and a complete set of somites. Noticeably, pigmentation at later stages is prominent, specifically in the retinal epithelium and in melanophores throughout the head, trunk, and tail. The circulatory system has also developed and by 24 hpf the heart contracts. The end of the pharyngula period signals the level High-pec stage, which by 42 hpf, the rudiments of the pectoral fins are seen and a division has occurred between the heart atrium and ventricle[22].

The hatching period (48 hpf - 72 hpf) comprises the final period of embryogenesis as the embryo transitions into its larval (fry) stages. Zebrafish from the same clutch will hatch asynchronously from their chorions (eggshell), and although many organ rudiments are complete by this time, rudimentary structures of the jaw, gills, and pectoral fins continue to develop. The yolk begins to deplete in preparation for free feeding, melanophores are prominent, and the mouth protrudes; all in preparation for the larval transition. Larvae can swim, due to the completed development of its eyes, pectoral fins, opercula, and specifically, the inflation of a swim bladder[22].

The larval stages last for approximately 6 weeks[111], and by ~10 – 12 dpf sex differences are detected[112]. Many factors contribute to sex determination, however, the underlying mechanisms driving these differences have yet to be clarified[113]. Gonadal differentiation

occurs by 25 dpf[114,115], where female gonads are detected around 35 dpf, and male gonads at 45 dpf[115]. Paired ovaries are elongated structures[116], containing oocytes, that can be identified throughout development at different stages such as: primary growth, cortical alveolus, vitellogenic, and mature oocyte[117]. Similarly, testes are paired and elongated, and contain varying types of reproductive cells such as Sertoli cells, Leydig cells, spermatogonia, spermatocytes, and mature spermatids[116]. Adults are sexually mature at approximately two months of age[118], whereby spawning in the laboratory is induced by the onset of light[119], and a single breeding pair of zebrafish provides, on average, 200-300 eggs a week[18].

As a sexually mature adult, the brain has clearly delineated into regions comprising the forebrain, midbrain, and hindbrain, and each region is further subdivided[120]. The forebrain, responsible for cognitive functioning and receiving and processing sensory information, is the most anterior structure[120]. The forebrain is further divided into two main domains, the telencephalon containing the olfactory bulb, pallium and subpallium, and the diencephalon, which contains the habenula, pineal body, and hypothalamus[120,121]. Although technically not classified as regions of the brain, the eyes develop as out-pockets of the forebrain[122]. The zebrafish eye is similar to other vertebrate eyes and comprises the cornea, lens, iris, choroid, retina, and optic nerve, which connects the eye to the brain[123]. The midbrain, required for visual and auditory processing, is further subdivided and includes the tectum and tegmentum[120]. Lastly, the hindbrain, which includes the cerebellum, is required for regulation of motor function and perception of sensory stimuli[124]. In summary, zebrafish development is rapid, with distinguishable stages and structures that highlight the significant changes needed for subsequent physiological processes.

1.3 Zebrafish, a model organism in development

Within the field of developmental biology there are many vertebrate and invertebrate model systems: house mouse (*Mus musculus*), African clawed frog (*Xenopus laevis*), fruit fly (*Drosophila melanogaster*), and nematode (*Caenorhabditis elegans*), to name a few[125]. While all model organisms have both favourable and unfavourable characteristics[125], zebrafish possess certain features that make them a powerful system in the laboratory. The

zebrafish, in particular, is advantageous in studying development as well as disease, due in part to the fact they are vertebrates, but also have a relative fast generation time, high fecundity, near-transparent embryos that develop outside the female[18], and show genetic similarities to humans[126].

Having a fully sequenced genome of a model organism is vitally important in driving genetic and molecular research and many sites are available including: Zebrafish Information Network (ZFIN)[127], Ensembl[32], UCSC Genome Browser[128], and NCBI[129]. Initiation of the zebrafish genome-sequencing project occurred in 2001, involving an initiative with the TU (Tübingen) wildtype zebrafish strain[126]. Although additional wildtype strains are currently in use, including the AB (Star-AB) and WIK (Wild India Kolkata) wildtype strains[130], more than half of published research is based on TU genome reference databases[131]. The TU genome contains 26,206 protein-coding genes and ~71% of the human protein-coding genes share a zebrafish orthologue[126]. However, one apparent difference, is that zebrafish lack heteromorphic (X and Y) sex chromosomes[132,133]. Tetrapods and zebrafish genomes show evolutionary differences of approximately 440 million years ago[134], with the zebrafish ancestor undergoing an additional genome duplication, referred to as teleost-specific genome duplication[135]. Consequently, this teleost duplication accounts for the presence of paralogous genes, with zebrafish having two copies of many human genes[126,135]. While loss-of-function of duplicated genes in probable, paralogues can alternatively gain new functions (neo-functionalization) or retain function (sub-functionalization) over the evolution of an organism[136].

Although noted genetic differences exist between humans and zebrafish, their popularity as a model preceded these differences and was related to other attributes of the system. As noted above zebrafish, compared to other vertebrates, develop relatively fast and have large clutch sizes[18]. Embryogenesis and larval development of zebrafish take approximately 6 weeks[111] and fish are sexually mature after only a few months[118], unlike *Xenopus*, who can take 1-2 years to become sexually active[137]. The *ex utero* fertilization and development of the zebrafish embryo also allows for easy manipulation and its relative transparency enables the direct visualization of developing organs[138] and real time cell imaging[139]. Additionally, various techniques and procedures such as *in situ* hybridization (visualization

of endogenous gene expression)[140], xenotransplantation (cell transplant)[141], and ease of genetic manipulation (see below) highlight the robustness of the zebrafish embryo. In contrast, the house mouse has litters of 6-8 pups[142] and a gestation period around 18-22 days[143]. This coupled with *in utero* development has obvious obstacles to accessing embryos in the pregnant female. Furthermore, large clutches and frequent breeding prominently place the zebrafish as the system for high-throughput chemical and drug screens[19]. Other attributes are available to the zebrafish, but as a vertebrate one major attraction is that it can be grown in a cost-effective manner[103], and more importantly, given its genetics and genomic relation to humans and the ease to modify this genome, it now sits at the forefront to study and model human diseases.

1.4 Molecular toolbox to manipulate the zebrafish genome

To create functional knockout zebrafish lines a plethora of approaches and technologies allow for sustained, heritable genetic disruptions. These involve endonucleases targeting specific sequence site(s) to induce DNA double stranded breaks (DSBs), and one of the approaches is using zinc finger nucleases (ZFNs)[144]. ZFNs are comprised of DNA binding domains containing zinc fingers and a DNA cleavage *Fokl* endonuclease domain[144]. Zinc fingers are small protein motifs that recognize a specific nucleotide sequence target of 3 base pairs in length[145]. When two ZFNs bind to the target site they create a functional *Fokl* dimer and a DSB occurs after digestion with *Fok1* and these are repaired through either non-homologous end joining (NHEJ) or homology-directed repair (HDR) if homologous donor templates are present[146]. Successful knockout of vascular endothelial growth factor-2 receptor (*kdr*a)[145] and forkhead box protein P2 (*foxP2*)[147] in zebrafish was performed using ZFNs and studies have shown that they cause between 1.6 – 33% mutagenic frequency[148,149]. Although ZFNs have been successful, their main limitations result from off-target effects and embryonic abnormalities not connected to the knockout of the target gene[145,150,151]. Thus, a degree of caution must be noted when implementing this knockout technique.

Transcription activator-like effector nucleases (TALENs) also use the endonuclease machinery to induce DSBs[152]. Similar to ZFNs, TALENs work in pairs to target the gene

sequence of interest whereby their dimerization allows for the recognition of the *FokI* endonuclease which causes breaks to occur[153,154]. TALENs are more specific and have better efficiency than ZFNs[152]. However, the main limitation to the TALEN approach is the TALEN size (~3 kb, kilobases), which poses challenges when trying to deliver the machinery into cells[155]. Despite these limitations there are advantages, highlighted in a study targeting the same site of the C-C chemokine receptor type 5 (*CCR5*) gene with ZFN and TALEN, with ZFNs producing more off-target mutations in the C-C chemokine receptor type 2 (*CCR2*) gene[156]. While ZFNs and TALENs have been successful in generating knockout zebrafish lines, the discovery of clustered regularly interspaced short palindromic repeats (CRISPR) mutagenesis has revolutionized genome editing in this and other organisms.

Zebrafish were the first vertebrate system where CRISPR-Cas9 induced mutagenesis was successful[157,158] and since 2013[126], many mutants have been established using this method[159]. The origins of the CRISPR system were first identified as part of the adaptive immune system in bacteria[160], where a guide RNA and a Cas9 endonuclease target an invading viral DNA[161]. In zebrafish, the 20 bp single guide RNA (sgRNA)[162] and the Cas9 mRNA (or protein) are injected as a ribonucleic/protein complex into the embryo at the 1-cell stage where the sgRNA signals to the Cas9 where to cause the DSB[163]. Cas9 cleavage at the Protospacer Adjacent Motif site (5'-NGG-3' just downstream of the sgRNA) induces activation of the endogenous non-homologous end joining repair mechanisms, causing *de novo* insertions and/or deletions of bases at the cut site[21]. In contrast, co-injecting a DNA cassette and homology directed repair allows for the insertion of exogenous DNA, thereby repairing or replacing the region of interest[21]. Homology directed repair in particular has been beneficial in the generation of zebrafish lines with specific single nucleotide polymorphisms and fluorescent reporters[21]. When knockouts are required, zebrafish mutants are considered as either transient or isogenic stable. With transients the mosaic loss or gain of function phenotype of F_0 zebrafish is assessed, whereas isogenic stables require further mating before a phenotype is examined[21]. In these lines, F_0 fish develop to sexual maturity (~2 months of age[118]) and are then outcrossed with WT fish to generate F_1 heterozygous carriers. The F_1s are then in-crossed to generate F_2 homozygous mutants now ready for phenotype assessment. Although more time consuming than the transient

approach, the isogenic knockouts can be done in approximately 6 months and provide genetic and phenotypic robustness[21]. Overall, CRISPR/Cas9 methods have shown six times higher mutagenic efficiency transmission than ZFNs or TALENs and a 99% success rate in mutation generation[164]. CRISPR is also limited by off-target effects, however, using paired Cas9 nickases to induce two single stranded breaks, appears to significantly lessen these drawbacks[165]. Thus, CRISPR-Cas9 in zebrafish has taken over the field as the go-to gene editing technique and has been used successfully to generate knockouts in at least five targets in a single fish[166] and importantly, provides the ability to model human disease.

1.5 Intersection between rare genetic diseases and zebrafish modelling

Today, generating rare genetic disease models is primarily through CRISPR-Cas9 gene editing, as this technique provides the most robust system to mirror rare genetic disease, understand their pathogenesis and even validate novel therapeutics[21]. Many zebrafish lines have been generated to phenocopy diseases of the nervous system[167,168], retina[169], eye[170,171], liver[172], kidney[173,174], craniofacial/skeletal[175,176], cardiovascular[177,178], hematological and immunological[179,180], and ciliopathies[181]. In particular, *in vivo* systems are extremely beneficial when studying neurological disorders as human CNS tissue is usually inaccessible for experimentation[16], where zebrafish provide an excellent alternative to study ocular and CNS disorders[18]. From an anatomical and physiological perspective, studying ocular disease in zebrafish is advantageous, as by 72 hpf the zebrafish eye has functioning vision and by that time its retinal architecture is similar to humans[138]. In addition, zebrafish have similar structures to the mammalian brain, sharing major brain regions and neurotransmitters (*e.g.*, dopamine, serotonin, and gamma-aminobutyric acid)[182]. Zebrafish models can also be utilized to study the behavioral attributes of disease which has been revealed with their ability to recapitulate autism spectrum disorder, ID, and epilepsy[183]. Worth noting is that ~90% of rare childhood diseases compromise behavior or the CNS[13], further stressing the importance of zebrafish CNS disease modelling. Pena and colleagues[167], exemplify the utilization of the zebrafish to recapitulate a rare genetic disease through modeling Pyridoxine-Dependent Epilepsy (PDE), a rare disease associated with pathogenic variants in the *Aldehyde Dehydrogenase 7 Family Member A1* (*ALDH7A1*)

gene, causing intractable seizures in neonates/infants. This group targeted zebrafish *aldh7a1* using CRISPR-Cas9 to generate mutants displaying disease characteristics of PDE (*e.g.*, seizures beginning in larval stages). Using drug screening techniques the researchers found pyridoxine and pyridoxal 5'-phosphate (which is the currently used treatment) mitigated the seizure-like behavior, and extended the life span of *aldh7a1* mutant zebrafish[167]. This study is particularly important as it was the first time a PDE animal model was created and is an example of a promising start to the utilization of the zebrafish model to answer questions about pathogenic mechanisms and specific treatment options for rare genetic diseases.

1.6 *PRR12* and zebrafish

To date, there is no literature describing any animal model recapitulating the *PRR12*-related Neuroocular Syndrome (NOC). Given the ocular and neurodevelopmental phenotypes of this syndrome and the advantages of using the zebrafish model to study neural development and the eye, the zebrafish is an attractive system to investigate this gene and potential syndrome. In Chapter 3, I explore the two orthologues of human *PRR12* in zebrafish, *proline rich 12a* (*prr12a*) and *proline rich 12b* (*prr12b*); two paralogous genes that are related through a duplication event[184]. Furthermore, temporal expression of the *prr12* paralogues has been detected from the one-cell stage through 5 dpf in zebrafish[185], alluding to its importance and role in early developmental processes.

To understand the intricate mechanisms of development, spatiotemporal gene expression information is needed to characterize the regulatory processes that govern embryonic development. Various techniques such as quantitative reverse-transcription polymerase chain reaction (qRT-PCR)[186], whole-mount *in situ* hybridization (WMISH)[187] and RNA-sequencing[188], can be used to investigate the developmental and/or tissue-specific expression patterns of target genes within the zebrafish. Such efforts are the first step in investigating gene regulation, and to ultimately understand and model human genetic diseases in zebrafish. Thus, in the present work, the pattern and expression of the *prr12* paralogues in early development and adulthood are characterized. The presented data expands on the relatively limited knowledge of the developmental role of *PRR12*, with

hopes to utilize the zebrafish model to demonstrate the spectrum of clinical phenotypes seen within this rare syndrome.

Disclaimer: The initial goal of this thesis was to create a CRISPR/Cas9 knockout of a *prr12a/prr12b* zebrafish disease model for the human *PRR12*-related Neuroocular Syndrome, as well as an investigation into the function of the *prr12* paralogues. I was not able to complete these experiments due to a suspected bacterial outbreak in the zebrafish housing system, leading to its closure (see **Appendix 1**); in addition to difficulties caused by the COVID-19 restrictions imposed by Western University, the Province of Ontario, and the Government of Canada. Therefore, the experiments that I had planned on completing for my M.Sc. thesis were revised, to focus instead on the spatiotemporal expression characteristics of the *prr12* paralogues in zebrafish embryos, larvae, and adult tissues.

1.7 Rationale, hypothesis, and objectives

Rationale of this study:

In vivo models, like that offered by the zebrafish, provide an unparalleled system to study development, genetics, and disease etiology. Due to the many attributes available to zebrafish including their rapid generation time, high fecundity, near-transparent embryos, and ease of genetic manipulation[18], my aim was to investigate the expression of *prr12a* and *prr12b* in zebrafish early development and adulthood. Towards that end, I characterized the spatiotemporal expression patterns of these transcripts using *in situ* hybridization, RT- and qPCR. Given the minimal literature describing *prr12* in any organism, the insight gained from these efforts provide significant knowledge of the role for *prr12* role in vertebrate development, and specifically will assist in delineating the pathogenesis of the variation of *PRR12* in the clinical population.

Hypothesis of this study:

I predict that during embryogenesis, larval development, and adulthood, the zebrafish *prr12* paralogues will be expressed in tissues as seen for human *PRR12*. Specifically, I hypothesize that human *PRR12* is conserved in its spatiotemporal expression patterns with the zebrafish paralogues, and that their biological function(s) is/are also similar. That said, studying the zebrafish paralogues provides a necessary platform to investigate underlying mechanisms that lead to human *PRR12*-related Neuroocular Syndrome.

Objectives of this study:

1. Identify the spatiotemporal expression of the *prr12* paralogues in embryonic and larval zebrafish development.

2. Analyze the tissue distribution and gene expression of the *prr12* paralogues in male and female adult zebrafish.

Chapter 2

2 Materials and Methods

2.1 Zebrafish husbandry: maintenance and embryo collection

All experiments were conducted in accordance with the guidelines outlined by the Canadian Council on Animal Care and approved by the Animal Care Committee at Western University (AUP #2019-149; **Appendix 1**), and Western's Biosafety Approval (BIO-UWO-0081).

Procedures for the assembly and start-up of the Aquaneering ZS560 Zebrafish Housing System were implemented according to the manufacturer's instructions[189]. System acclimation was conducted for approximately 8 weeks where water flow, pH, ammonia, and nitrate levels were monitored, adjusted, and checked daily; in addition to all other system maintenance outlined by Aquaneering[189]. TU and AB wildtype zebrafish (generously donated by Dr. B. Ciruna, The Hospital for Sick Children, Toronto, ON and Dr. M. Ekker, University of Ottawa, respectively) were housed separately by zebrafish strain in the system and used for experimentation. Zebrafish nutritional culture standard operational procedures were established from Aquaneering protocols, and zebrafish were fed according to guides provided by Aquaneering[189] and the Zebrafish Book[190]. Briefly, paramecia (*Paramecium multimicronucleatum*) (Ward's Science, Henrietta, NY, USA) were purchased and fed to zebrafish aged 5-15 dpf; brine shrimp nauplii (hatched cysts) (Brine Shrimp Direct, Salt Lake City, UT, USA) were fed to zebrafish aged 16 – 30 dpf; and slow sinking (1.0mm) dry food pellets (Zeigler, Gardners, PA, USA) with brine shrimp nauplii were fed to zebrafish after 31 dpf on alternating days. Paramecia cultures were passaged every 5 weeks and examined for contamination every 2 days using the SZO-4 OPTIKA stereomicroscope (OPTIKA Microscopes Italy). Brine shrimp eggs (cysts) were hatched according to the manufacturer's protocol[189].

Adult zebrafish were stocked at 6-8 fish per liter with an approximately equal male to female ratio and held under a 14-hr light/10-hr dark light cycle at 28.5ºC. Breeding procedures were outlined in the Zebrafish Book[190] and the Kelly Laboratory Protocol (AUP

#2019-149; **Appendix 1**). For pair-wise breeding one female and one male were placed in static tanks overnight. Approximately 30 minutes after light cycle initiation, embryos were collected using a 4-inch nylon mesh strainer. Zebrafish embryos were raised in embryo medium (E3) solution (1% methylene blue) at 28.5ºC that was changed daily[190]. Five dpf zebrafish were introduced to the housing system, where age and overall morphology was assessed according to a staging guide[22].

2.2 Embryo, larval, and adult mRNA expression analysis

2.2.1 Embryo and larval mRNA isolation

Total mRNA was isolated from TU wildtype strain embryos and larval (fry) at 2-cell (0.75 hpf), 32-cell (1.75 hpf), 128-cell (2.25 hpf), 1k-cell (3 hpf), 50%-epiboly (5.3 hpf), 1-4 somite (10.3 hpf), 14-19 somite (16 hpf), Prim-6 (24 hpf), Long pec (48 hpf), Protruding mouth (3 dpf), Day 4 (4 dpf), and Day 5 (5 dpf). Approximately 30 embryos or fry were pooled at each timepoint, according to a staging guide[22], and RNA isolation was performed according to Peterson and Freeman, 2009[191]. Briefly, samples were homogenized using a pellet pestle (Thermo Scientific, 12-141-364), mRNA was isolated using TRIzol reagent (Invitrogen, 15596026) and chloroform eluted in a final volume of 100 µL of RNase-free water and quantified using a NanoDrop™ 2000c Spectrophotometer (Thermo Fisher Scientific). RNA was reverse transcribed into cDNA using the High-Capacity cDNA Reverse Transcription Kit (Applied Biosystems, 4368814) as per manufacturer's instructions.

2.2.2 Adult tissue dissection and mRNA isolation

A total of 3 male and 3 female 8-month-old TU wildtype strain zebrafish siblings were used for dissections of the brain, eye, liver, kidney, and reproductive organs. Dissections were performed by the Zebrafish Genetics and Disease Models Core Facility at the Hospital for Sick Children (Toronto, ON) as described in Gupta and Mullins, 2010[192] with minor modifications. Briefly, zebrafish were individually immersed in 0.2% tricaine and euthanized in an incubation of ice water and then laterally pinned on a dissecting mat under a stereomicroscope. The ventral underside of the fish anterior to the anal fin was cut to the

operculum and the gill was excised. The remaining skin and underlying muscle from the lateral sides of the fish were removed. The testes or ovaries were excised, and the fat was dissociated prior to collection. The gastrointestinal system was removed from the body cavity of the fish and the whole intestine and liver collected. The swim bladder was removed, and fish were placed dorsal-side upwards to collect the head, body and tail of the kidney located on the dorsal wall. For collection of the eye and the brain, the head was removed with a razor blade and the skull opened on the dorsal side from the anterior forehead. The right eye of all zebrafish was excised and collected. The whole brain was also excised and macro-dissected on dry ice into 3 brain regions: the telencephalon, mesencephalon and rhombencephalon, with the optic tectum used as a landmark. All dissections were performed using sterile/RNase free dissecting scissors, razor blades and forceps and collected on dry ice immediately after excision. RNA was isolated using the Trizol reagent and chloroform following the manufacturer's protocol (Invitrogen) and eluted in a final volume of 15 μL of RNase-free water and quantified using a NanoDrop™ 2000c Spectrophotometer (Thermo Fisher Scientific). As the tissue was small in size, glycogen (Thermo Fisher Scientific, R0551) was added as a carrier molecule directly to Trizol for isolation of RNA. RNA was reverse transcribed into cDNA using the High-Capacity cDNA Reverse Transcription Kit (Applied Biosystems, 4368813) as per the manufacturer's instructions.

2.3 Qualitative (endpoint, RT-PCR) and quantitative reverse-transcription (qRT-PCR) polymerase chain reaction

Specific primers for *prr12a* and *prr12b* were designed using the Ensembl Genome Browser (Zebrafish, GRCz11)[32] and the NCBI Primer-BLAST tool[193]. RT-PCR was performed under the following reaction conditions: 500 nanomolar (nM) forward and reverse primers (**Table 2**), 25 μL DreamTaq Green PCR Master Mix (Thermo Fisher Scientific, K1081) and 1 μL of cDNA template. Reactions were performed using a C1000 Touch Thermal Cycler (Bio-Rad Laboratories) for 35 cycles. Samples for endpoint RT-PCR were visualized on a 2% agarose gel (1X TAE), containing RedSafe (iNtRON Biotechnology Inc., 21141) and gels imaged using the ChemiDoc Touch Imaging System (Bio-Rad

Laboratories). *Like-sm protein 12 homolog b* (*lsm12b*) was used as a reference gene to normalize amplification of target genes[194].

Table 2. Endpoint RT-PCR primer sequences for zebrafish target genes

Gene	Forward Primer (5' to 3')	Reverse Primer (5' to 3')	Tm
prr12a	ACAGCCATCCTATGGG TCCT	AACCAGAGAGGCACGA CTTG	58ºC
prr12b	AGATGTCCTGGGAGGG AGAC	TCCTCTTGAGCTCCTCG TCA	53ºC
lsm12b	AGTTGTCCCAAGCCTA TGCAATCAG	CCACTCAGGAGGATAA AGACGAGTC	54ºC

qRT-PCR was performed under the following reaction conditions: 500 nM forward and reverse primers (**Table 3**), 10 µL SensiFAST™ SYBR Mix (Bioline, FroggaBio Inc., BIO-98050) and 1 µL cDNA template. Reactions were performed using a CFX Connect Real-Time PCR Detection System (Bio-Rad Laboratories) for 40 cycles. Relative mRNA gene expression was calculated using the comparative Ct method ($2^{-\Delta Ct}$) and normalized to the constitutively active *glyceraldehyde-3-phosphate dehydrogenase* (*gapdh*)[195].

Table 3. qRT-PCR primer sequences for zebrafish target genes

Gene	Forward Primer (5' to 3')	Reverse Primer (5' to 3')	Tm
prr12a	TGGAGGCATTCGCCC GTTAT	GGCTAGGACAGCCAC CCAAA	53ºC
prr12b	ATCTCCCACCCATGC GGAAG	CCCAGATGCACTTTCA CCGC	54ºC
gapdh	CGCTGGCATCTCCCT CAA	TCAGCAACACGATGG CTGTAG	55ºC

2.4 Spatiotemporal expression analysis

2.4.1 Plasmid preparation and *in vitro* transcription for *in situ* hybridization

In situ hybridization RNA probes (riboprobes) were designed using the Ensembl Genome Browser (Zebrafish, GRCz11)[32] and NCBI Primer-BLAST[193] tool for the creation of antisense and sense *prr12a* and *prr12b* 3' riboprobes. Primers were designed targeting the 3' untranslated regions (UTR) for specificity, and EcoRI or BamHI restriction sites were included for directional cloning (**Table 4**). *prr12a* and *prr12b* fragments were amplified

via RT-PCR (as described in Section 2.3) using a C1000 Touch Thermal Cycler (Bio-Rad Laboratories) from 4 dpf zebrafish embryonic cDNA, purified using a QIAquick PCR Purification Kit (QIAGEN, 28104) and digested with EcoRI (New England Biolabs, R3101S) and BamHI (New England Biolabs, R0136S) as per the manufacturer's protocol.

Table 4. Primer sequences for zebrafish *in situ* hybridization probes

Gene	Forward Primer (5' to 3')	Reverse Primer (5' to 3')	Tm
prr12a	GGACGAATTCTTGGA GACGGCCTCAAT	ATAAGGATCCATGAA TCCGTCAGTCCG	58ºC
prr12b	ATTAGGATCCTCCAC GATCCAAACACGTCC	GGAGGGAATTCTGTC TCTGTGCAGACAACTG	58ºC

A 1:3 vector to insert ratio was used to ligate insert into EcoRI and BamHI digested BluescriptSK+ plasmid (generously donated by Dr. L. Dagnino, UWO, London, ON). T4 DNA ligase (New England Biolabs, M0202S) was used for overnight incubation at 16ºC before plasmids were transformed into *E. coli* (DH5-Alpha). Colonies were selected and plasmids were isolated using QIAprep Spin Miniprep Kit (QIAGEN, 27104) as per the manufacturer's protocol. Insertion of *prr12a* and *prr12b* was confirmed by sequencing (London Regional Genomics Centre, Roberts Research Institute, London, ON).

prr12a, *prr12b,* and *dlx3* and *krox-20* plasmids (the latter two generously donated by Dr. B. Ciruna, The Hospital for Sick Children, Toronto, ON) were used as templates for *in vitro* transcription of antisense and sense riboprobes. Briefly, plasmids were linearized (**Table 5**), DNA was precipitated in 100% ethanol and 3 M sodium acetate (Sigma-Aldrich) at -80ºC, and the pellet vacuum dried and suspended in 20 µL RNase-free water. DNA concentrations were quantified using a NanoDrop™ 2000c Spectrophotometer (Thermo Fisher Scientific). Riboprobes were synthesized by *in vitro* transcription using a DIG (Digoxigenin) RNA Labelling Kit (Roche, 11175025910) as per the manufacturer's instructions.

Table 5. Restriction enzyme and RNA polymerases for *in vitro* transcription

Plasmid Name	Vector	RNA Polymerase	Restriction Enzyme
***prr12a* sense**	Bluescript SK+	T7	BamHI
***prr12a* antisense**	Bluescript SK+	T3	EcoRI
***prr12b* sense**	Bluescript SK+	T3	EcoRI
***prr12b* antisense**	Bluescript SK+	T7	BamHI
***dlx3* antisense**	Bluescript KS+	T7	Sall
***krox-20* antisense**	Bluescript KS+	T3	Pstl

2.4.2 Whole-mount *in situ* hybridization (WMISH)

AB wildtype zebrafish embryos were fixed at 6, 16, 24, 48 and 72 hpf, by the Zebrafish Genetics and Disease Models Core Facility at the Hospital for Sick Children (Toronto, ON). Briefly, embryos were exposed to 0.003% 1-phenyl 2-thiourea to inhibit pigmentation, as described in Karlsson *et al*., 2001[196]. Embryos were then fixed in 4% paraformaldehyde, washed in 1X PBS, manually dechorionated using sterile forceps, transferred to 100% methanol, and shipped to the Kelly Lab at The University of Western Ontario (London, ON).

Embryos were rehydrated and processed for WMISH as described in Kelly *et al.*, 2003[197] with minor modifications. Briefly, embryos underwent incubation in hybridization solution containing antisense or sense riboprobes, extensively washed to ensure removal of unbound probe, and blocked in 5% heat inactivated sheep serum at room temperature. Embryos were incubated overnight at 4ºC in blocking solution containing anti-digoxigenin (Roche, 11093274910) conjugated to alkaline phosphatase. Next, embryos were washed in PBST (phosphate-buffered saline, Tween 20) and washed 3 times in staining buffer (5 M NaCl, 1 M MgCl2, 1 M Tris, pH 9.5, 10% Tween 20). Embryos were incubated in staining buffer containing NBT/BCIP (4-nitro blue tetrazolium chloride/5-bromo-4-chloro-3-indolylphosphate) (Roche, 11681451001). Staining proceeded in the dark until a signal was visualized within embryos incubated with the sense probe. Stained embryos were fixed in 100% methanol and placed in 2:1 ratio of benzyl benzoate (Sigma-Aldrich, B6630-250ML)/benzyl alcohol (Sigma-Aldrich, 305197-100ML) and imaged at 45x magnification using an SZO-4 OPTIKA stereomicroscope with a OPTIKA C-B5+ camera

(OPTIKA Microscopes Italy). Images were processed using the OPTIKA LITEView software (OPTIKA Microscopes Italy) and scale bars were added using ImageJ (NIH)[198].

2.5 *In silico* analysis

2.5.1 Analysis of proline rich 12 sequences

Sequences for zebrafish and human genomic DNA and proteins were obtained from the Ensembl Genome Browser database[32]. Zebrafish (*prr12a* and *prr12b*) and human (*PRR12*) exon-intron structures were generated using an Exon-Intron Graphic Maker[199]. The human PRR12 protein schematic outlining specific protein domains was constructed using Adobe Illustrator 7.0 (Adobe), as described in Chowdhury *et al.*, 2021[27]. Alignments of human (PRR12) and zebrafish (Prr12a and Prr12b) amino acid sequences were performed using Clustal Omega Multiple Sequence Alignment Tool[200]. The location of the critical domains were identified with reference to the residue numbers stated by the Clustal Omega Multiple Sequence Alignment Tool and as described in PRR12 literature[24,25,27]. Total nucleotide and amino acid sequence identities were calculated using a Multiple Sequence Alignment (CLUSTALW)[201].

2.5.2 Whole zebrafish RNA-sequencing

Zebrafish temporal expression data was obtained from a publicly available RNA sequencing database (White *et al.,* 2017[185]). *prr12a* and *prr12b* TPM (Transcripts per Million) values were selected for various developmental time points (12 time points, N=5). Data was analyzed using GraphPad Software version 9.2.0 (283) for Mac OS X, GraphPad Software, San Diego, California USA, www.graphpad.com. The expression for the *prr12* paralogues at the selected developmental time points was analyzed for an overall trend.

2.6 Statistical analysis

Data for the tissue distribution across selected tissues and gene expression analyses in individual tissues were representative of 3 biological replicates of individual fish. Tissue distribution analyses were performed using a one-way ANOVA with Tukey's honest significant difference (HSD) post-hoc test to compare gene expression of *prr12a* or *prr12b*

across selected male or female zebrafish tissues. Gene expression analyses in individual tissues were performed using a two-way ANOVA with Tukey's HSD post-hoc test to compare gene expression of *prr12a* and *prr12b* amongst male and female tissues. A P value < 0.05 was considered significant for both one-way and two-way ANOVA and reported error bars represent standard error of the mean (± S.E.M). All statistical analysis was performed using GraphPad Prism version 9.2.0 for Mac OS X, GraphPad Software, San Diego, California USA, www.graphpad.com.

Chapter 3

3 Results

3.1 Exonic structure arrangement of human *PRR12*, zebrafish *prr12a*, and zebrafish *prr12b*

ZFIN[127] and the Ensembl Genome Browser[32] report the *prr12* zebrafish paralogues; *prr12a* and *prr12b,* that are zebrafish orthologues of the human *PRR12* gene. To investigate the overall exonic structure of these transcripts, nucleotide sequences were obtained from the Ensembl Genome Browser[32] and processed through an Exon-Intron Graphic Maker[199], to allow for proportional analysis and identification of homologous exons between species. Analysis was performed on the following: long human *PRR12* isoform, short human *PRR12* isoform (RefSeq, NM_020719.3), zebrafish *prr12a,* (RefSeq, XM_005156014), and zebrafish *prr12b* (RefSeq, XM_680992)[32]. *In silico* analysis revealed similar exonic length in human long and short *PRR12*, *prr12a,* and *prr12b*; with the majority number of exons and exon length conserved. In comparison, to the long human *PRR12* isoform, zebrafish *prr12a* has 1 additional exon and zebrafish *prr12b* has 2 additional exons (**Figure 4**). As calculated by a Multiple Sequence Alignment (CLUSTALW)[201], zebrafish *prr12a* and zebrafish *prr12b*, share 30% and 27% sequence identity with the long human *PRR12* isoform, respectively.

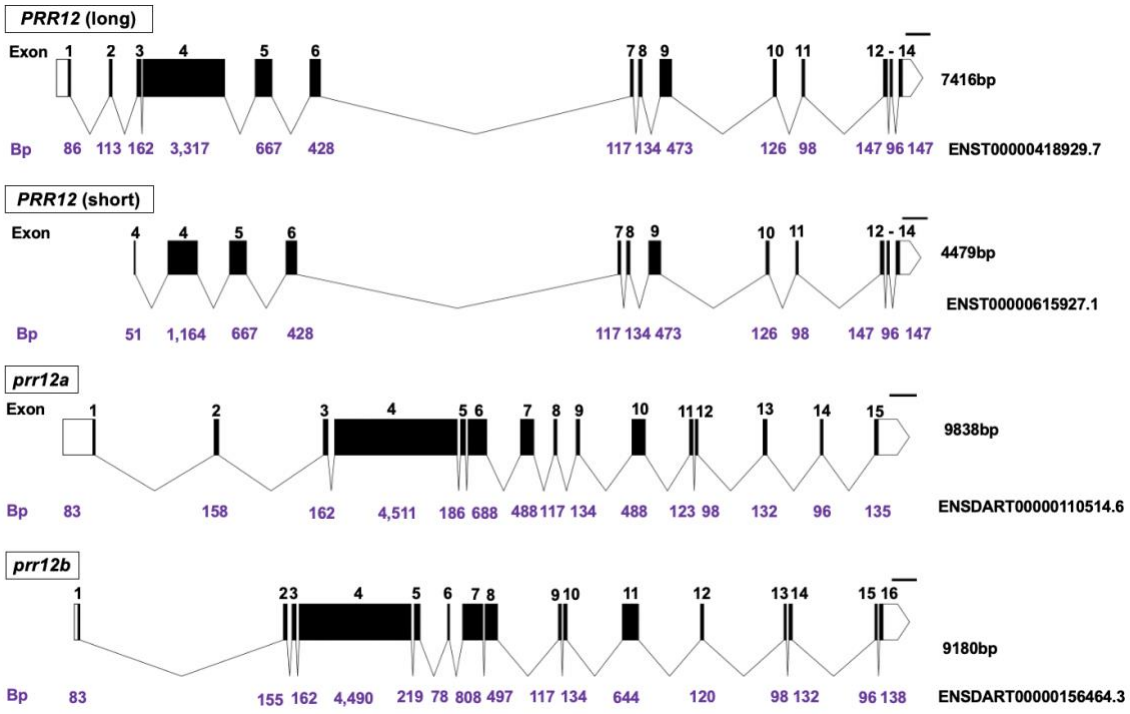

Figure 4. Exonic structure arrangement of human *PRR12* isoforms and zebrafish *prr12a*, and zebrafish *prr12b*. Human *PRR12* long and short isoforms, and zebrafish *prr12a* and *prr12b*, show overall similar exon-intron structure. Black boxes are exons, lines are introns, white boxes indicate the 5' UTR and white triangles the 3' UTR. Each exon is numbered, overall transcript length is indicated in base pairs (bp) and each Ensembl transcript ID is indicated. Nucleotide sequences were obtained from Ensembl[32] and processed through an Exon-Intron Graphic Maker[199]. Scale bar: 1000bp.

3.2 Schematic representation of the AT-hook domain regions within human PRR12, zebrafish Prr12a, and zebrafish Prr12b

The long and short PRR12 isoforms encode proline rich polypeptides (Ensembl, ENSP00000394510.1) with nuclear localization owing to their two predictive AT-hook binding domains[24,25]. To test if the two predicted AT-hook domains in both long and short human isoforms are conserved in zebrafish Prr12a (Ensembl, ENSDARP00000137218.1) and Prr12b (Ensembl, ENSDART00000156464.3), amino acid sequences were obtained from the Ensembl Genome Browser[32] and aligned through a Clustal Omega Multiple Sequence Alignment Tool[200]. A protein schematic of human PRR12 was modelled to identify domains of the PRR12 protein (**Figure 5A**)[25,27]. As the DNA binding ability of PRR12 is one of its defining characteristics[24,25,27], the two AT-hook domains was selected to investigate domain conservation in human and zebrafish. The results demonstrated the presence of the first and second AT-hook domains, corresponding to 93% and 62% amino acid identity, respectively, between human and zebrafish (**Figure 5B**). Multiple Sequence Alignment (CLUSTALW)[201] showed the total amino acid sequence identity between PRR12 and Prr12a is 28%, and 26% between PRR12 and Prr12b.

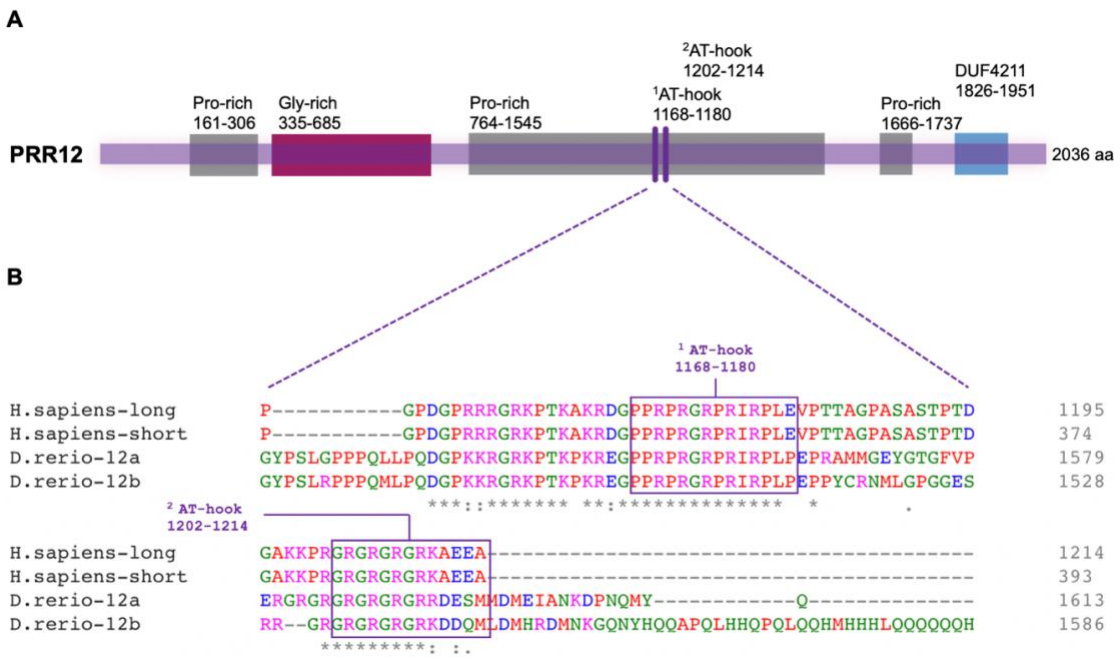

Figure 5. Schematic representation of the AT-hook domain regions within human PRR12, zebrafish Prr12a, and zebrafish Prr12b. A. Full-length human PRR12 protein schematic highlighting specific domain regions, adapted and modified from Chowdhury *et al.*, 2021[27]. Pro-rich: proline rich domains, Gly-rich: glycine rich domains, AT-hook: DNA-binding protein motif, DUF4211: domain of unknown function. **B.** Amino acid sequences were obtained from Ensembl[32] and processed through the Clustal Omega Multiple Sequence Alignment Tool[200] showing the conserved AT-hook domain sequences between human and zebrafish. The two predictive AT-hook binding sites are denoted with a purple box. Asterisks (*): a fully conserved residue, colon (:): strongly similar properties between groups and period (.): weakly similar properties between groups. Residue type of amino acids are coloured based on property accordingly (Red: small + hydrophobic (incl. aromatic – Y), Blue: acidic, Magenta: basic – H, Green: hydroxyl + sulfhydryl + amine G, *etc.*). Schematic not drawn to scale.

3.3 Transcriptome profiling of *prr12a* and *prr12b* in zebrafish development

To date there is no literature indicating the role *prr12a* and *prr12b* play in zebrafish development, however, transcriptome profiling of the *prr12* paralogues throughout embryogenesis and larval development was publicly accessible through an RNA sequencing database[185]. This study pooled 12 Hubrecht Long Fin wildtype strain embryos per time point (N=5), isolated total RNA and performed a poly(A) pulldown RNA-seq and 3' end enrichment method to generate a temporal zebrafish expression database. The global expression profile of the *prr12* paralogues throughout development was analyzed by obtaining the respective Transcripts per Million (TPM) values of each paralogue. Values were obtained from the database and expression of each gene was assessed over the selected developmental timepoints. The results demonstrated that both *prr12a* and *prr12b* were expressed globally throughout embryonic and larval development, where *prr12a* showed overall elevated expression levels throughout development in comparison to *prr12b* (**Figure 6A and 6B**). *prr12a* highest expression value, ~60 TPM, was seen at the 128-cell stage, when the embryo is entering into the blastula stage[22] (**Figure 6A**), whereas *prr12b* highest expression value, ~25 TPM, was observed at 48 hpf, when larvae are entering the hatching period[22]. In addition, when observing overall trends of expression, *prr12a* was more abundant than *prr12b* in early development (**Figure 6A**). These relatively low *prr12b* expression levels steadily increased later in development (**Figure 6B**).

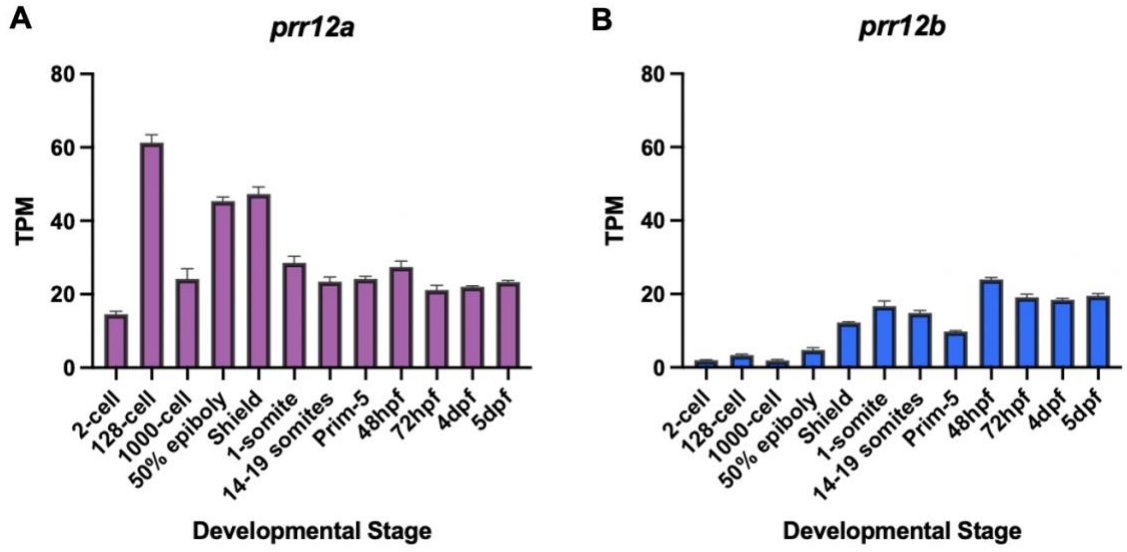

Figure 6. Transcriptome profiling of *prr12a* and *prr12b* in zebrafish development. Global RNA-sequencing expression demonstrating **A.** *prr12a* and **B.** *prr12b* expression at 12 developmental time points; hpf: hours post fertilization and dpf: days post fertilization. Each bar represents the mean value of 5 biological replicates of 12 pooled embryos, ± S.E.M. Each timepoint is represented as Transcripts per Million (TPM). Raw data obtained from White *et al.*, 2017[185].

3.4 Representative temporal expression profile of *prr12a* and *prr12b* in zebrafish development

To corroborate the transcriptomic expression profiles revealed by the RNA sequencing data (**Figure 6A** and **6B**), I performed RT-PCR targeting the *prr12* paralogues. Specifically, total RNA was isolated from ~30 pooled embryos or larvae, and reverse transcribed into cDNA for RT-PCR analysis using *prr12a*, *prr12b*, and *lsm12b* (reference gene)[194] specific primers. RNA was collected from 13 stages encompassing the 2-cell stage through 5 dpf (**Figure 7A**) and as expected, *prr12a* and *prr12b* showed a similar overall expression trend throughout development to the RNA sequencing data (**Figure 6A** and **6B**). RT-PCR of *prr12a* showed expression in all tested stages, where it is maternally expressed as evident by a band seen at the 2-cell, 32-cell, and 128-cell stages. Maternal *prr12a* expression prior to the MBT, continued after the 512-cell stage, when zygotic gene expression is active[22]. *prr12a* transcript was also detected in larval development (72 hpf, 4 dpf, and 5 dpf) (**Figure 7B**). In comparison, the *prr12b* transcript amplicon was seen, albeit weak, early in development (**Figure 7B**), mirroring the *prr12b* RNA-sequencing data (**Figure 6B**). Interestingly, *prr12b* exhibited a dynamic expression pattern, as its detection suggests that the gene is upregulated and downregulated at varying stages. These results seen in **Figure 7B** are similar in the earlier selected timepoints but contrast those from the RNA sequencing analysis that showed sustained *prr12b* expression throughout later developmental stages (**Figure 6B**). Later stages (24 hpf through 5 dpf) correspond to the completion of organ morphogenesis[22], and my results would suggest a potential temporal-specific role for *prr12b* during these processes.

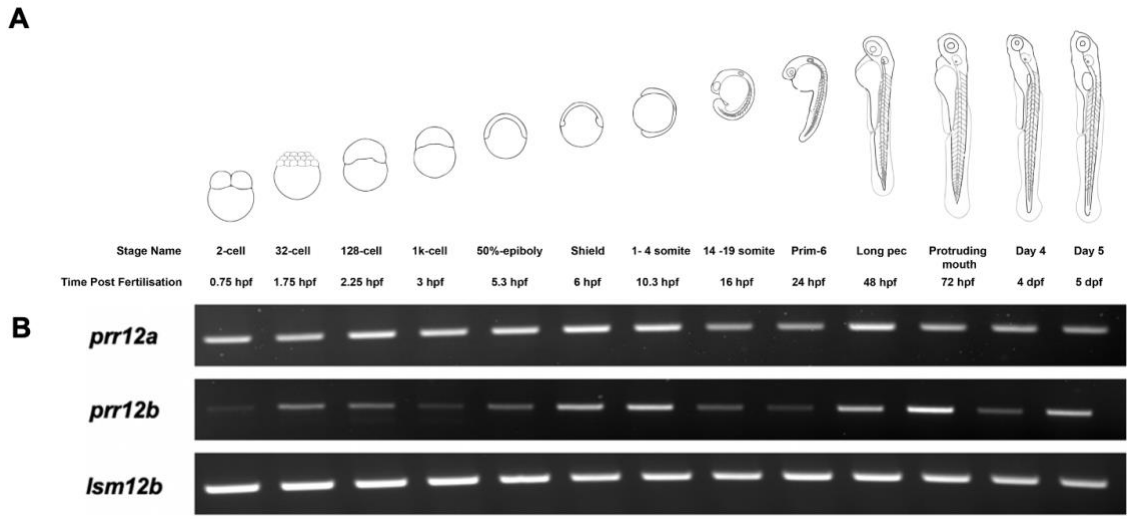

Figure 7. Representative temporal expression of *prr12a* and *prr12b* in zebrafish development. A. Zebrafish diagrams showing representative 2-cell, 32-cell, 128-cell, 1k-cell, 50%-epiboly, Shield, 1-4 somite, 14-19 somite, Prim-6, Long pec, Protruding mouth, Day-4, and Day-5, adapted and modified from White *et al*., 2017[185], and not drawn to scale. Hpf represents hours post fertilization and dpf represents days post fertilization. **B.** Agarose gel electrophoresis (2% agarose) of amplicons showing temporal expression of *prr12a* and *prr12b*, relative to the *lsm12b* loading control. Each lane represents global mRNA expression of ~30 embryos or larvae, N=1.

3.5 Whole-mount *in situ* hybridization assay of *prr12a* expression in zebrafish development

Temporal analyses revealed that *prr12a* was expressed throughout embryogenesis and larval development (**Figure 6A** and **7B**). However, WMISH was employed to elucidate the spatiotemporal expression pattern of these targets (**Figure 8**). Five of the 13 developmental time points from the previous RT-PCR analyses (**Figure 7B**) were selected: 6 hpf (Shield), 16 hpf (14-19 somite), 24 hpf (Prim-6), 48 hpf (Long pec), and 72 hpf (Protruding mouth) (**Figure 8A**). *prr12a* expression was detected in the selected developmental stages, consistent with the RT-PCR data (**Figure 7B**) and WMISH showed there was a diffuse expression pattern throughout embryonic and larval stages (**Figure 8B-J**). Specifically, global expression at 6 hpf (early gastrulation period) (**Figure 8B**) and 16 hpf (segmentation period) (**Figure 8C** and **C'**) was seen with the *prr12a* probe. The same was true for 24 hpf (pharyngula period) (Figure **D**, **D'** and **E**) and during organogenesis at 48 hpf (**Figure 8F, G** and **G'**). Of note, no distinct *prr12* expression boundaries were seen at 24 hpf and 48 hpf in the telencephalon, diencephalon, mesencephalon, and rhombencephalon. However, at 72 hpf in the hatching period (**Figure 8H**) *prr12a* expression appeared to be localized to the eye and brain regions of the larvae. *dlx3*[202] and *krox-20*[203] were used as positive controls and, as expected, highly localized expression patterns were seen at 16 and 24 hpf, respectively. The negative control, sense-strand *prr12a* probe showed some background staining (**Figure 8B'**).

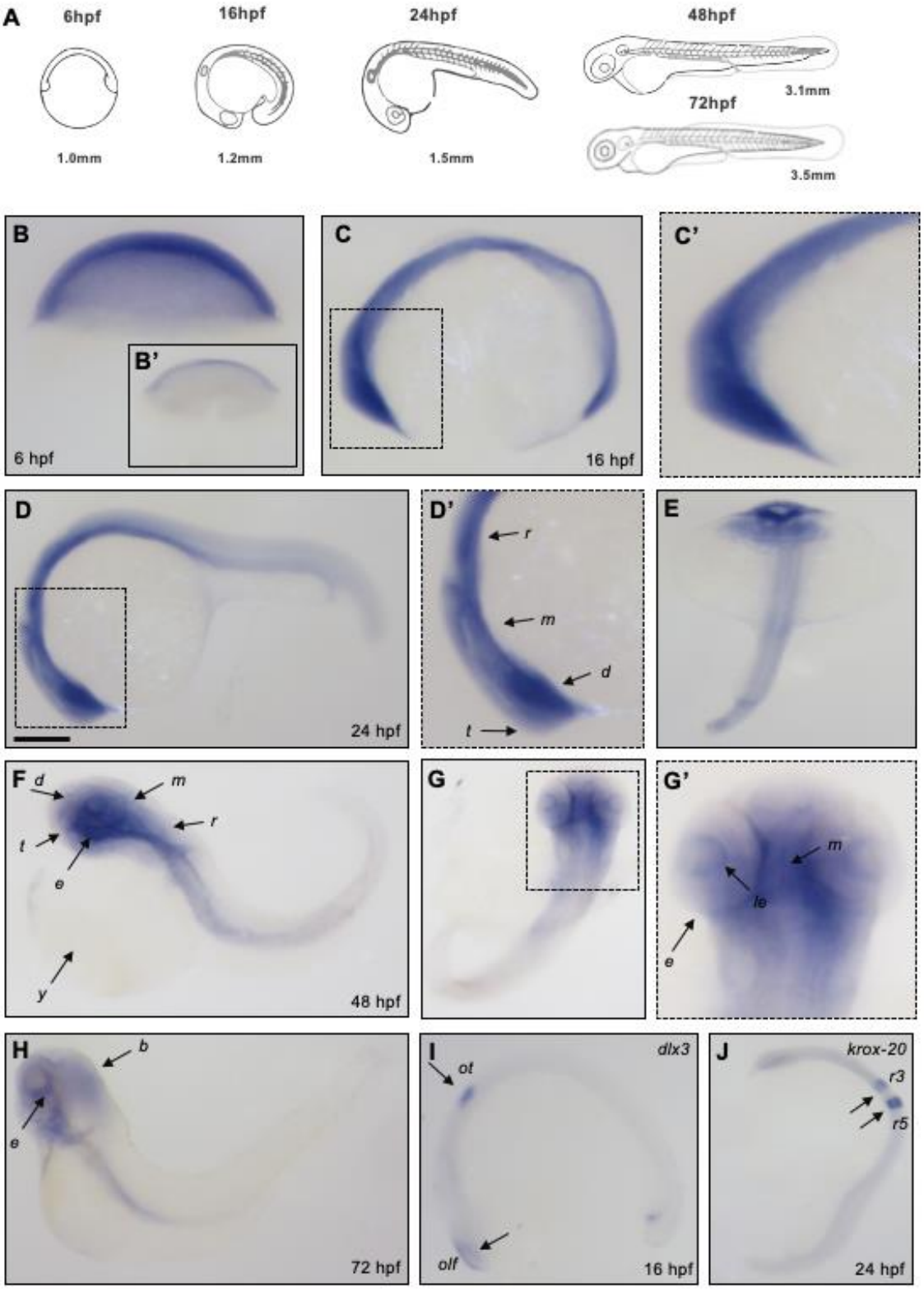
A
6hpf
16hpf
24hpf
48hpf
1.0mm
1.2mm
1.5mm
3.1mm
72hpf
3.5mm
B
B'
6 hpf
C
16 hpf
C'
D
24 hpf
D'
r
m
d
t
E
F
d
m
r
t
e
y
48 hpf
G
G'
m
le
e
H
b
e
72 hpf
I
dlx3
ot
olf
16 hpf
J
krox-20
r3
r5
24 hpf

Figure 8. Whole-mount *in situ* hybridization (WMISH) showing *prr12a* expression in zebrafish development. Diagrams (**A**) are adapted and modified from White *et al*., 2017[185]. Representative WMISH of *prr12a* expression in embryos/larvae at 6 hpf (**B** and **B'**), 16 hpf (**C** and **C'**), 24 hpf (**D**, **D'** and **E**), 48 hpf (**F**, **G** and **G'**), and 72 hpf (**H**). (**I**) *dlx3* expression at 16 hpf in olfactory and otic cells (indicated with arrows) and (**J**) showing *krox-20* labeling of rhombomeres 3 and 5 (indicated with arrows). **B-D'**, **F** and **H-J** are lateral views, and **E**, **G** and **G'** are dorsal views. The box in area **B'** shows background staining in a sense strand control embryo. Scale bar is equal to 100 μm and images **C'**, **D'** and **G'** are digitally enlarged. Image labeled acronyms; *b (brain), d (diencephalon), t (telencephalon), m (mesencephalon), r (rhombencephalon), e (eye), le (lens), y (yolk), ot (otic placode), olf (olfactory placode), r3 (rhombomere 3), and r5 (rhombomere 5).*

3.6 Whole-mount *in situ* hybridization assay of *prr12b* expression in zebrafish development

The spatiotemporal expression profile of *prr12b* was examined by WMISH (**Figure 9**) and given the RNA sequencing and RT-PCR data, I expected its expression to vary across the developmental stages, becoming localized at later timepoints. To address this, the same developmental time points were used in the *prr12a* analysis, specifically: 6 hpf (Shield), 16 hpf (14-19 somite), 24 hpf (Prim-6), 48 hpf (Long pec), and 72 hpf (Protruding mouth) (**Figure 9A**). Results showed *prr12b* had a similar expression profile to *prr12a* (**Figure 8B-H**), with diffuse expression seen in all embryonic and larval tissues, corresponding to the early gastrulation (6 hpf, **Figure 9B**), a segmentation period (16 hpf, **Figure 9C** and **C'**), pharyngula periods 24 hpf (**Figure 9D, D'** and **E**), and 48 hpf (**Figure 9F, G and G'**). Like *prr12a*, *prr12b* transcript was detected in the eye and brain regions of the larvae at 72 hpf, which constitutes the end of the hatching period (**Figure 9H**). Thus, the *prr12b* profile was like that for *prr12a* (**Figure 8**), and the same was true for the expression in the telencephalon, diencephalon, mesencephalon, and rhombencephalon. *dlx3*[202] and *krox-20*[203] was highly localized in embryos at 16 hpf (**Figure 9I**) and 24 hpf (**Figure 9J**), respectively. Furthermore, the sense strand, negative control for *prr12b*, showed some background staining (**Figure 9B'**).

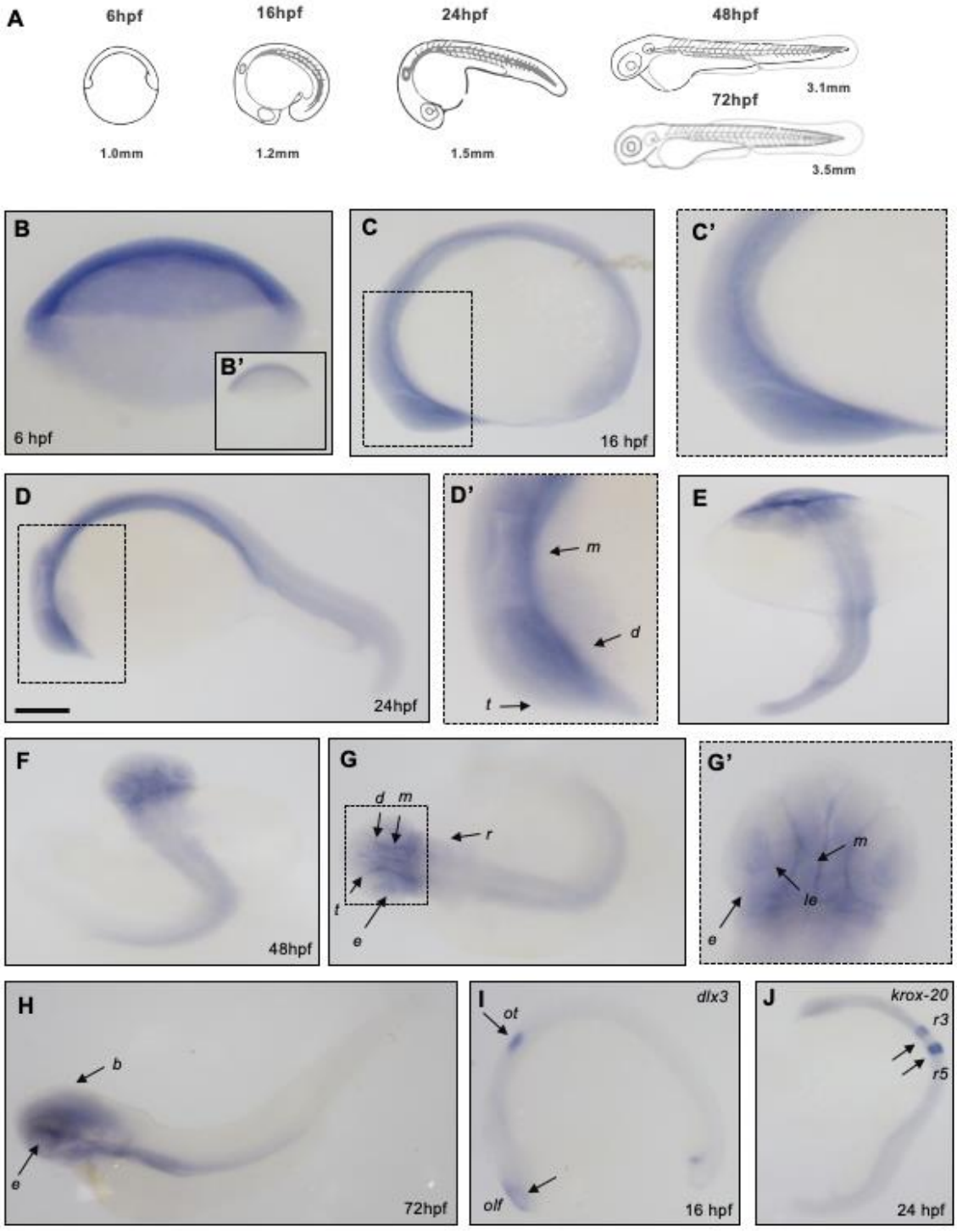
A
6hpf
16hpf
24hpf
48hpf
72hpf
1.0mm
1.2mm
1.5mm
3.1mm
3.5mm
B
B'
6 hpf
C
16 hpf
C'
D
24hpf
D'
m
d
t
E
F
48hpf
G
d
m
r
t
e
G'
m
le
e
H
b
e
72hpf
I
dlx3
ot
olf
16 hpf
J
krox-20
r3
r5
24 hpf

Figure 9. Whole-mount *in situ* hybridization (WMISH) showing *prr12b* expression in zebrafish development. Diagrams (**A**) are adapted and modified from White *et al*., 2017[185]. Representative WMISH of *prr12b* expression in embryos/larvae at 6 hpf (**B** and **B'**), 16 hpf (**C** and **C'**), 24 hpf (**D**, **D'** and **E**), 48 hpf (**F**, **G** and **G'**), and 72 hpf (**H**). (**I**) *dlx3* expression at 16 hpf in olfactory and otic cells (indicated with arrows) and (**J**) showing *krox-20* labeling of rhombomeres 3 and 5 (indicated with arrows). **B-D'** and **H-J** are lateral views, **E**, **G** and **G'** are dorsal views, and **F** is a frontal view. The box in area **B'** shows staining in a sense strand control embryo. Scale bar is equal to 100 μm and images **C'**, **D'** and **G'** are digitally enlarged images. Image labeled acronyms; *b (brain), d (diencephalon), t (telencephalon), m (mesencephalon), r (rhombencephalon), e (eye), le (lens), y (yolk), ot (otic placode), olf (olfactory placode), r3 (rhombomere 3), and r5 (rhombomere 5).*

3.7 *prr12a* expression in male and female adult zebrafish tissues

Although the diffuse expression pattens of *prr12a* and *prr12b* would suggest a general role in zebrafish embryogenesis and early larval development (**Figure 6, 7, 8,** and **9**), their spatial expression patterns in adult tissues, heretofore not reported, and may provide insight into roles that are organ-specific. To address this question, tissues in male and female 8-month-old adult TU wildtype zebrafish were dissected; specifically, brain (telencephalon, mesencephalon, and rhombencephalon), eye, kidney, liver, testes and/or ovaries. Total RNA was isolated from these selected tissues and reverse transcribed to cDNA for qRT-PCR analysis using specific *prr12a* and *gapdh* primers analyzed through a one-way ANOVA. Results showed *prr12a* expression in males within all 7 selected tissues, and there was no statistical difference in the levels amongst these tissues (**Figure 10A**). In contrast, *prr12a* expression was significantly enriched in the ovary ($P<0.0001$; **Figure 10B**) compared to the other tissues in the female zebrafish. *prr12a* expression was elevated in female liver in comparison to the telencephalon, mesencephalon, and rhombencephalon, eye, and kidney, although these levels were not statistically significant (**Figure 10B**).

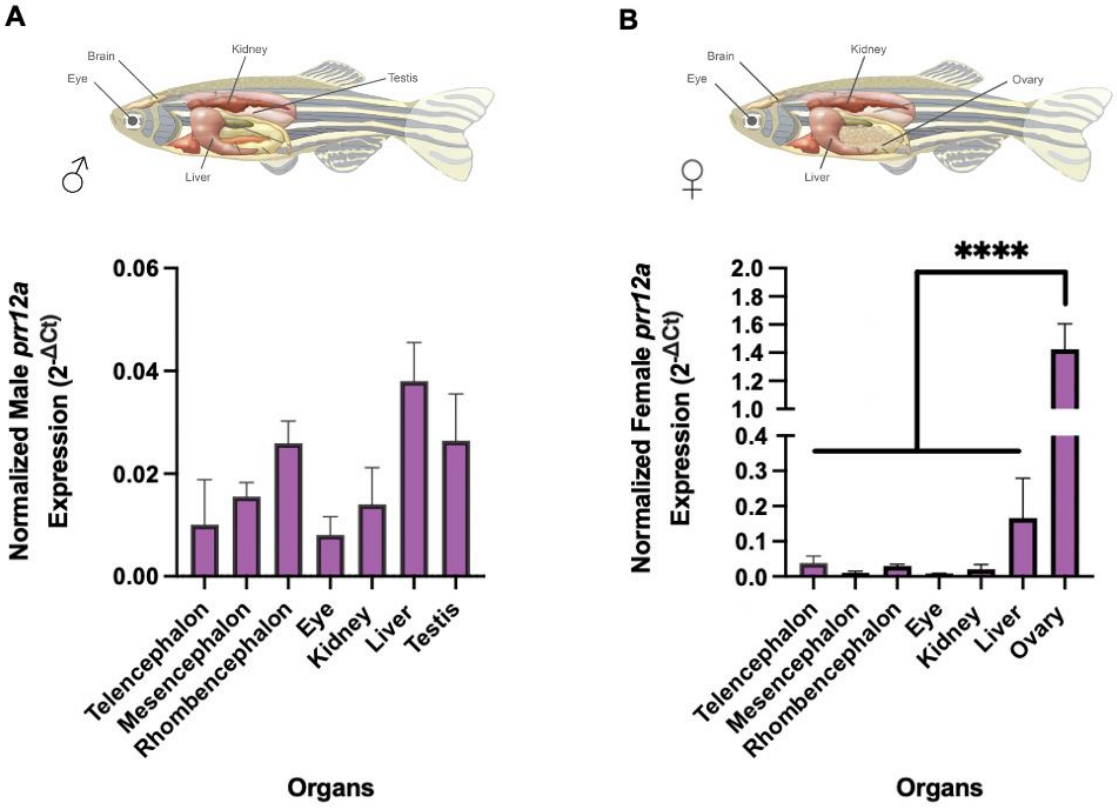

Figure 10. Tissue distribution of *prr12a* expression in male and female zebrafish. qRT-PCR analysis of *prr12a* expression in **A.** male and **B.** female zebrafish organ tissues. Expression of *prr12a* was normalized to *gapdh* according to the $2^{-\Delta Ct}$ method. Diagrams of male and female adult are adapted and modified from Santoriello and Zon, 2012[18] and Nguyen, 2015[204]. Bars represent mean $2^{-\Delta Ct}$ values ± S.E.M, N=3. Asterisks indicate significant difference (****$P<0.0001$) as tested by a one-way ANOVA followed by a Tukey test relative to the constitutively expressed *gapdh* gene.

3.8 *prr12b* expression in male and female adult zebrafish tissues

Since *prr12a* expression showed sex-specific enrichment in the ovary compared to other female tissues (**Figure 10B**) and given my hypothesis that the expression of the *prr12* paralogues would be overlapping, then *prr12b* should also show this enrichment pattern. To address this, the same dissected tissues used were examined using qRT-PCR with *prr12b* and *gapdh* primers and analyzed through a one-way ANOVA. In males, *prr12b* was detected in all tissues; however, low expression was seen in the kidney. Furthermore, *prr12b* showed significantly higher levels in the male mesencephalon compared to eye ($P<0.05$), kidney ($P<0.01$), and testis ($P<0.05$). Other regions, including the telencephalon and rhombencephalon, showed no statistical differences compared to other selected tissues (**Figure 11A**), would suggest a mesencephalon-specific role of *prr12b* in adult males. *prr12b* expression in female fish showed no significant difference between the selected tissues, which contradicted that seen with *prr12a*. Overall, female *prr12b* expression was more enriched in the brain, liver and ovary compared to eye and kidney (**Figure 11B**), but these apparent differences were not statistically significant.

Together, these data show that some sex-specific, tissue expression differences exist between the *prr12* paralogues in the adult zebrafish, and although these genes are expressed rather ubiquitously in all tissues, these noted differences may contribute to unique adult roles.

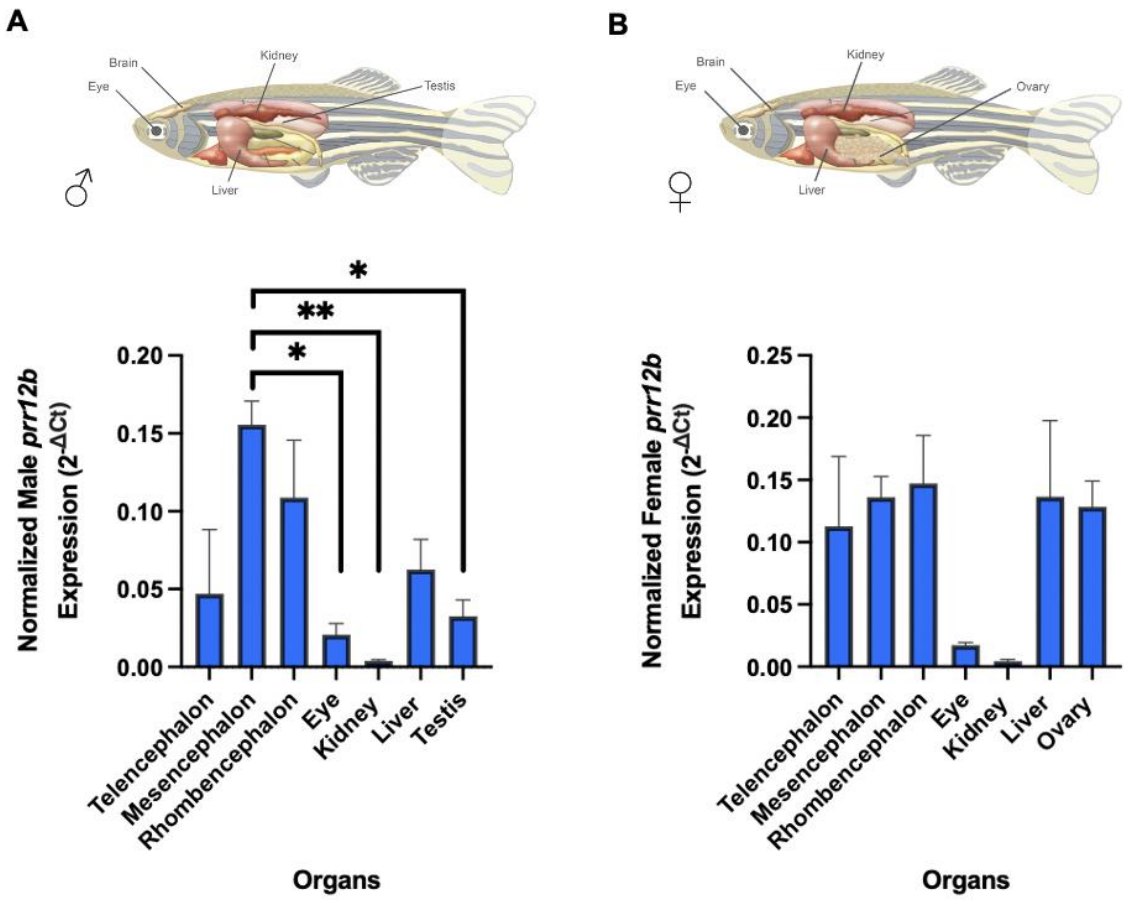

Figure 11. Tissue distribution of *prr12b* expression in male and female zebrafish. qRT-PCR analysis of *prr12b* expression in **A.** male and **B.** female zebrafish organ tissues. Expression of *prr12b* was normalized to *gapdh* according to the $2^{-\Delta Ct}$ method. Diagrams of male and female adult are adapted and modified from Santoriello and Zon, 2012[18] and Nguyen, 2015[204]. Bars represent mean $2^{-\Delta Ct}$ values ± S.E.M, N=3. Asterisks indicate significant difference (*$P<0.05$, **$P<0.01$) as tested by one-way ANOVA followed by a Tukey test relative to the constitutively expressed *gapdh* gene.

3.9 *prr12a* and *prr12b* expression in the brain and eye of male and female adult zebrafish

To further analyze the expression prolife of the *prr12* paralogues in adult zebrafish, I investigated if there were differences in individual tissues of the brain (telencephalon, mesencephalon, rhombencephalon) and eye, for *prr12a* and *prr12b* gene expression between the sexes, in the same adult zebrafish analyzed previously (**Figure 10** and **11**). qRT-PCR results analyzed with a two-way ANOVA of the telencephalon showed no significant differences exist in *prr12a* and *prr12b* expression between male and female fish (**Figure 12A**). *prr12b* expression, however, was significantly enriched in male and female mesencephalon compared to *prr12a* expression (**Figure 12B**). Similarly, *prr12b* expression, compared to *prr12a* expression, was significantly higher in the male and female rhombencephalon (**Figure 12C**) and eye (**Figure 12D**).

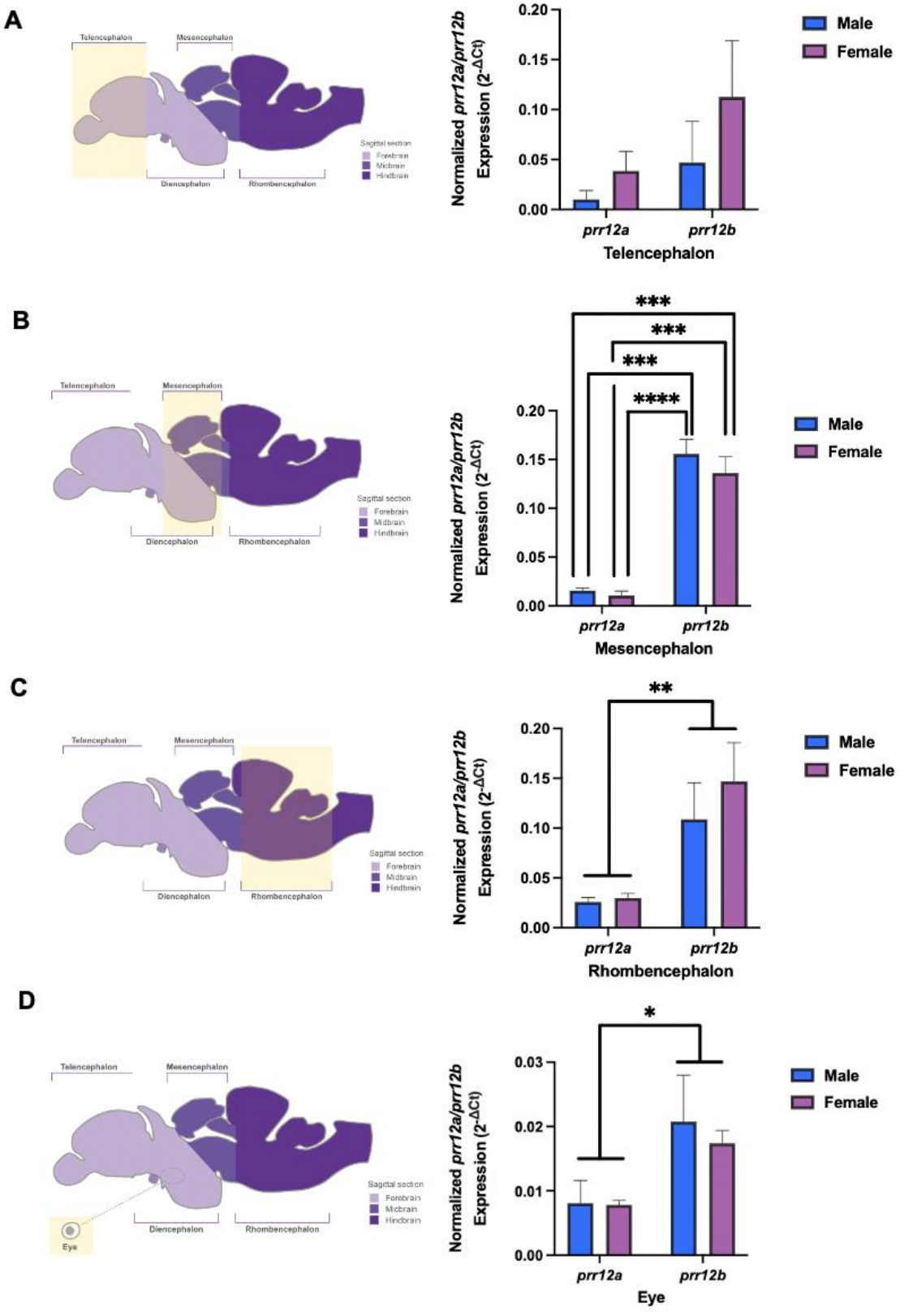
A
Telencephalon
Mesencephalon
Diencephalon
Rhombencephalon
Sagittal section
Forebrain
Midbrain
Hindbrain
Normalized prr12a/prr12b Expression (2-ΔCt)
0.20
0.15
0.10
0.05
0.00
prr12a
prr12b
Telencephalon
Male
Female
B
***
***
***
****
Mesencephalon
C
**
Rhombencephalon
D
*
Eye

Figure 12. Expression of *prr12a* and *prr12b* in the brain and eye of male and female adult zebrafish. qRT-PCR of *prr12a* and *prr12b* expression in the **A.** telencephalon, **B.** mesencephalon, **C.** rhombencephalon, and **D.** eye. Diagrams of sagittal adult zebrafish brain are adapted and modified from Vaz *et al*., 2019[120], with yellow highlighted regions indicating the tissue dissection region. Expression of *prr12a* and *prr12b* was normalized to *gapdh* according to the $2^{-\Delta Ct}$ method. Bars represent mean $2^{-\Delta Ct}$ values ± S.E.M, N=3. Asterisks indicate significant difference (**P*<0.05, ***P*<0.01, ****P*<0.001, *****P*<0.0001) as tested by two-way ANOVA followed by a Tukey test relative to the constitutively expressed *gapdh* gene.

Chapter 4

4 Discussion

4.1 Summary of findings

PRR12-related Neuroocular Syndrome is a rare autosomal dominant disorder (OMIM #619539) characterized by a spectrum of clinical phenotypes including developmental impairment, ocular defects, hypotonia, renal and cardiac anomalies, and growth delays[24–27]. This syndrome is thought to be caused by LOF variants in *PRR12* encoding for a protein of unknown function. The majority of *PRR12* pathogenic alleles are *de novo* frameshift and nonsense variants. These unique sequence variants predominantly affect exons 3-7, introducing a premature stop codon, where the mRNA is expected to undergo nonsense-mediated decay[25–27]. While the pathogenic mechanisms of disrupted *PRR12* have not been elucidated, its involvement in neural development have been reported, showing abundant *Prr12* mRNA/protein identified in embryonic mouse brain cells[24] and elevated *PRR12* mRNA in fetal brain structures[27,205]. However, no published studies have investigated the developmental role of *PRR12* in nonmammalian species. To address this, I characterized the *prr12* paralogues in the zebrafish and report on the temporal and tissue-specific expression profiles of these paralogues during selected embryonic, larval, and adult stages.

Zebrafish have two *PRR12* orthologues, *prr12a* and *prr12b*[32,127] and *PRR12* orthologues are also found in mammals, amphibians, fish, birds, and reptiles[32] (**Appendix 2**). Moreover, it has been reported that the coding regions of the long and short isoforms of *PRR12*[24], are conserved amongst vertebrates[25,33]. Despite the conservation, there are additional exonic regions in the *prr12* paralogues, likely due to evolutionary divergence in the coding regions[206]. Overall, *prr12a* and *prr12b* share 30% and 27% sequence identity with human *PRR12*, respectively (CLUSTALW)[201]. While there are overlapping similarities in exonic structure between these orthologues, the percent sequence identity is relatively low (**Figure 4**). Nevertheless, the analysis of the conserved protein functional domains between human PRR12 and zebrafish Prr12a and Prr12b were investigated (see below).

As *prr12a* and *prr12b* are currently genes of unknown function[32,127], identifying co-expressed genes might also provide insight into the biological function and/or the transcriptional regulatory programs involved with these targets. Co-expression analysis confirmed *prr12a* and *prr12b* are co-expressed, and genes that co-express with *prr12a* are linked to transcriptional regulation, including coiled coil, nuclear, zinc-finger, and bromodomain-containing proteins. Likewise, similar genes are co-expressed with *prr12b*, which mimics that for *PRR12* (COXPRESdb7.3; DAVID)[27,43–45]. Although the function of some of these proteins have been investigated in zebrafish transcriptional regulation[207,208], this co-expression with *prr12a* and *prr12b* intimates sharing similar biological functions with their human counterpart; suggesting that they are in fact orthologues. Therefore, similarities with co-expressed genes and the proteins they encode as reported by Chowdhury and colleagues[27], specifically bromodomain-containing[42], and zinc-finger containing proteins[209], lends further credence for commonalities between human *PRR12*[27] and the zebrafish paralogues. Ultimately, replacement/rescue studies where *prr12a* and *prr12b* are expressed in mammalian cells deficient in *PRR12* would provide insight as to whether they act in a functionally redundant manner.

RT-PCR was used to identify the temporal expression of the *prr12* paralogues in development (**Figure 7**). *prr12a* transcripts were present before the MBT, indicating that they are maternally expressed[22], while *prr12b* displayed weak expression before the MBT, there appeared to be an upregulation at select timepoints throughout embryogenesis and larval development, with amplicons detected later in development. Although the data was from endpoint PCR and not quantifiable, the apparent differences in fluorescent intensity of amplicons would indicate *prr12a* as being the dominant maternal paralogue. These analyses reveal insight into when these genes are required in development, but essentially, they are both expressed maternally and as transcripts are depleted, they are replaced after the MBT when the zygote activates its genome[108] and are required in the embryo and larvae. Therefore, the profile of the zebrafish *prr12* paralogues is similar to that of the mouse *Prr12* expression, which is relatively ubiquitous throughout embryonic development (E1 – E18) (MGI)[210].

A publicly available RNA-sequencing dataset exploring the transcriptomic profile of zebrafish embryos and larvae identified *prr12a* and *prr12b* as being differentially expressed (**Figure 6**)[185]. These results were encouraging with *prr12a* showing consistent expression throughout early stages, but an apparent upregulation of the gene at the 128-cell stage, during the blastula period before MBT[22], was not expected. Moreover, the RNA-sequencing results for *prr12b* revealed dynamic expression and increase throughout development with relatively consistent expression 48 hpf – 5 dpf; however, there was downregulation at 4 dpf in the RT-PCR results. Both differences in expression noted for *prr12a* and *prr12b* are likely due to differences in the techniques, with RNA-sequencing being much more sensitive and accurate than endpoint RT-PCR. Overall, both the RNA-sequencing and RT-PCR results reveal a similar expression profile and provide insight into when these genes are temporally regulated.

Determining the conservation of the amino acid sequences encoded by *PRR12/prr12* was of interest as it could add to the phylogenetic (functional) relationship(s) between zebrafish and human PRR12. I used comparative *in silico* protein sequence analysis, targeting the two AT-hook domains as this region in PRR12 was proposed as having DNA-binding activity and conferring gene regulation[24,25,27]. The AT-hook domains were highly conserved amongst zebrafish and human, 93% and 62%, respectively (**Figure 5**) (Clustal Omega)[200], suggesting that zebrafish Prr12a/12b may act functionally similar to PRR12 and allow these proteins to bind to DNA elements. It is, however, noteworthy that the total protein sequence identity between PRR12 and Prr12a is 28%, and 26% between PRR12 and Prr12b (CLUSTALW)[201]. Other zebrafish paralogues, including *bach1* (*bach1a* and *bach1b)* and *bach2 (bach2a* and *bach2b)*, have low amino acid sequence identity with some mammalian species, but they still maintain conserved functional domains[211]. Thus, and although not tested, given the presence of conserved AT-hook domains in zebrafish Prr12a and Prr12b, there is precedence for functional conservation. AT-hook domain regions are associated with high mobility group proteins[38] and interestingly, other AT-hook domain containing proteins such as MeCP2 (Methyl-CpG Binding Protein 2) and AHDC1 (AT-Hook DNA Binding Motif Containing Protein 1) are associated with neurological disorders[212,213]. Specifically, pathogenic variants of *MeCP2* disrupting the AT-hook domain regions, caused the most severe phenotypes within patients[214], with *mecp2*-null

zebrafish lines recapitulating similar behavioral phenotypes as seen in the patient population[215]. Moreover, *de novo* frameshift or nonsense *AHDC1* variants predicted to cause LOF are associated with intellectual disability and developmental delay[213], mirroring many of the genetic and clinical characteristics of the *PRR12*-related Neuroocular Syndrome[24–27]. In addition, a developmental transcriptome database containing varying human brain structures identified *AHDC1* as having the most similar expression profile to *PRR12* (BrainSpan atlas)[35]. Therefore, these findings would suggest that *PRR12* and *AHDC1* may be functionally related, and/or they participate in the same regulatory pathway. If so, investigation of the zebrafish *prr12* paralogues would provide further insight into the function of these pathways in vertebrate systems.

WMISH was used to investigate the spatial expression of *prr12a* and *prr12b* at selected timepoints in zebrafish development. Both *prr12a* and *prr12b* revealed similar expression profiles and thus, would indicate theses paralogues are not spatially distinct from each other in early development (**Figure 8** and **9**). Specifically, at 6 hpf and 16 hpf, *prr12a* and *prr12b* showed diffuse expression throughout the embryo proper, suggesting that these transcripts are needed in many tissues for various biological functions in early embryogenesis. Likewise, the patterns at 24 hpf and 48 hpf demonstrated diffuse signals, and no distinct expression boundaries of either transcript were detected in various neural tissue regions including the telencephalon, diencephalon, mesencephalon, and rhombencephalon. At 72 hpf both transcripts continued to be expressed, mainly showing expression in the eye and brain tissue regions, but this could be due to other reasons including tissue thickness and/or cell density. Publicly available single cell RNA sequencing data from the UCSC Cell Browser[128,216] highlights both transcripts being expressed in the CNS and further support for my *in situ* studies comes from *prr12a* and *prr12b* to being predominately identified within neurons at 24 hpf, 48 hpf, and 5 dpf zebrafish[216] (**Appendix 4**). It is interesting to note that my WMISH analysis of 48 hpf embryos showed diffuse expression throughout the brain, which is similar to the spatial expression mapping of *Prr12* in E11.5 mouse brain but with strong signal detected in the mesencephalon (MGI)[210]. Considering that these neural regions are common expression sites for these genes in embryonic mouse and zebrafish, they provide additional evidence for a role of *PRR12* in neural progenitor cell

proliferation and differentiation. Thus, it is tempting to speculate that these genes may encode proteins required for various biological functions in these tissues.

While my spatiotemporal analyses and the RNA-sequencing datasets allowed for further characterization of the *prr12* paralogues in zebrafish development, the expression of these genes in adult stages or their distribution in male versus female tissues has not been reported in many vertebrates. To address this, I used qRT-PCR to analyze *prr12a* and *prr12b* expression in zebrafish brain, eye and kidney, which were specifically selected due to their relevance in the *PRR12*-related NOC cohort[24–27]. Other zebrafish tissues, including the liver, ovaries, and testes, were also examined using this method. In male adults, analysis revealed *prr12a* was distributed in all selected tissues, and in females there was significant expression in the ovary (**Figure 10**). This enrichment in the ovary is consistent in other vertebrates, as evident in African clawed frog (Xenbase)[217] and mouse (MGI)[210]. Additionally, two human expression databases also show enriched *PRR12* expression in female reproductive tissues, including the ovary (GTEx; BioGPS)[34,218]. Therefore, the presence of *prr12a* in the ovary and its presence prior to MBT in zebrafish before it even appears would suggest that transcripts are deposited in primordial germ cells. In comparison, *prr12b* was detected in majority of the selected adult tissues, but significant expression was seen in the mesencephalon region of the adult male. In females while there appeared to be elevated *prr12b* levels in the selected brain tissues, no region showed significant expression (**Figure 11**). Prescence of *prr12b* in neural tissues of the adult zebrafish are consistent with mouse *Prr12* (MGI)[210] and human *PRR12* expression (GTEx; BioGPS)[34,218], and *prr12b* enrichment in the male mesencephalon may suggest a sex-specific role. That said, studies investigating gene expression in male and female zebrafish have identified sexually dimorphic patterns in the brain[219,220], but reports that male zebrafish have higher brain weights than females[221], may account for total transcript accumulation. Regardless, the consideration of sex is an important biological variable when investigating the *prr12* paralogues regarding brain function and regulation.

To further test if there were expression differences between *prr12a* and *prr12b* in male versus female, the same selected brain and eye tissues were analyzed through a two-way ANOVA. qRT-PCR analyses revealed *prr12b* expression in both male and female tissue

was significantly expressed in the mesencephalon, rhombencephalon, and eye in comparison to *prr12a* (**Figure 12**). Interestingly, the human mesencephalon, which structurally contains the tectum and tegmentum[222] is analogous to the zebrafish mesencephalon[120], and known to process auditory and visual information, in addition to regulating motor control[223]. It is interesting to speculate that lack of *PRR12* expression in the mesencephalon region may be relevant to the underlying phenotypes seen within the *PRR12*-related Neuroocular Syndrome cohort, such as motor and speech delay, and hearing loss[25–27]. In addition, a zebrafish co-expression database revealed that the top 50 genes co-expressed with *prr12b*, but not *prr12a,* were also enriched for central nervous system development and neuron cellular homeostasis (COXPRESdb7.3; DAVID)[43–45]. Taken together, these findings suggest that *prr12b* may have a neuronal-specific role in adulthood, alleviating *prr12a* from such function.

Overall, the findings from the developmental and tissue-specific analyses highlight that despite the fact the *prr12* paralogues present with overlapping expression profiles, *prr12a* seems to be predominately required in early development and is maternally expressed, potentially, a unique requirement for this paralogue. In comparison, while *prr12b* appears to be expressed in the latter stages of early development, it is enriched in certain adult CNS tissues, calling attention for its potential role in neural function and regulation.

4.2 Limitations and future directions

Little is known about the gene and/or protein of the mouse *Prr12* or human *PRR12* homologue and until now zebrafish *prr12a* and *prr12b* were relatively unexplored. This study sheds new light on the expression profile of the zebrafish paralogues in early development and adulthood, and the conservation in mammalian systems. Unfortunately, the *in vivo* role of *prr12a* and *prr12b* in development was not determined (see **Appendices 1**, **5** and **6**), and although numerous techniques were used to identify when and where the *prr12* paralogues are expressed, such approaches are not without limitation(s).

Firstly, the temporal analysis of these paralogues was performed using endpoint RT-PCR, and while an expression profile for each gene could be examined, the technique does not lend itself to detect quantitative differences amongst these targets. Therefore, the approach was to use qRT-PCR and focus on specific tissues in the adult zebrafish. Secondly, *in situ* hybridization was able to detect the expression of these genes in a morphological context; however, background noise was detected using the sense probes. In fact, non-specific probe detection with chromogenic enzyme reactions can produce false-positive results[187]. Therefore, in subsequent studies it would be ideal to synthesize and assay additional sets of *prr12a* and *prr12b* antisense and sense riboprobes to confirm my results. It is, however, important to recognize that since there are no published *in situ* hybridization assays from developing zebrafish embryo and/or larval stages, the WMISH technique and the background noted above, may not be sensitive to detect low RNA levels of these targets[224]. One approach would be to use a method employing *in situ* hybridization chain reaction, which allows for mapping of multiple target mRNAs, simultaneously within a whole-mount embryo, using an enzyme-free approach[225]. In comparison to the enzyme-based *in situ* method, such an approach can reduce the amount of nonspecific signal, time and labor required when detecting RNAs. Lastly, histological sectioning and staining with hematoxylin and eosin would further accurately validate the localization of the *prr12a* and *prr12b* transcripts and potentially reveal distinct cellular signals within specific embryonic tissues.

One additional limitation recognized in this study relates to sample size, specifically N=1, ~30 pooled embryos/larvae per timepoint (**Figure 7**) and N=3, for each individual organ/tissue per male and female zebrafish (**Figure 10**, **11**, and **12**). Regarding the latter, although I reported the overall trend for some tissue targets, due to variation, an increase in sample size would improve the statistical power. Moreover, adding to the current data with that from other targets including, heart, intestine, and muscle would help to further delineate the spatial relevance of the *prr12* paralogues. Despite these shortfalls, the reported data is relevant and more importantly, serves as reference for future transcriptomic analyses.

With the novelty of *PRR12* and the related occurrence of the *PRR12*-related Neuroocular Syndrome, little has been reported on the molecular consequences of its LOF[24–27]. Zebrafish mutant line(s) targeting the *prr12* paralogues would likely have contributed evidence into the pathogenesis of this disease, and ultimately would have been the platform to model the *PRR12*-related Neuroocular Syndrome. I had designed and synthesized sgRNAs to knockout *prr12a*, *prr12b* and *prr12a/prr12b* (**Appendix 5**) at the one-cell stage in WT TU zebrafish embryos. After preliminary experiments, I had demonstrated the feasibility of *prr12a*-specifc guides and CRISPR-Cas9, as a means to genetically edit exon 2 of *prr12a.* sgRNAs were microinjected into embryos, and the knockout efficiency of *prr12a* was confirmed by Sanger sequencing and TIDE analysis[226]. Simultaneously, sgRNA and Cas9 mRNA efficiency was assessed by targeting the tyrosinase (*tyr*) gene (Ensembl, ENSDARG00000039077), and creating zebrafish *tyr* mutants. Specifically, these mutants were used as a technical control, as lack of pigmentation was the confirmatory phenotype (**Appendix 6**). Unfortunately, due to a suspected bacterial outbreak, all mutant and wildtype zebrafish were culled according to Animal Care Committee at Western University (AUP #2019-149; **Appendix 1**). In future, the use of these already synthesized sgRNAs (*prr12a* and *prr12b*), and Cas9 mRNA will resume and *prr12* functional knockout studies will be considered. Although high-fidelity Cas9 enzymes have been since reported[227], it would be prudent to design another set of guides intended to induce mutations in the AT-hook domains and/or for other identified domains such as the domain of unknown function (DUF4211)[24], which also shows conservation

with the DUF4211 in human PRR12 (**Appendix 3**). Gross morphological examination of *prr12* mutants was not performed because of the cull, but this and histological staining would have provided invaluable information, possibly modelling the clinical characteristics seen within the *PRR12*-related Neuroocular Syndrome cohort.

Although it may have been difficult to determine if the knockout of *prr12a* and/or *prr12b* showed obvious morphological defects, subtle behavioural changes may have provided evidence for the role of these genes in development. Within the clinical cohort, ~97% of individuals present with developmental and/or intellectual deficits[24–27]. To detect behavioural changes in larvae zebrafish, would require tracking and analysis of individual fish using DanioVision and accompanying software[228], which assesses stimuli response and swimming behaviour[120]. With respect to adult zebrafish, specific assays also test social interactions (*e.g.*, shoaling tests) analyzing sociability, anxiety, and fear[120]; analogous to ADHD and autism, observed in individuals with *PRR12* pathogenic variants[25–27]. Moreover, overall growth and size of *prr12* mutants would also have been amenable to this tracking system, as short stature and failure to thrive are additional clinical features seen amongst individuals with pathogenic *PRR12* variants[25–27]. Unfortunately, although this data was not collected, it would have contributed to our understanding of *PRR12* in humans.

Another issue that needs to be addressed relates to the rescue of mutant phenotypes, which has been successfully demonstrated in *ptk7*[229] and *kars1*[230] established zebrafish mutant lines. One caveat is expressing wildtype *prr12a* and *prr12b,* which based on the size of the coding sequence (~9 kb), not to mention the vector backbone would be technically difficult to construct and clone. Alternative strategies such as introduction of a bacterial artificial chromosome could be implemented[231], and have been proven successful in zebrafish[232,233]. Nonetheless, technical problems are associated with this project, and were recognized from the beginning. Despite these shortfalls, we have learned a great deal about the spatiotemporal expression profiles of *prr12a* and *prr12b* in zebrafish development and such limitations in the short term can be revisited.

4.3 Conclusion

This thesis aimed to characterize the spatiotemporal expression profiles of the two zebrafish orthologues of human *PRR12*. Zebrafish *prr12a* and *prr12b* are diffusely expressed in the developing embryo, with *prr12a* appearing to be the predominant maternal transcript expressed, but also expressed later in development and in larval stages and adult. In contrast, *prr12b* was weakly expressed maternally, and there were apparent increases and decreases in its embryonic expression profile. In comparison to *prr12a*, adult males had enriched *prr12b* expression in the mesencephalon and transcripts were upregulated in certain CNS tissues in comparison to *prr12a*. Expression of the *prr12* paralogues recapitulated a similar spatiotemporal expression profile seen in human *PRR12*, which had been predicted. Moreover, the data showed *prr12a* may be required for oocyte development and early processes, whereas *prr12b* is needed later, having a more neuronal-specific role. Therefore, although *prr12a* and *prr12b* may have different biological functions later in zebrafish development, the presence of each transcript prior to germ layer formation, before the presence of specific tissues/organs, indicate they are in the same cells and possibly functioning to regulate gene expression. Further studies, however, are required to definitively state if these paralogues are phenocopying human *PRR12* expression and more specifically, if the proteins they encode are acting in a functionally similar role. Experiments to create the *prr12*$^{-/-}$ zebrafish mutant lines have been initiated and together, with what we have learned from this study, will help establish the zebrafish as a model of this human rare disorder.

References

1. Boycott KM, Rath A, Chong JX, *et al*. International cooperation to enable the diagnosis of all rare genetic diseases. *Am J Hum Genet*. 2017;100(5):695-705. doi:10.1016/J.AJHG.2017.04.003

2. Canadian Organization for Rare Disorders (CORD). Our work, Canadian organization for rare disorders. Published 2021. Accessed November 26, 2021. https://www.raredisorders.ca/our-work/

3. Amberger J, Bocchini CA, Scott AF, Hamosh A. McKusick's online mendelian inheritance in man (OMIM). *Nucleic Acids Res*. 2009;37(Database issue):D793-D796. doi:10.1093/NAR/GKN665

4. Amberger JS, Bocchini CA, Schiettecatte F, Scott AF, Hamosh A. OMIM.org: online mendelian inheritance in man (OMIM®), an online catalog of human genes and genetic disorders. *Nucleic Acids Res*. 2015;43(Database issue):D789-D798. doi:10.1093/NAR/GKU1205

5. Wright CF, FitzPatrick DR, Firth H V. Paediatric genomics: diagnosing rare disease in children. *Nat Publ Gr*. 2018;19:253-268. doi:10.1038/nrg.2017.116

6. Michaels-Igbokwe C, McInnes B, MacDonald K V., *et al.* (Un)standardized testing: the diagnostic odyssey of children with rare genetic disorders in Alberta, Canada. *Genet Med*. 2020;23(2):272-279. doi:10.1038/s41436-020-00975-0

7. Global Genes. RARE facts. Published 2021. Accessed September 16, 2021. https://globalgenes.org/rare-facts/

8. Blöß S, Klemann C, Rother A-K, *et al*. Diagnostic needs for rare diseases and shared prediagnostic phenomena: results of a German-wide expert delphi survey. *PLoS One*. 2017;12(2):e0172532. doi:10.1371/JOURNAL.PONE.0172532

9. Shashi V, McConkie-Rosell A, Rosell B, *et al.* The utility of the traditional medical genetics diagnostic evaluation in the context of next-generation sequencing for

undiagnosed genetic disorders. 2013;16:176-182. doi:10.1038/gim.2013.99

10. Chae JH, Vasta V, Cho A, *et al*. Utility of next generation sequencing in genetic diagnosis of early onset neuromuscular disorders. *J Med Genet*. 2015;52(3):208-216. doi:10.1136/JMEDGENET-2014-102819

11. Kingsmore SF, Dinwiddie DL, Miller NA, Soden SE, Saunders CJ, Team* for the CMGM. Adopting orphans: comprehensive genetic testing of mendelian diseases of childhood by next-generation sequencing. *Expert Rev Mol Diagn*. 2014;11(8):855-868. doi:10.1586/ERM.11.70

12. Kaufmann P, Pariser AR, Austin C. From scientific discovery to treatments for rare diseases - the view from the national center for advancing translational sciences - office of rare diseases research. *Orphanet J Rare Dis*. 2018;13(1):196. doi:10.1186/s13023-018-0936-x

13. Lee CE, Singleton KS, Wallin M, Faundez V. Rare genetic diseases: nature's experiments on human development. *iScience*. 2020;23(5):101123. doi:10.1016/j.isci.2020.101123

14. Limb L, Nutt S, Sen A. Experiences of rare diseases: an insight from patients and families. Rare Disease, UK. Published 2010. Accessed April 25, 2021. www.raredisease.org.uk

15. Uhlenbusch N, Löwe B, Depping MK. Perceived burden in dealing with different rare diseases: a qualitative focus group study. *BMJ Open*. 2019;9(12):e033353. doi:10.1136/BMJOPEN-2019-033353

16. Adamson KI, Sheridan E, Grierson AJ, Neuroscience T, Andrew D, Grierson J. Use of zebrafish models to investigate rare human disease. *J Med Genet*. 2018;55(1):641-649. doi:10.1136/jmedgenet-2018-105358

17. Veldman MB, Lin S. Zebrafish as a developmental model organism for pediatric research. *Pediatr Res*. 2008;64(5):470-476. doi:10.1203/PDR.0b013e318186e609

18. Santoriello C, Zon LI. Hooked! modeling human disease in zebrafish. *J Clin Invest*. 2012;122(7):2337-2343. doi:10.1172/JCI60434

19. Patton EE, Zon LI, Langenau DM. Zebrafish disease models in drug discovery: from preclinical modelling to clinical trials. *Nat Rev Drug Discov*. 2021;20(8):611-628. doi:10.1038/s41573-021-00210-8

20. Dang M, Henderson RE, Garraway LA, Zon LI. Long-term drug administration in the adult zebrafish using oral gavage for cancer preclinical studies. *Dis Model Mech*. 2016;9(7):811-820. doi:10.1242/DMM.024166

21. Cornet C, Di Donato V, Terriente J. Combining zebrafish and CRISPR/Cas9: toward a rore efficient rrug discovery pipeline. *Front Pharmacol*. 2018;(9):703. doi:10.3389/FPHAR.2018.00703

22. Kimmel CB, Ballard WW, Kimmel SR, Ullmann B, Schilling TF. Stages of embryonic development of the zebrafish. *Dev Dyn*. 1995;203(3):253-310. doi:10.1002/AJA.1002030302

23. Avey MT, Fenwick N, Griffin G. The use of systematic reviews and reporting guidelines to advance the implementation of the 3Rs. *J Am Assoc Lab Anim Sci*. 2015;54(2):153-162. doi:/pmc/articles/PMC4382619/

24. Córdova-Fletes C, Domínguez MG, Delint-Ramirez I, *et al*. A de novo t(10;19)(q22.3;q13.33) leads to ZMIZ1/PRR12 reciprocal fusion transcripts in a girl with intellectual disability and neuropsychiatric alterations. *Neurogenetics*. 2015;16(4):287-298. doi:10.1007/s10048-015-0452-2

25. Leduc MS, Mcguire M, Madan-Khetarpal S, *et al*. De novo apparent loss-of-function mutations in PRR12 in three patients with intellectual disability and iris abnormalities. *Hum Genet*. 2018;137(3):257-264. doi:10.1007/s00439-018-1877-0

26. Reis LM, Costakos D, Wheeler PG, *et al.* Dominant variants in PRR12 result in unilateral or bilateral complex microphthalmia. *Clin Genet*. 2020;99(3):437-442. doi:10.1111/cge.13897

27. Chowdhury F, Wang L, Al-Raqad M, *et al*. Haploinsufficiency of PRR12 causes a spectrum of neurodevelopmental, eye, and multisystem abnormalities. *Genet Med*. 2021;23:1234-1245. doi:10.1038/s41436-021-01129-6

28. Verma AS, FitzPatrick DR. Anophthalmia and microphthalmia. *Orphanet J Rare Dis*. 2007;2:47. doi:10.1186/1750-1172-2-47

29. NORD (National Organization for Rare Disorders). Williams syndrome. Accessed September 13, 2021. https://rarediseases.org/rare-diseases/williams-syndrome/

30. Gregory-Evans CY, Williams MJ, Halford S, Gregory-Evans K. Ocular coloboma: a reassessment in the age of molecular neuroscience. *J Med Genet*. 2004;41(12):881-891. doi:10.1136/JMG.2004.025494

31. Gunton KB, Wasserman BN, Debenedictis C. Strabismus. *Prim Care Clin Off Pract*. 2015;42(3):393-407. doi:10.1016/j.pop.2015.05.006

32. Howe KL, Achuthan P, Allen J, *et al*. Ensembl 2021. *Nucleic Acids Res*. 2021;49(D1):D884-D891. doi:10.1093/NAR/GKAA942

33. SOPHiA GENETICS. Alamut Visual Plus. Accessed September 18, 2021. https://www.interactive-biosoftware.com/

34. Carithers LJ, Ardlie K, Barcus M, *et al*. A novel approach to high-quality postmortem tissue procurement: the GTEx project. *Biopreserv Biobank*. 2015;13(5):311-319. doi:10.1089/BIO.2015.0032

35. Miller JA, Ding SL, Sunkin SM, *et al*. Transcriptional landscape of the prenatal human brain. *Nature*. 2014;508(7495):199-206. doi:10.1038/nature13185

36. Fishilevich S, Nudel R, Rappaport N, *et al*. GeneHancer: genome-wide integration of enhancers and target genes in GeneCards. *Database J Biol Databases Curation*. 2017:bax028. doi:10.1093/DATABASE/BAX028

37. Harikumar A, Meshorer E. Chromatin remodeling and bivalent histone

modifications in embryonic stem cells. *EMBO Rep*. 2015;16(12):1609-1619. doi:10.15252/EMBR.201541011

38. Aravind L, Landsman D. AT-hook motifs identified in a wide variety of DNA-binding proteins. *Nucleic Acids Res*. 1998;26(19):4413-4421. doi:10.1093/NAR/26.19.4413

39. Reeves R. Molecular biology of HMGA proteins: hubs of nuclear function. *Gene*. 2001;277(1-2):63-81. doi:10.1016/S0378-1119(01)00689-8

40. Consortium TU, Bateman A, Martin M-J, *et al.* UniProt: the universal protein knowledgebase in 2021. *Nucleic Acids Res*. 2021;49(D1):D480-D489. doi:10.1093/NAR/GKAA1100

41. Choudhary C, Kumar C, Gnad F, *et al*. Lysine acetylation targets protein complexes and co-regulates major cellular functions. *Science*. 2009;325(5942):834-840. doi:10.1126/science.1175371

42. Josling GA, Selvarajah SA, Petter M, Duffy MF. The role of bromodomain proteins in regulating gene expression. *Genes (Basel)*. 2012;3(2):320-343. doi:10.3390/GENES3020320

43. Obayashi T, Kagaya Y, Aoki Y, Tadaka S, Kinoshita K. COXPRESdb v7: a gene coexpression database for 11 animal species supported by 23 coexpression platforms for technical evaluation and evolutionary inference. *Nucleic Acids Res*. 2019;47(D1):D55-D62. doi:10.1093/NAR/GKY1155

44. Huang DW, Sherman BT, Lempicki RA. Systematic and integrative analysis of large gene lists using DAVID bioinformatics resources. *Nat Protoc*. 2009;4(1):44-57. doi:10.1038/NPROT.2008.211

45. Huang DW, Sherman BT, Lempicki RA. Bioinformatics enrichment tools: paths toward the comprehensive functional analysis of large gene lists. *Nucleic Acids Res*. 2009;37(1):1-13. doi:10.1093/NAR/GKN923

46. Yuhang M, Gang S, Zuopeng S, Jiarui D, Fulin X, Yong Y. RAD21 inhibited transcription of tumor suppressor MIR4697HG and led to glioma tumorigenesis. *Biomed Pharmacother*. 2020;123:109759. doi:10.1016/J.BIOPHA.2019.109759

47. Online Mendelian Inheritance in Man, OMIM®. McKusick-Nathans Institute of Genetic Medicine, Johns Hopkins University (Baltimore, MD). Published 2021. https://omim.org/

48. Amberger JS, Hamosh A. Searching online mendelian inheritance in man (OMIM): a knowledgebase of human genes and genetic phenotypes. *Curr Protoc Bioinforma*. 2017;2017:1.2.1-1.2.12. doi:10.1002/cpbi.27

49. Boycott KM, Vanstone MR, Bulman DE, MacKenzie AE. Rare-disease genetics in the era of next-generation sequencing: discovery to translation. *Nat Rev Genet*. 2013;14(10):681-691. doi:10.1038/nrg3555

50. Hall MN. mTOR-what does it do? *Transplant Proc*. 2008;40:S5-S8. doi:10.1016/j.transproceed.2008.10.009

51. Woo S-Y, Kim D-H, Jun C-B, *et al*. PRR5, a novel component of mTOR complex 2, regulates platelet-derived growth factor receptor β expression and signaling. *J Biol Chem*. 2007;282(35):25604-25612. doi:10.1074/JBC.M704343200

52. Johnstone CN, Castellví-Bel S, Chang LM, *et al*. PRR5 encodes a conserved proline-rich protein predominant in kidney: analysis of genomic organization, expression, and mutation status in breast and colorectal carcinomas. *Genomics*. 2005;85(3):338-351. doi:10.1016/J.YGENO.2004.11.002

53. Krieger KL, Hu W-F, Ripperger T, Woods NT. Functional impacts of the BRCA1-mTORC2 interaction in breast cancer. *Int J Mol Sci Artic*. 2019;20(23):5876. doi:10.3390/ijms20235876

54. Cheng S, Xie W, Miao Y, *et al*. Identification of key genes in invasive clinically non-functioning pituitary adenoma by integrating analysis of DNA methylation and mRNA expression profiles. *J Transl Med*. 2019;17:407. doi:10.1186/s12967-019-

02148-3

55. Niu T, Liu N, Zhao M, *et al*. Identification of a novel FGFRL1 microRNA target site polymorphism for bone mineral density in meta-analyses of genome-wide association studies consortium for healthy gging (NCHA). *Hum Mol Genet*. 2015;24(16):4710-4727. doi:10.1093/hmg/ddv144

56. Mao Q, Zhang P-H, Yang J, *et al.* iTRAQ-based proteomic analysis of ginsenoside F 2 on human gastric carcinoma cells SGC7901. *Evidence-based Complement Altern Med*. 2016; 2016:2635483. doi:10.1155/2016/2635483

57. Martin J, Masri J, Bernath A, Nishimura RN, Gera J. Hsp70 associates with rictor and is required for mTORC2 formation and activity. *Biochem Biophys Res Commun*. 2008;372(4):578-583. doi:10.1016/j.bbrc.2008.05.086

58. Kravchick DO, Karpova A, Hrdinka M, *et al*. Synaptonuclear messenger PRR7 inhibits c-Jun ubiquitination and regulates NMDA -mediated excitotoxicity. *EMBO J*. 2016;35(17):1923-1934. doi:10.15252/EMBJ.201593070/FORMAT/PDF

59. Murata Y, Doi T, Taniguchi H, Fujiyoshi Y. Proteomic analysis revealed a novel synaptic proline-rich membrane protein (PRR7) associated with PSD-95 and NMDA receptor. *Biochem Biophys Res Commun*. 2005;327:183-191. doi:10.1016/j.bbrc.2004.11.154

60. Lee SH, Shin SM, Zhong P, *et al*. Reciprocal control of excitatory synapse numbers by Wnt and Wnt inhibitor PRR7 secreted on exosomes. *Nat Commun*. 2018;9(1):3434. doi:10.1038/s41467-018-05858-2

61. Hrdinka M, Dráber P, Štěpánek O, *et al*. PRR7 is a transmembrane adaptor protein expressed in activated T cells involved in regulation of T Cell receptor signaling and apoptosis. *J Biol Chem*. 2011;286(22):19617-19629. doi:10.1074/JBC.M110.175117

62. Stepanek O, Draber P, Horejsi V. Palmitoylated transmembrane adaptor proteins in leukocyte signaling. *Cell Signal*. 2014;26(5):895-902.

doi:10.1016/J.CELLSIG.2014.01.007

63. Hu H, Song Z, Yao Q, *et al*. Proline-Rich protein 11 regulates self-renewal and tumorigenicity of gastric cancer stem cells. *Cell Physiol Biochem*. 2018;47(4):1721-1728. doi:10.1159/000491005

64. Ji Y, Xie M, Lan H, *et al*. PRR11 is a novel gene implicated in cell cycle progression and lung cancer. *Int J Biochem Cell Biol*. 2013;45(3):645-656. doi:10.1016/J.BIOCEL.2012.12.002

65. Ni R, Huang Y, Wang J, Liu Y. Knockdown of lncRNA DLX6-AS1 inhibits cell proliferation, migration and invasion while promotes apoptosis by downregulating PRR11 expression and upregulating miR-144 in non-small cell lung cancer. *Biomed Pharmacother*. 2019;109:1851-1859. doi:10.1016/J.BIOPHA.2018.09.151

66. Zhan Y, Wu X, Zheng G, *et al*. Proline-rich protein 11 overexpression is associated with a more aggressive phenotype and poor overall survival in ovarian cancer patients. *World J Surg Oncol*. 2020;18(1):318. doi:10.1186/S12957-020-02077-2

67. Wang C, Yu L, Hu F, *et al.* Upregulation of proline rich 11 is an independent unfavorable prognostic factor for survival of tongue squamous cell carcinoma patients. *Oncol Lett*. 2017;14(4):4527. doi:10.3892/OL.2017.6780

68. Wang C, Yu L, Ren X, *et al.* The oncogenic potential of PRR11 gene in tongue squamous cell carcinoma cells. *J Cancer*. 2019;10(11):2541. doi:10.7150/JCA.29265

69. Chen J, Kang C-Y, Niu Z-X, Zhou H-C, Yang H-M. A chalcone inhibits the growth and metastasis of KYSE-4 esophageal cancer cells. *J Int Med Res*. 2020;48(6):300060520928831. doi:10.1177/0300060520928831

70. Li J, Sun P, Yue Z, Zhang D, You K, Wang J. miR-144-3p induces cell cycle arrest and apoptosis in pancreatic cancer cells by targeting proline-rich protein 11 expression via the mitogen-activated protein kinase signaling pathway. *DNA Cell Biol*. 2017;36(8):619-626. doi:10.1089/DNA.2017.3656

71. Wang Y, Weng H, Zhang Y, *et al.* The PRR11-SKA2 bidirectional transcription unit is negatively regulated by p53 through NF-Y in lung cancer cells. *Int J Mol Sci*. 2017;18(3):534. doi:10.3390/IJMS18030534

72. Zhao Q. RNAi-mediated silencing of praline-rich gene causes growth reduction in human lung cancer cells. *Int J Clin Exp Pathol*. 2015;8(2):1760-1767. /pmc/articles/PMC4396257/

73. Qiao W, Wang H, Zhang X, Luo K. Proline-rich protein 11 silencing inhibits hepatocellular carcinoma growth and epithelial-mesenchymal transition through β-catenin signaling. *Gene*. 2019;681:7-14. doi:10.1016/J.GENE.2018.09.036

74. Larance M, Ahmad Y, Kirkwood KJ, Ly T, Lamond AI. Global subcellular characterization of protein degradation using quantitative proteomics. *Mol Cell Proteomics*. 2013;12(3):638-650. doi:10.1074/MCP.M112.024547

75. Siegel RL, Miller KD, Jemal A. Cancer statistics, 2018. *CA Cancer J Clin*. 2018;68(1):7-30. doi:10.3322/CAAC.21442

76. Zhu J, Hu H, Wang J, Yang Y, Yi P. PRR11 overexpression facilitates ovarian carcinoma cell proliferation, migration, and invasion through activation of the PI3K/AKT/β-catenin pathway. *Cell Physiol Biochem*. 2018;49(2):696-705. doi:10.1159/000493034

77. Zhang L, Lei Y, Zhang Y, *et al*. Silencing of PRR11 suppresses cell proliferation and induces autophagy in NSCLC cells. *Genes Dis*. 2018;5(2):158. doi:10.1016/J.GENDIS.2017.12.003

78. Song Z, Liu W, Xiao Y, *et al.* PRR11 is a prognostic marker and potential oncogene in patients with gastric cancer. *PLos One.* 2015;10(8):e0128943 doi:10.1371/journal.pone.0128943

79. Wang Y, Zhang C, Mai L, Niu Y, Wang Y, Bu Y. PRR11 and SKA2 gene pair is overexpressed and regulated by p53 in breast cancer. *BMB Rep*. 2019;52(2):157-162. doi:10.5483/BMBREP.2019.52.2.207

80. Chen Y, Cha Z, Fang W, *et al.* The prognostic potential and oncogenic effects of PRR11 expression in hilar cholangiocarcinoma. *Oncotarget*. 2015;6(24):20419. doi:10.18632/ONCOTARGET.3983

81. Luo H, Li J, Lin Q, *et al.* Ultrasonic irradiation and sonovue microbubbles-mediated RNA interference targeting PRR11 inhibits breast cancer cells proliferation and metastasis, but promotes apoptosis. *Biosci Rep*. 2020;40(11). doi:10.1042/BSR20201854

82. Nenasheva V V., Kovaleva G V., Khaidarova N V., *et al.* Trim14 overexpression causes the same transcriptional changes in mouse embryonic stem cells and human HEK293 cells. *Vitr Cell Dev Biol*. 2013;50(2):121-128. doi:10.1007/S11626-013-9683-4

83. Hamanaka S, Nakagawa T, Hiwasa T, *et al.* Investigation of novel biomarkers for predicting the clinical course in patients with ulcerative colitis. *J Gastroenterol Hepatol*. 2018;33(12):1975-1983. doi:10.1111/JGH.14297

84. Zhao D, Zhang W, Li X, *et al.* The mRNA expression of BRCA1, ERCC1, TUBB3, PRR13 genes and their relationship with clinical chemosensitivity in primary epithelial ovarian cancer. *Chinese J Oncol*. 2012;34(3):196-200. doi:10.3760/CMA.J.ISSN.0253-3766.2012.03.008

85. Poleshko A, Mansfield KM, Burlingame CC, Andrake MD, Shah NR, Katz RA. The human protein PRR14 tethers heterochromatin to the nuclear lamina during interphase and mitotic exit. *Cell Rep*. 2013;5(2):292-301. doi:10.1016/J.CELREP.2013.09.024

86. Ren X, Long M, Li Z, *et al.* Oncogene PRR14 promotes breast cancer through activation of PI3K signal pathway and inhibition of CHEK2 pathway. *Cell Death Dis*. 2020;11(6):464. doi:10.1038/S41419-020-2640-8

87. Li F, Zhang C, Fu L. PRR14 overexpression promotes cell growth, epithelial to mesenchymal transition and metastasis of colon cancer via the AKT pathway. *PLoS*

One. 2019;14(10):e0218839. doi:10.1371/JOURNAL.PONE.0218839

88. Poleshko A, Katz RA. Specifying peripheral heterochromatin during nuclear lamina reassembly. *Nucleus*. 2014;5(1):32-39. doi:10.4161/NUCL.28167

89. Yang M, Yuan Z-M. A novel role of PRR14 in the regulation of skeletal myogenesis. *Cell Death Dis 2015 64*. 2015;6(4):e1734-e1734. doi:10.1038/cddis.2015.103

90. Xiao S, Yang M. Discovery of a novel target for cancer: PRR14. *Cell Death Dis*. 2016;7(12):e2502. doi:10.1038/CDDIS.2016.401

91. Dunlevy KL, Medvedeva V, Wilson JE, *et al.* The PRR14 heterochromatin tether encodes modular domains that mediate and regulate nuclear lamina targeting. *J Cell Sci*. 2020;133(10):jcs240416. doi:10.1242/JCS.240416

92. Bai K, He S, Shu L, *et al.* Identification of cancer stem cell characteristics in liver hepatocellular carcinoma by WGCNA analysis of transcriptome stemness index. *Cancer Med*. 2020;9(12):4290. doi:10.1002/CAM4.3047

93. Yamamoto K, Gandin V, Sasaki M, *et al.* Largen: a molecular regulator of mammalian cell size control. *Mol Cell*. 2014;53(6):904-915. doi:10.1016/J.MOLCEL.2014.02.028

94. Liu X, Chen Q, Tsai H-J, *et al*. Maternal preconception body mass index and offspring cord blood DNA methylation: exploration of early life origins of disease. *Environ Mol Mutagen*. 2014;55(3):223-230. doi:10.1002/EM.21827

95. Snezhkina A, Lukyanova E, Fedorova M, *et al*. Novel genes associated with the development of carotid paragangliomas. *Mol Biol*. 2019;53(4):547-559. doi:10.1134/S0026893319040137

96. Williamson MP. The structure and function of proline-rich regions in proteins. *Biochem J*. 1994;297 (Pt 2)(Pt 2):249-260. doi:10.1042/BJ2970249

97. Zebrafish show their stripes. *Lab Anim (NY)*. 2012;41(9):247.

doi:10.1038/laban0912-247

98. Engeszer RE, Patterson LB, Rao AA, Parichy DM. Zebrafish in the wild: a review of natural history and new notes from the field. *Zebrafish*. 2007;4(1):21-40. doi:10.1089/zeb.2006.9997

99. Spence R, Gerlach G, Lawrence C, Smith C. The behaviour and ecology of the zebrafish, *Danio rerio*. *Biol Rev*. 2008;83(1):13-34. doi:10.1111/J.1469-185X.2007.00030.X

100. Arunachalam M, Raja M, Vijayakumar C, Malaiammal P, Mayden RL. Natural history of zebrafish (*Danio rerio*) in India. *Zebrafish*. 2013;10(1):1-14. doi:10.1089/ZEB.2012.0803

101. Facciol A, Gerlai R. Zebrafish shoaling, its behavioral and neurobiological mechanisms, and Its alteration by embryonic alcohol exposure: a review. *Front Behav Neurosci*. 2020;14:572175. doi:10.3389/FNBEH.2020.572175

102. Kishi S, Slack BE, Uchiyama J, Zhdanova I V. Zebrafish as a genetic model in biological and behavioral gerontology: where development meets aging in vertebrates – a mini-review. *Gerontology*. 2009;55(4):430-441. doi:10.1159/000228892

103. Lieschke GJ, Currie PD. Animal models of human disease: zebrafish swim into view. *Nat Rev Genet*. 2007;8(5):353-367. doi:10.1038/NRG2091

104. Urushibata H, Sasaki K, Takahashi E, *et al.* Control of developmental speed in zebrafish embryos using different incubation temperatures. *Zebrafish*. 2021;18(5):316-325. doi:10.1089/ZEB.2021.0022

105. Lee MT, Bonneau AR, Giraldez AJ. Zygotic genome activation during the maternal-to-zygotic transition. *Annu Rev Cell Dev Biol*. 2014;30:581-613. doi:10.1146/ANNUREV-CELLBIO-100913-013027

106. Lepage S. Adapted from zebrafish developmental timeline, by BioRender.com

(2021). https://app.biorender.com/biorender-templates

107. Kane DA, Kimmel CB. The zebrafish midblastula transition. *Development*. 1993;119(2):447-456. doi:10.1242/DEV.119.2.447

108. Tadros W, Lipshitz HD. The maternal-to-zygotic transition: a play in two acts. *Development*. 2009;136(18):3033-3042. doi:10.1242/DEV.033183

109. Feldman B, Gates MA, Egan ES, *et al.* Zebrafish organizer development and germ-layer formation require nodal-related signals. *Nature*. 1998;395(6698):181-185. doi:10.1038/26013

110. Gilbert SF. *Developmental Biology*. 6th ed. (Sunderland MA, ed.). Sinauer Associates; 2000.

111. Singleman C, Holtzman NG. Growth and maturation in the zebrafish, *Danio rerio*: a staging tool for teaching and research. *Zebrafish*. 2014;11(4):396-406. doi:10.1089/ZEB.2014.0976

112. Tong S-K, Hsu H-J, Chung B. Zebrafish monosex population reveals female dominance in sex determination and earliest events of gonad differentiation. *Dev Biol*. 2010;344(2):849-856. doi:10.1016/J.YDBIO.2010.05.515

113. Liew WC, Orbán L. Zebrafish sex: a complicated affair. *Brief Funct Genomics*. 2014;13(2):172-187. doi:10.1093/BFGP/ELT041

114. Uchida D, Yamashita M, Kitano T, Iguchi T. Oocyte apoptosis during the transition from ovary-like tissue to testes during sex differentiation of juvenile zebrafish. *J Exp Biol*. 2002;205(6):711-718. doi:10.1242/JEB.205.6.711

115. Chen W, Ge W. Gonad differentiation and puberty onset in the zebrafish: evidence for the dependence of puberty onset on body growth but not age in females. *Mol Reprod Dev*. 2013;80(5):384-392. doi:10.1002/MRD.22172

116. Menke AL, Spitsbergen JM, Wolterbeek APM, Woutersen RA. Normal anatomy

and histology of the adult zebrafish. *Toxicol Pathol*. 2011;39(5):759-775. doi:10.1177/0192623311409597

117. Deniz Koç N, Aytekin Y, Yüce R. Ovary maturatıon stages and histological investigation of ovary of the zebrafish (*Danio rerio*) nazan. *Brazilian Arch Biol Technol*. 2008;51(3):513-522.

118. Liu C, Yue S, Solarz J, Lee J, Li L. Improving the sexual activity and reproduction of female zebrafish with high testosterone levels. *Sci Rep*. 2021;11(1):1-11. doi:10.1038/s41598-021-83085-4

119. Nasiadka A, Clark MD. Zebrafish breeding in the laboratory environment. *ILAR J*. 2012;53(2):161-168. doi:10.1093/ILAR.53.2.161

120. Vaz R, Hofmeister W, Lindstrand A. Zebrafish models of neurodevelopmental disorders: limitations and benefits of current tools and techniques. *Int J Mol Sci*. 2019;20(6):1296. doi:10.3390/IJMS20061296

121. Cheng R-K, Jesuthasan SJ, Penney TB. Zebrafish forebrain and temporal conditioning. *Philos Trans R Soc B Biol Sci*. 2014;369(1637):20120462. doi:10.1098/RSTB.2012.0462

122. Gestri G, Link BA, Neuhauss SCF. The visual system of zebrafish and its use to model human ocular Diseases. *Dev Neurobiol*. 2012;72(3):302-327. doi:10.1002/dneu.20919

123. Chhetri J, Jacobson G, Gueven N. Zebrafish - on the move towards ophthalmological research. *Eye*. 2014;28(4):367-380. doi:10.1038/eye.2014.19

124. Bae YK, Kani S, Shimizu T, *et al.* Anatomy of zebrafish cerebellum and screen for mutations affecting its development. *Dev Biol*. 2009;330(2):406-426. doi:10.1016/J.YDBIO.2009.04.013

125. Wheeler GN, Brändli AW. Simple vertebrate models for chemical genetics and drug discovery screens: lessons from zebrafish and *Xenopus*. *Dev Dyn*.

2009;238(6):1287-1308. doi:10.1002/DVDY.21967

126. Howe K, Clark MD, Torroja CF, *et al.* The zebrafish reference genome sequence and its relationship to the human genome. *Nature*. 2013;496(7446):498-503. doi:10.1038/nature12111

127. Ruzicka L, Howe DG, Ramachandran S, *et al.* The zebrafish information network: new support for non-coding genes, richer gene ontology annotations and the alliance of genome resources. *Nucleic Acids Res*. 2019;47(D1):D867-D873. doi:10.1093/NAR/GKY1090

128. Kent WJ, Sugnet CW, Furey TS, *et al.* The human genome browser at UCSC. *Genome Res*. 2002;12(6):996-1006. doi:10.1101/GR.229102

129. Coordinators NR. Database resources of the national center for biotechnology information. *Nucleic Acids Res*. 2016;44(D1):D7-D19. doi:10.1093/NAR/GKV1290

130. Holden LA, Brown KH. Baseline mRNA expression differs widely between common laboratory strains of zebrafish. *Sci Rep*. 2018;8(1):1-10. doi:10.1038/s41598-018-23129-4

131. Suurväli J, Whiteley AR, Zheng Y, Gharbi K, Leptin M, Wiehe T. The laboratory domestication of zebrafish: from diverse populations to inbred substrains. *Mol Biol Evol*. 2020;37(4):1056-1069. doi:10.1093/MOLBEV/MSZ289

132. Traut W, Winking H. Meiotic chromosomes and stages of sex chromosome evolution in fish: zebrafish, platyfish and guppy. *Chromosom Res*. 2001;9(8):659-672. doi:10.1023/A:1012956324417

133. Anderson JL, Marí AR, Braasch I, *et al.* Multiple sex-associated regions and a putative sex chromosome in zebrafish revealed by RAD mapping and population genomics. *PLoS One*. 2012;7(7):e40701. doi:10.1371/JOURNAL.PONE.0040701

134. Amores A, Catchen J, Ferrara A, Fontenot Q, Postlethwait JH. Genome evolution

and meiotic maps by massively parallel DNA sequencing: spotted gar, an outgroup for the teleost genome duplication. *Genetics*. 2011;188(4):799-808. doi:10.1534/GENETICS.111.127324

135. Meyer A, Schartl M. Gene and genome duplications in vertebrates: the one-to-four (-to-eight in fish) rule and the evolution of novel gene functions. *Curr Opin Cell Biol*. 1999;11(6):699-704. doi:10.1016/S0955-0674(99)00039-3

136. Kassahn KS, Dang VT, Wilkins SJ, Perkins AC, Ragan MA. Evolution of gene function and regulatory control after whole-genome duplication: comparative analyses in vertebrates. *Genome Res*. 2009;19(8):1404-1418. doi:10.1101/GR.086827.108

137. Hellsten U, Harland RM, Gilchrist MJ, *et al.* The genome of the western clawed frog *Xenopus* tropicalis. *Science*. 2010;328(5978):633-636. doi:10.1126/SCIENCE.1183670

138. Richardson R, Tracey-White D, Webster A, Moosajee M. The zebrafish eye-a paradigm for investigating human ocular genetics. *Eye*. 2017;31(1):68-86. doi:10.1038/eye.2016.198

139. Greiling TM, Clark JI. Early lens development in the zebrafish: a three-dimensional time-lapse analysis. *Dev Dyn*. 2009;238(9):2254-2265. doi:10.1002/DVDY.21997

140. Veldman MB, Lin S. Zebrafish as a developmental model organism for pediatric research. *Pediatr Res*. 2008;64(5):470-476. doi:10.1203/pdr.0b013e318186e609

141. Zhang B, Xuan C, Ji Y, Zhang W, Wang D. Zebrafish xenotransplantation as a tool for in vivo cancer study. *Fam Cancer*. 2015;14(3):487-493. doi:10.1007/S10689-015-9802-3/FIGURES/4

142. Flurkey K, Currer J, Eds. *The Jackson Laboratory Handbook on Genetically Standardized Mice*. Jackson Laboratory; 2009.

143. Murray SA, Morgan JL, Kane C, *et al.* Mouse gestation length is genetically

determined. *PLoS One*. 2010;5(8):e12418. doi:10.1371/JOURNAL.PONE.0012418

144. Sertori R, Trengove M, Basheer F, Ward AC, Liongue C. Genome editing in zebrafish: a practical overview. *Brief Funct Genomics*. 2016;15(4):322-330. doi:10.1093/BFGP/ELV051

145. Meng X, Noyes MB, Zhu LJ, Lawson ND, Wolfe SA. Targeted gene inactivation in zebrafish using engineered zinc-finger nucleases. *Nat Biotechnol*. 2008;26(6):695-701. doi:10.1038/NBT1398

146. Urnov FD, Rebar EJ, Holmes MC, Zhang HS, Gregory PD. Genome editing with engineered zinc finger nucleases. *Nat Rev Genet*. 2010;11(9):636-646. doi:10.1038/nrg2842

147. Xing L, Hoshijima K, Grunwald DJ, *et al.* Zebrafish foxP2 zinc finger nuclease mutant has normal axon pathfinding. *PLoS One*. 2012;7(8):e43968. doi:10.1371/JOURNAL.PONE.0043968

148. Sood R, Carrington B, Bishop K, *et al.* Efficient methods for targeted mutagenesis in zebrafish using zinc-finger nucleases: data from targeting of nine genes using CompoZr or CoDA ZFNs. *PLoS One*. 2013;8(2):e57239. doi:10.1371/JOURNAL.PONE.0057239

149. Liu Y, Kretz CA, Maeder ML, *et al.* Targeted mutagenesis of zebrafish antithrombin III triggers disseminated intravascular coagulation and thrombosis, revealing insight into function. *Blood*. 2014;124(1):142-150. doi:10.1182/BLOOD-2014-03-561027

150. Doyon Y, McCammon JM, Miller JC, *et al.* Heritable targeted gene disruption in zebrafish using designed zinc-finger nucleases. *Nat Biotechnol*. 2008;26(6):702-708. doi:10.1038/nbt1409

151. Foley JE, Yeh JRJ, Maeder ML, *et al.* Rapid mutation of endogenous zebrafish genes using zinc finger nucleases made by oligomerized pool engineering. *PLoS One*. 2009;4(2):e4348. doi:10.1371/JOURNAL.PONE.0004348

152. Li H, Yang Y, Hong W, Huang M, Wu M, Zhao X. Applications of genome editing technology in the targeted therapy of human diseases: mechanisms, advances and prospects. *Signal Transduct Target Ther*. 2020;5(1):1-23. doi:10.1038/s41392-019-0089-y

153. Rafferty SA, Quinn TA. A beginner's guide to understanding and implementing the genetic modification of zebrafish. *Prog Biophys Mol Biol*. 2018;138:3-19. doi:10.1016/J.PBIOMOLBIO.2018.07.005

154. Nemudryi AA, Valetdinova KR, Medvedev SP, Zakian SM. TALEN and CRISPR/Cas genome editing systems: tools of discovery. *Acta Naturae*. 2014;6(3):19-40. doi:10.32607/20758251-2014-6-3-19-40

155. Gupta RM, Musunuru K. Expanding the genetic editing tool kit: ZFNs, TALENs, and CRISPR-Cas9. *J Clin Invest*. 2014;124(10):4154-4161. doi:10.1172/JCI72992

156. Mussolino C, Morbitzer R, Lütge F, Dannemann N, Lahaye T, Cathomen T. A novel TALE nuclease scaffold enables high genome editing activity in combination with low toxicity. *Nucleic Acids Res*. 2011;39(21):9283-9293. doi:10.1093/NAR/GKR597

157. Hwang WY, Fu Y, Reyon D, *et al.* Efficient genome editing in zebrafish using a CRISPR-Cas system. *Nat Biotechnol*. 2013;31(3):227-229. doi:10.1038/nbt.2501

158. Liu K, Petree C, Requena T, Varshney P, Varshney GK. Expanding the CRISPR toolbox in zebrafish for studying development and disease. *Front Cell Dev Biol*. 2019;4(7):13. doi:10.3389/FCELL.2019.00013

159. Liu J, Zhou Y, Qi X, *et al.* CRISPR/Cas9 in zebrafish: an efficient combination for human genetic diseases modeling. *Hum Genet*. 2016;136(1):1-12. doi:10.1007/S00439-016-1739-6

160. Zhan T, Rindtorff N, Betge J, Ebert MP, Boutros M. CRISPR/Cas9 for cancer research and therapy. *Semin Cancer Biol*. 2019;55:106-119. doi:10.1016/J.SEMCANCER.2018.04.001

161. Lee C. CRISPR/Cas9-based antiviral strategy: Current status and the potential challenge. *Molecules*. 2019;24(7):1349. doi:10.3390/molecules24071349

162. Matson AW, Hosny N, Swanson ZA, Hering BJ, Burlak C. Optimizing sgRNA length to improve target specificity and efficiency for the GGTA1 gene using the CRISPR/Cas9 gene editing system. *PLoS One*. 2019;14(12):e0226107. doi:10.1371/JOURNAL.PONE.0226107

163. Sorlien EL, Witucki MA, Ogas J. Efficient production and identification of CRISPR/Cas9-generated gene knockouts in the model system *Danio rerio*. *J Vis Exp*. 2018;(138):56969. doi:10.3791/56969

164. Varshney GK, Pei W, Lafave MC, et al. High-throughput gene targeting and phenotyping in zebrafish using CRISPR/Cas9. *Genome Res*. 2015;25(7):1030-1042. doi:10.1101/gr.186379.114

165. Cho SW, Kim S, Kim Y, *et al.* Analysis of off-target effects of CRISPR/Cas-derived RNA-guided endonucleases and nickases. *Genome Res*. 2014;24(1):132-141. doi:10.1101/GR.162339.113

166. Jao L-E, Wente SR, Chen W. Efficient multiplex biallelic zebrafish genome editing using a CRISPR nuclease system. *Proc Natl Acad Sci*. 2013;110(34):13904-13909. doi:10.1073/PNAS.1308335110

167. Pena IA, Roussel Y, Daniel K, *et al.* Pyridoxine-dependent epilepsy in zebrafish caused by aldh7a1 deficiency. *Genetics*. 2017;207(4):1501-1518. doi:10.1534/GENETICS.117.300137

168. Liu C, Li C, Hu C, *et al.* CRISPR/Cas9-induced shank3b mutant zebrafish display autism-like behaviors. *Mol Autism*. 2018;9(1):1-13. doi:10.1186/S13229-018-0204-X

169. Cai S, Chen Y, Shang Y, Cui J, Li Z, Li Y. Knockout of zebrafish interleukin 7 receptor (IL7R) by the CRISPR/Cas9 system delays retinal neurodevelopment. *Cell Death Dis*. 2018;9(3):1-11. doi:10.1038/s41419-018-0337-z

170. Lee J, Willer JR, Willer GB, Smith K, Gregg RG, Gross JM. Zebrafish blowout provides genetic evidence for Patched1 mediated negative regulation of Hedgehog signaling within the proximal optic vesicle of the vertebrate eye. *Dev Biol*. 2008;319(1):10-22. doi:10.1016/J.YDBIO.2008.03.035

171. den Hollander AI, Biyanwila J, Kovach P, *et al.* Genetic defects of GDF6 in the zebrafish out of sight mutant and in human eye developmental anomalies. *BMC Genet*. 2010;11:102. doi:10.1186/1471-2156-11-102

172. Ellis JL, Bove KE, Schuetz EG, *et al.* Zebrafish abcb11b mutant reveals strategies to restore bile excretion impaired by bile salt export pump deficiency. *Hepatology*. 2018;67(4):1531-1545. doi:10.1002/HEP.29632

173. Anderson BR, Howell DN, Soldano K, *et al.* In vivo modeling implicates APOL1 in nephropathy: evidence for dominant negative effects and epistasis under anemic stress. *PLOS Genet*. 2015;11(7):e1005349. doi:10.1371/JOURNAL.PGEN.1005349

174. Bolar NA, Golzio C, Živná M, *et al.* Heterozygous loss-of-function SEC61A1 mutations cause autosomal-dominant tubulo-interstitial and glomerulocystic kidney disease with anemia. *Am J Hum Genet*. 2016;99(1):174-187. doi:10.1016/J.AJHG.2016.05.028

175. Talbot JC, Nichols JT, Yan YL, *et al.* Pharyngeal morphogenesis requires fras1-itga8-dependent epithelial-mesenchymal interaction. *Dev Biol*. 2016;416(1):136-148. doi:10.1016/J.YDBIO.2016.05.035

176. Zhang Y, Huang H, Zhao G, *et al.* ATP6V1H deficiency impairs bone development through activation of MMP9 and MMP13. *PLOS Genet*. 2017;13(2):e1006481. doi:10.1371/JOURNAL.PGEN.1006481

177. Wang J, Luo J, Chen Q, *et al.* Identification of LBX2 as a novel causal gene of atrial septal defect. *Int J Cardiol*. 2018;265:188-194. doi:10.1016/J.IJCARD.2018.04.038

178. Sasagawa S, Nishimura Y, Okabe S, *et al.* Downregulation of GSTK1 is a common

mechanism underlying hypertrophic cardiomyopathy. *Front Pharmacol*. 2016;7:162. doi:10.3389/FPHAR.2016.00162/BIBTEX

179. Ear J, Hsueh J, Nguyen M, *et al.* A zebrafish model of 5q-syndrome using CRISPR/Cas9 targeting RPS14 reveals a p53-independent and p53-dependent mechanism of erythroid failure. *J Genet Genomics*. 2016;43(5):307-318. doi:10.1016/J.JGG.2016.03.007

180. Pazhakh V, Clark S, Keightley MC, Lieschke GJ. A GCSFR/CSF3R zebrafish mutant models the persistent basal neutrophil deficiency of severe congenital neutropenia. *Sci Rep*. 2017;7(1):1-11. doi:10.1038/srep44455

181. Van De Weghe JC, Rusterholz TDS, Latour B, *et al.* Mutations in ARMC9, which encodes a basal body protein, cause joubert syndrome in humans and ciliopathy phenotypes in zebrafish. *Am J Hum Genet*. 2017;101(1):23-36. doi:10.1016/J.AJHG.2017.05.010

182. Guo S. Using zebrafish to assess the impact of drugs on neural development and function. *Expert Opin Drug Discov*. 2009;4(7):715-726. doi:10.1517/17460440902988464

183. Sakai C, Ijaz S, Hoffman EJ. Zebrafish models of neurodevelopmental disorders: past, present, and future. *Front Mol Neurosci*. 2018;(11):294. doi:10.3389/FNMOL.2018.00294

184. Koonin E V. Orthologs, paralogs, and evolutionary genomics. *Annu Rev Genet*. 2005;39:309-338. doi:10.1146/ANNUREV.GENET.39.073003.114725

185. White RJ, Collins JE, Sealy IM, *et al.* A high-resolution mRNA expression time course of embryonic development in zebrafish. *Elife*. 2017;6:e30860. doi:10.7554/ELIFE.30860

186. Lan C-C, Tang R, Un I, Leong S, Love DR. Quantitative real-time RT-PCR (qRT-PCR) of zebrafish transcripts: optimization of RNA extraction, quality control considerations, and data analysis. *Cold Spring Harb Protoc*.

2009;(10):pdb.prot5314. doi:10.1101/pdb.prot5314

187. Thisse C, Thisse B. High-resolution in situ hybridization to whole-mount zebrafish embryos. *Nat Protoc*. 2008;3(1):59-69. doi:10.1038/nprot.2007.514

188. Hostelley TL, Nesmith JE, Zaghloul NA. Sample preparation and analysis of RNAseq-based gene expression data from zebrafish. *J Vis Exp*. 2017;(128):56187. doi:10.3791/56187

189. Aquaneering. *Aquaneering, Zebrafish (Danio Rerio) Stand Alone Aquatic Housing System*. Aquaneering Incorporated; 2017.

190. Westerfield M. *The Zebrafish Book. A Guide for the Laboratory Use of Zebrafish (Danio Rerio)*. 4th ed. University of Oregon Press, Eugene; 2000.

191. Peterson SM, Freeman JL. RNA isolation from embryonic zebrafish and cDNA synthesis for gene expression analysis. *J Vis Exp*. 2009;(30):1470. doi:10.3791/1470

192. Gupta T, Mullins MC. Dissection of organs from the adult zebrafish. *J Vis Exp*. 2010;(37):1717. doi:10.3791/1717

193. Ye J, Coulouris G, Zaretskaya I, Cutcutache I, Rozen S, Madden T. Primer-BLAST: a tool to design target-specific primers for polymerase chain reaction. *BMC Bioinformatics*. 2012;13(1):1-11. doi:10.1186/1471-2105-13-134

194. Hu Y, Xie S, Yao J. Identification of novel reference genes suitable for qRT-PCR normalization with respect to the zebrafish developmental stage. *PLoS One*. 2016;11(2):e0149277. doi:10.1371/JOURNAL.PONE.0149277

195. Qian Y, Wang C, Wang J, *et al.* Fipronil-induced enantioselective developmental toxicity to zebrafish embryo-larvae involves changes in DNA methylation. *Sci Rep*. 2017;7(1):1-11. doi:10.1038/s41598-017-02255-5

196. Karlsson J, Von Hofsten J, Olsson E. Generating transparent aebrafish: a refined method to improve detection of gene expression during embryonic development.

Mar Biotechnol. 2001;3(6):522-527. doi:10.1007/s1012601-0053-4

197. Knowlton MN, Chan BMC, Kelly GM. The zebrafish band 4.1 member Mir is involved in cell movements associated with gastrulation. *Dev Biol*. 2003;264(2):407-429. doi:10.1016/J.YDBIO.2003.09.001

198. Schneider CA, Rasband WS, Eliceiri KW. NIH image to imageJ: 25 years of image analysis. *Nat Methods*. 2012;9(7):671-675. doi:10.1038/NMETH.2089

199. Bhatla N. Exon-Intron Graphic Maker. WormWeb.org. Accessed August 2, 2021. http://wormweb.org/exonintron

200. Madeira F, Park YM, Lee J, *et al.* The EMBL-EBI search and sequence analysis tools APIs in 2019. *Nucleic Acids Res*. 2019;47(W1):W636-W641. doi:10.1093/NAR/GKZ268

201. Thompson JD, Higgins DG, Gibson TJ. CLUSTAL W: improving the sensitivity of progressive multiple sequence alignment through sequence weighting, position-specific gap penalties and weight matrix choice. *Nucleic Acids Res*. 1994;22(22):4673-4680. doi:10.1093/nar/22.22.4673

202. Solomon KS, Fritz A. Concerted action of two dlx paralogs in sensory placode formation. *Development*. 2002;129(13):3127-3136. doi:10.1242/dev.129.13.3127

203. Oxtoby E, Jowett T. Cloning of the zebrafish krox-20 gene (krx-20) and its expression during hindbrain development. *Nucleic Acids Res*. 1993;21(5):1087-1095. doi:10.1093/NAR/21.5.1087

204. Nguyen LL. Developmental toxicity of tetrakis (hydromethyl) phosphonium chloride (THPC) in zebrafish (*Danio rerio*) embryos. *Georg South Univ*. Published online 2015.

205. Miller JA, Ding S-L, Sunkin SM, *et al.* Transcriptional landscape of the prenatal human brain. *Nature*. 2014;508(7495):199-206. doi:10.1038/nature13185

206. Xu G, Guo C, Shan H, Kong H. Divergence of duplicate genes in exon–intron structure. *Proc Natl Acad Sci*. 2012;109(4):1187-1192. doi:10.1073/PNAS.1109047109

207. Dibenedetto AJ, Guinto JB, Ebert TD, Bee K, Schmidt MM, Jackman TR. Zebrafish brd2a and brd2b are paralogous members of the bromodomain-ET (BET) family of transcriptional coregulators that show structural and expression divergence. *BMC Dev Biol*. 2008;8:39. doi:10.1186/1471-213X-8-39

208. Drummond I, Rohwer-Nutter P, Sukhatme V. The zebrafish egr1 gene encodes a highly conserved, zinc-finger transcriptional regulator. *DNA Cell Biol*. 2009;13(10):1047-1055. doi:10.1089/DNA.1994.13.1047

209. Cassandri M, Smirnov A, Novelli F, *et al.* Zinc-finger proteins in health and disease. *Cell Death Discov*. 2017;3(1):17071. doi:10.1038/cddiscovery.2017.71

210. Bult CJ, Blake JA, Smith CL, et al. Mouse genome database (MGD) 2019. *Nucleic Acids Res*. 2019;47(D1):D801-D806. doi:10.1093/nar/gky1056

211. Luo Q, Wu C, Sun S, *et al*. The spatial-temporal expression and functional divergence of bach homologs in zebrafish *Danio rerio*. *J Fish Biol*. 2016;88(4):1584-1597. doi:10.1111/JFB.12931

212. Ausió J, Martínez de Paz A, Esteller M. MeCP2: the long trip from a chromatin protein to neurological disorders. *Trends Mol Med*. 2014;20(9):487-498. doi:10.1016/J.MOLMED.2014.03.004

213. Yang H, Douglas G, Monaghan KG, *et al*. De novo truncating variants in the AHDC1 gene encoding the AT-hook DNA-binding motif-containing protein 1 are associated with intellectual disability and developmental delay. *Cold Spring Harb Mol Case Stud*. 2015;1(1):a000562. doi:10.1101/MCS.A000562

214. Baker SA, Chen L, Wilkins AD, Yu P, Lichtarge O, Zoghbi HY. A newly characterized AT-hook domain in MeCP2 determines clinical course of rett syndrome and related disorders. *Cell*. 2013;152(5):984-996.

doi:10.1016/J.CELL.2013.01.038

215. Pietri T, Roman A-C, Guyon N, *et al*. The first mecp2-null zebrafish model shows altered motor behaviors. *Front Neural Circuits*. 2013;7:118. doi:10.3389/FNCIR.2013.00118

216. Farnsworth DR, Saunders LM, Miller AC. A single-cell transcriptome atlas for zebrafish development. *Dev Biol*. 2020;459(2):100-108. doi:10.1016/J.YDBIO.2019.11.008

217. Karimi K, Fortriede JD, Lotay VS, *et al*. Xenbase: a genomic, epigenomic and transcriptomic model organism database. *Nucleic Acids Res*. 2018;46(D1):D861-D868. doi:10.1093/NAR/GKX936

218. Wu C, Jin X, Tsueng G, Afrasiabi C, Su A. BioGPS: building your own mash-up of gene annotations and expression profiles. *Nucleic Acids Res*. 2016;44(D1):D313-D316. doi:10.1093/NAR/GKV1104

219. Ampatzis K, Dermon CR. Sex differences in adult cell proliferation within the zebrafish (*Danio rerio)* cerebellum. *Eur J Neurosci*. 2007;25(4):1030-1040. doi:10.1111/J.1460-9568.2007.05366.X

220. Ampatzis K, Makantasi P, Dermon C. Cell proliferation pattern in adult zebrafish forebrain is sexually dimorphic. *Neuroscience*. 2012;226:367-381. doi:10.1016/J.NEUROSCIENCE.2012.09.022

221. Karoglu-Eravsar ET, Tuz-Sasik MU, Adams MM. Environmental enrichment applied with sensory components prevents age-related decline in synaptic dynamics: evidence from the zebrafish model organism. *Exp Gerontol*. 2021;149:111346. doi:10.1016/j.exger.2021.111346

222. Caminero F, Cascella M. Neuroanatomy, mesencephalon midbrain. *StatPearls*. Published online November 2, 2020. Accessed October 3, 2021. https://www.ncbi.nlm.nih.gov/books/NBK551509/

223. Ruchalski K, Hathout GM. A medley of midbrain maladies: a brief review of midbrain anatomy and syndromology for radiologists. *Radiol Res Pract*. 2012;2012(7):1-11. doi:10.1155/2012/258524

224. Jensen E. Technical review: in situ hybridization. *Anat Rec*. 2014;297(8):1349-1353. doi:10.1002/AR.22944

225. Choi H, Chang J, Trinh L, Padilla JE, Fraser SE, Pierce NA. Programmable in situ amplification for multiplexed imaging of mRNA expression. *Nat Biotechnol*. 2010;28(11):1208-1212. doi:10.1038/NBT.1692

226. Brinkman EK, Chen T, Amendola M, van Steensel B. Easy quantitative assessment of genome editing by sequence trace decomposition. *Nucleic Acids Res*. 2014;42(22):e168-e168. doi:10.1093/NAR/GKU936

227. Liu M-S, Gong S, Yu H-H, Jung K, Johnson KA, Taylor DW. Engineered CRISPR/Cas9 enzymes improve discrimination by slowing DNA cleavage to allow release of off-target DNA. *Nat Commun*. 2020;11(1):1-13. doi:10.1038/s41467-020-17411-1

228. Colón-Rodríguez A, Uribe-Salazar JM, Weyenberg KB, *et al*. Assessment of autism zebrafish mutant models using a high-throughput larval phenotyping platform. *Front Cell Dev Biol*. 2020;8:1324. doi:10.3389/FCELL.2020.586296

229. Hayes M, Gao X, Yu LX, *et al*. Ptk7 mutant zebrafish models of congenital and idiopathic scoliosis implicate dysregulated Wnt signalling in disease. *Nat Commun*. 2014;5:4777. doi:10.1038/ncomms5777

230. Lin SJ, Vona B, Barbalho PG, *et al*. Biallelic variants in KARS1 are associated with neurodevelopmental disorders and hearing loss recapitulated by the knockout zebrafish. *Genet Med*. 2021;23(10):1933-1943. doi:10.1038/s41436-021-01239-1

231. Fuentes F, Reynolds E, Lewellis SW, Venkiteswaran G, Knaut H. A plasmid set for efficient bacterial artificial chromosome (BAC) transgenesis in zebrafish. *G3 Genes, Genomes, Genet*. 2016;6(4):829-834. doi:10.1534/G3.115.026344

232. Iwashita M, Watanabe M, Ishii M, *et al.* Pigment pattern in jaguar/obelix zebrafish is caused by a Kir7.1 mutation: implications for the regulation of melanosome movement. *PLoS Genet*. 2006;2(11):e197. doi:10.1371/journal.pgen.0020197

233. Yan YL, Talbot WS, Egan ES, Postlethwait JH. Mutant rescue by BAC clone injection in zebrafish. *Genomics*. 1998;50(2):287-289. doi:10.1006/geno.1998.5304

234. Saitou N, Nei M. The neighbor-joining method: a new method for reconstructing phylogenetic trees. *Mol Biol Evol*. 1987;4(4):406-425. doi:10.1093/oxfordjournals.molbev.a040454

235. Felsenstein J. Confidence limits on phylogenies: an approach using the bootstrap. *Evolution (N Y)*. 1985;39(4):783-791. doi:10.2307/2408678

236. Tamura K, Nei M, Kumar S. Prospects for inferring very large phylogenies by using the neighbor-joining method. *Proc Natl Acad Sci U S A*. 2004;101(30):11030-11035. doi:10.1073/pnas.0404206101

237. Tamura K, Stecher G, Kumar S. MEGA11: molecular evolutionary genetics analysis version 11. *Mol Biol Evol*. 2021;38(7):3022-3027. doi:10.1093/molbev/msab120

238. Stecher G, Tamura K, Kumar S. Molecular evolutionary genetics analysis (MEGA) for macOS. *Mol Biol Evol*. 2020;37(4):1237-1239. doi:10.1093/molbev/msz312

239. Moreno-Mateos MA, Vejnar CE, Beaudoin J-D, *et al*. CRISPRscan: designing highly efficient sgRNAs for CRISPR-Cas9 targeting in vivo. *Nat Methods*. 2015;12(10):982-988. doi:10.1038/nmeth.3543

240. Camp E, Lardelli M. Tyrosinase gene expression in zebrafish embryos. *Dev Genes Evol*. 2001;211(3):150-153. doi:10.1007/S004270000125

241. Brinkman EK, Chen T, Amendola M, van Steensel B. Easy quantitative assessment of genome editing by sequence trace decomposition. *Nucleic Acids Res*. 2014;42(22):e168-e168. doi:10.1093/NAR/GKU936

Appendices

Appendix 1. Animal use protocol

AUP Number: 2019-149

Biosafety Approval: BIO-UWO-0081

AUP Title: Cell Signaling in Embryonic Epithelial to Mesenchymal Transitions

Disease Outbreak and Zebrafish Facility Shutdown:

Clinical symptoms of sickness were identified, in October 2020. Those presenting were euthanized, fixed in formalin, and sent to clinical veterinarian staff of the Animal Care Committee. Bacterial culture and histopathology were conducted (Animal Health Laboratory, University of Guelph, ON). Findings suggested Motile *Aeromonas* Septicemia as the cause of the bacterial outbreak. The zebrafish colony was culled, and the facility was closed. Continuation of research was completed through purchase of samples from the Zebrafish Genetics and Disease Models Core, The Hospital for Sick Children, Toronto, Canada.

Appendix 2. Phylogenetic relationship of *proline rich 12* amongst vertebrates

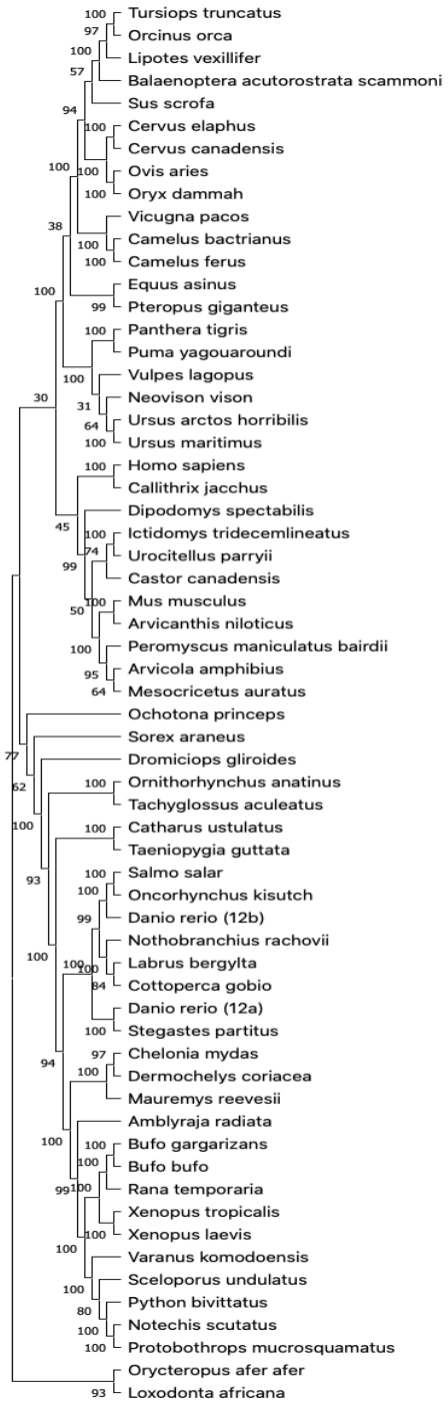

Figure 13. *Proline rich 12* evolutionary history amongst vertebrates inferred using the Neighbor-joining method[234]. The bootstrap consensus tree inferred from 500 replicates[235] is taken to represent the evolutionary history of the taxa analyzed[235]. Branches

corresponding to partitions reproduced in less than 50% bootstrap are collapsed. The percentage of replicate trees in which the associated taxa clustered together in the bootstrap test (500 replicates) are shown next to the branches[235]. The evolutionary distances were computed using the Maximum Composite Likelihood method[236] and are in the units of the number of base substitutions per site. This analysis involved 62 nucleotide sequences retrieved from NCBI[129]. All ambiguous positions were removed for each sequence pair (pairwise deletion option). Evolutionary analyses were conducted in MEGA11[237,238].

Appendix 3. Schematic representation of DUF4122 region within human PRR12, zebrafish Prr12a, and zebrafish Prr12b

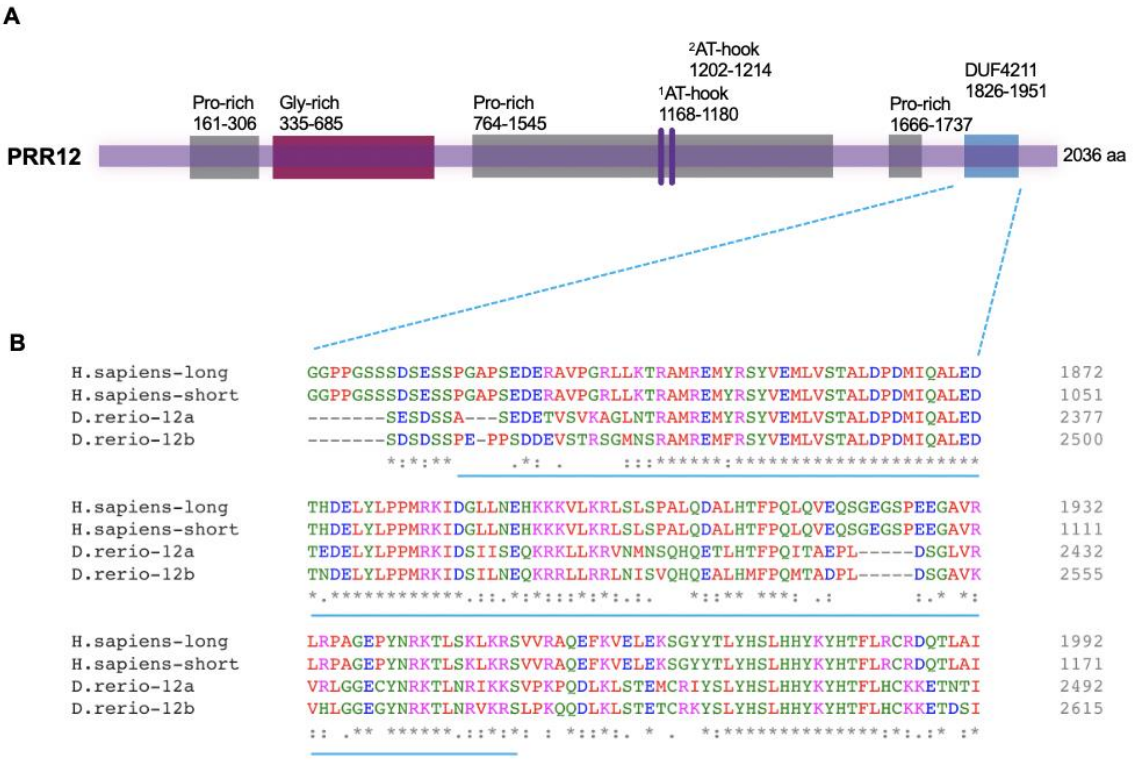

Figure 14. Schematic representation of conserved DUF4211 region within human PRR12, zebrafish Prr12a, and zebrafish Prr12b. A. Full-length human PRR12 protein schematic highlighting specific domain regions, adapted and modified from Chowdhury *et al.*, 2021[27]. Pro-rich: proline rich domains, Gly-rich: glycine rich domains, AT-hook: DNA-binding protein motif, DUF4211: domain of unknown function. **B.** Clustal Omega Multiple Sequence Alignment Tool showing the conserved DUF4211 domain sequence across human and zebrafish. The predicted DUF4211 region is highlighted with a blue line. The last amino acid of the displayed sequence is indicated at the end of each row. Asterisks (*): fully conserved residue, colon (:): strongly similar properties, and period (.): weakly similar properties. Residue type of amino acids are coloured based on property accordingly (Red: small + hydrophobic (incl. aromatic – Y), Blue: acidic, Magenta: basic – H, Green: hydroxyl + sulfhydryl + amine G, *etc.*). Schematic not drawn to scale. Multiple Sequence Alignment image and analysis obtained from Clustal Omega[200].

Appendix 4. Zebrafish *prr12a* and *prr12b* single cell RNA-sequencing analysis

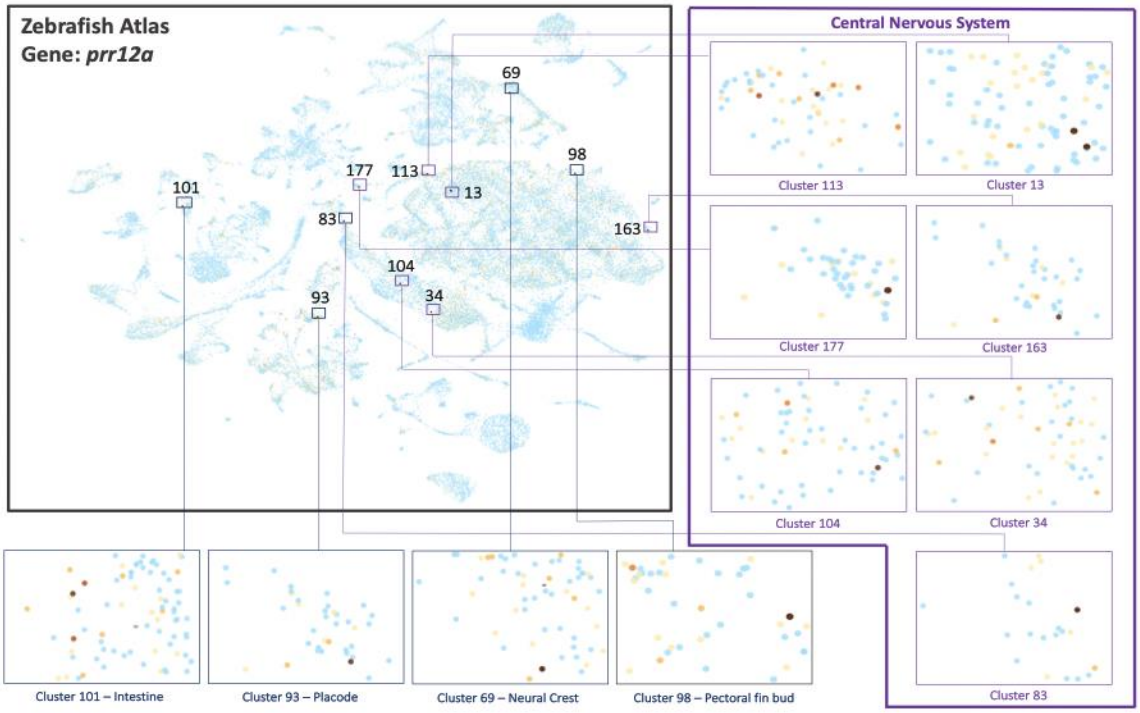

prr12a

Cluster ID	Tissue	Cell Type	Subtype	Day of origin
13	Central Nervous System	Neuron	Mid-hindbrain boundary	2,5
34	Central Nervous System	Neuroblast	Retinal	1
69	Neural crest	Cardiac neural crest		1
83	Central Nervous System	Neuron	Retinal, differentiating neurons	2,5
93	Placode	Otic		1,2,5
98	Pectoral fin bud			1,2
101	Intestine	Intestinal epithelial cell		1,2,5
104	Central Nervous System	Neuron	Retinal, differentiating neurons	2,5
113	Central Nervous System	Neuron	Retinal, differentiating neurons	2,5
163	Central Nervous System	Neuroblast	Hindbrain	1,2,5
177	Central Nervous System	Neuron	Retinal	5

Range	Frequency
0	83.0%
1	14.3%
2	2.2%
3	0.39%
4	0.08%
5	0.03%

Figure 15. Zebrafish *prr12a* single-cell RNA-sequencing analysis. *prr12a* transcript abundance present in central nervous system structures during early embryonic development. Cell clustering analysis of 11 clusters expressing *prr12a* transcripts. 7 clusters expressed in the central nervous system and 4 clusters expressed in: intestine, placode, neural crest, and pectoral fin bud. Cell colours on atlas represent *prr12a* UMI count (absolute number of *prr12a* transcripts). Highest number of *prr12a* transcripts are represented with brown cells, and no *prr12a* transcripts are represented with blue cells. Refer to legend for full range frequency. Seurat software and Uniform Manifold Approximation and Projection (UMAP) was used for data analysis. Cell atlas image

adapted and modified from UCSC Cell Browser, 2020[128] and raw data obtained from Farnsworth *et al*., 2020[216].

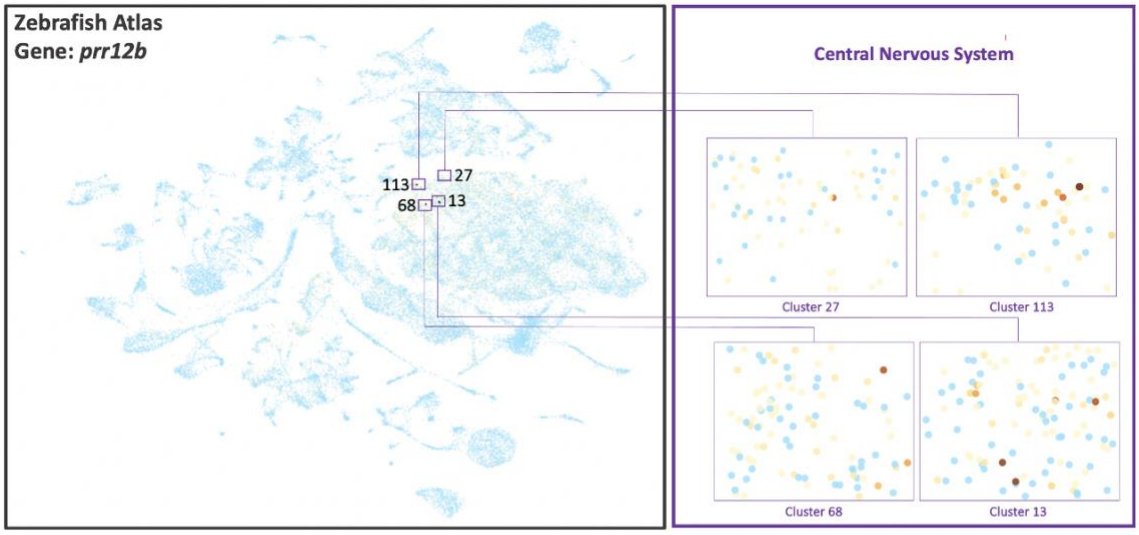

prr12b

Cluster ID	Tissue	Cell Type	Subtype	Day of origin
13	Central Nervous System	Neuron	Mid-hindbrain boundary	2,5
27	Central Nervous System	Neuron	Mid-hindbrain boundary, Glut	1,2,5
113	Central Nervous System	Neuron	Retinal, differentiating neurons	2,5
68	Central Nervous System	Neuron, differentiating	Fore-midbrain boundary	1,2

Range	Frequency
0	82.1%
1-2	16.7%
2-4	1.0%
4-5	0..07%
5-7	0.07%
7-8	0.01%
8-9	0.00%
9-11	0.01%
11-12	0.00%
12-23	0.01%

Figure 16. Zebrafish *prr12b* single-cell RNA-sequencing analysis. *prr12b* transcript abundance present in central nervous system structures during early embryonic development. Cell clustering analysis of 4 clusters expressing *prr12b* transcripts. 4 clusters expressed in the central nervous system. Cell colours on atlas represent *prr12b* UMI count (absolute number of *prr12b* transcripts). Highest number of *prr12b* transcripts are represented with brown cells, and no *prr12b* transcripts are represented with blue cells. Refer to legend for full range frequency. Seurat software and Uniform Manifold Approximation and Projection (UMAP) was used for data analysis. Cell atlas image adapted and modified from UCSC Cell Browser, 2020[128] and raw data obtained from Farnsworth *et al.*, 2020[216].

Appendix 5. Generation of knockout zebrafish lines

Single guide RNA and SpCas9 mRNA synthesis

CRISPRscan software[239] and the Ensembl Genome Browser (Zebrafish, GRCz11)[32] were used to identify single guide RNAs (sgRNAs) (**Table 6**) for CRISPR-Cas9 editing of *prr12a or prr12b* (**Figure 17**). Two sgRNAs were designed per gene, targeting different exons, to determine the most efficient Cas9 mediated cleavage. sgRNAs were synthesized using the EnGen sgRNA Synthesis Kit *S. pyogenes* (New England Biolabs, E3322S), purified using an RNA Clean and Concentrator (ZYMO RESEARCH, R1017) and quantified using a NanoDrop™ 2000c Spectrophotometer (Thermo Fisher Scientific). *Streptococcus pyogenes* CRISPR-associated protein (SpCas9) mRNA was prepared by digesting the pT3TS-nCas9n expression vector (generously donated by Dr. B. Ciruna, The Hospital for Sick Children, Toronto, ON) with *Xbal* (New England Biolabs, R0145S) followed by *in vitro* transcription using the mMESSAGE mMACHINE™ T3 kit (Thermo Fisher Scientific, AM1348) as per the manufacturer's instructions.

Table 6: sgRNA sequences for CRISPR-Cas9 embryo microinjection

Gene	**Sequence (5' to 3')**
#1. *prr12a*	**TTAATACGACTCACTATAGGTGGGGCTTGGGGTGCAGC GTTTTAGAGCTAGAAATAG**
#2. *prr12a*	**TTAATACGACTCACTATAGGGGGCTGGGAATGTGACTG GTTTTAGAGCTAGAAATAG**
#1. *prr12b*	**TTAATACGACTCACTATAGGGTGCGAAATTGGGAGAGA GTTTTAGAGCTAGAAATAG**
#2. *prr12b*	**TTAATACGACTCACTATAGGAAAAGCTTATGGAAGTCTT GTTTTAGAGCTAGAAATAG**
tyr (control)[240]	**TTAATACGACTCACTATAGGACTGGAGGACTTCTGGGG GTTTTAGAGCTAGAAATAGC**

For each guide, an oligonucleotide was created where 18 nucleotides in yellow represent the T7 promoter site, 20 bp nucleotides in green represent the target sequence, followed by the 19 nucleotides in red representing the scaffold overlap sequence.

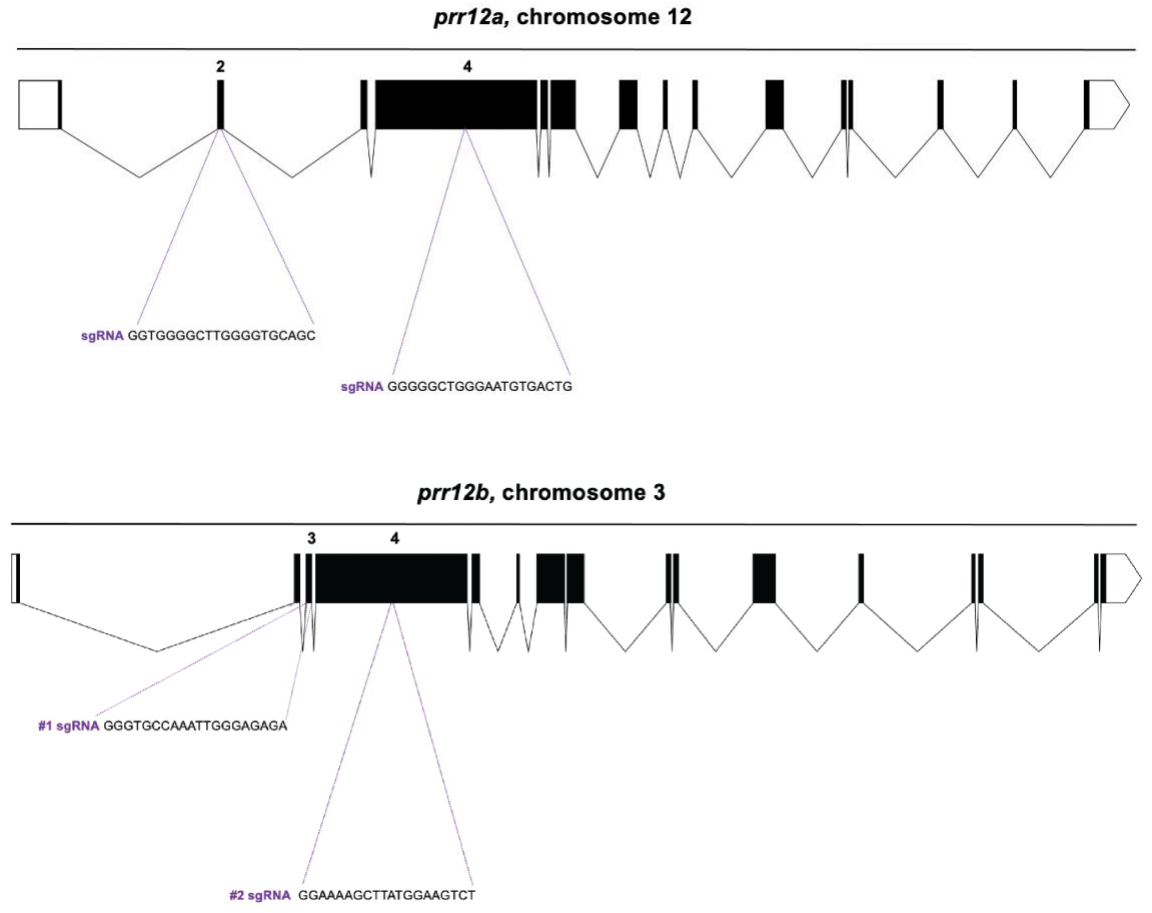

Figure 17. *prr12a* and *prr12b* sgRNA target sites within the zebrafish. *prr12a* #1 sgRNA targeting exon 2 and #2 sgRNA targeting exon 4. *prr12b* #1 sgRNA targeting exon 3 and #2 sgRNA targeting exon 4.

Zebrafish embryo microinjections and TIDE analysis

Zebrafish embryos were collected (as described in Section 2.1) and injected with 10 μL either 50 pg (picograms) *prr12a* sgRNA, 300pg Cas9, and phenol red dye or phenol red dye alone in RNase-free water at the 1-cell stage using a PLI-100 Pico-Injector (Medical Systems Corp.). Embryos were incubated in embryo medium (E3 solution) at 28.5ºC. *prr12a* sgRNA and Cas9 mRNA efficiency was compared to a concurrently derived *tyr* (tyrosinase) knockout, where *tyr* deficient embryos present with little to no melanin pigmentation[240].

Genomic DNA of a subset of injected fish was isolated and samples were processed using a PTC-100 Programmable Thermal Controller (MJ Research, Inc.), under the following conditions: 95ºC for 10 min, 4ºC held, addition of Proteinase K, 55ºC for 60 min, when 17.8mg/ml of proteinase K was added, then heat inactivated at 95ºC for 10 min. Followed by PCR amplification using *prr12a* forward and reverse primers (**Table 7**) flanking the CRISPR-Cas9 cut site, amplicons were purified using a QIAquick PCR Purification Kit (QIAGEN, 28104) and products were sequenced (London Regional Genomics Centre, Robarts Research Institute, London, ON). Resulting chromatograms from wildtype embryos (control injected) were compared to *prr12a* sgRNA/Cas9-injected embryos and analyzed using Tracking of Indels by Decomposition (TIDE)[241].

Table 7: Primer sequences for zebrafish RT-PCR genotyping target gene

Gene	Forward Primer (5' to 3')	Reverse Primer (5' to 3')	Tm
prr12a	GGGAGACTACCTCAGGCAAAC	AGCACCAAAGCACTTGTGGAA	55ºC

Appendix 6. Preliminary analysis of *prr12a* genetic disruption

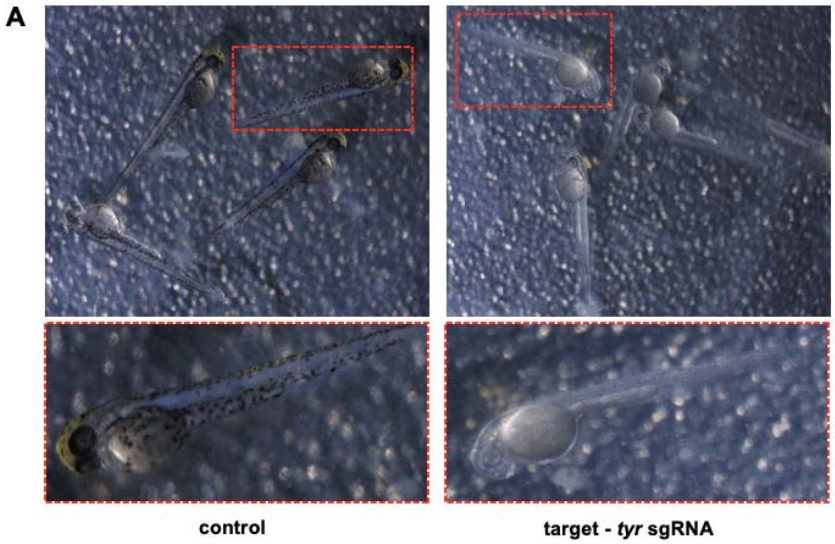

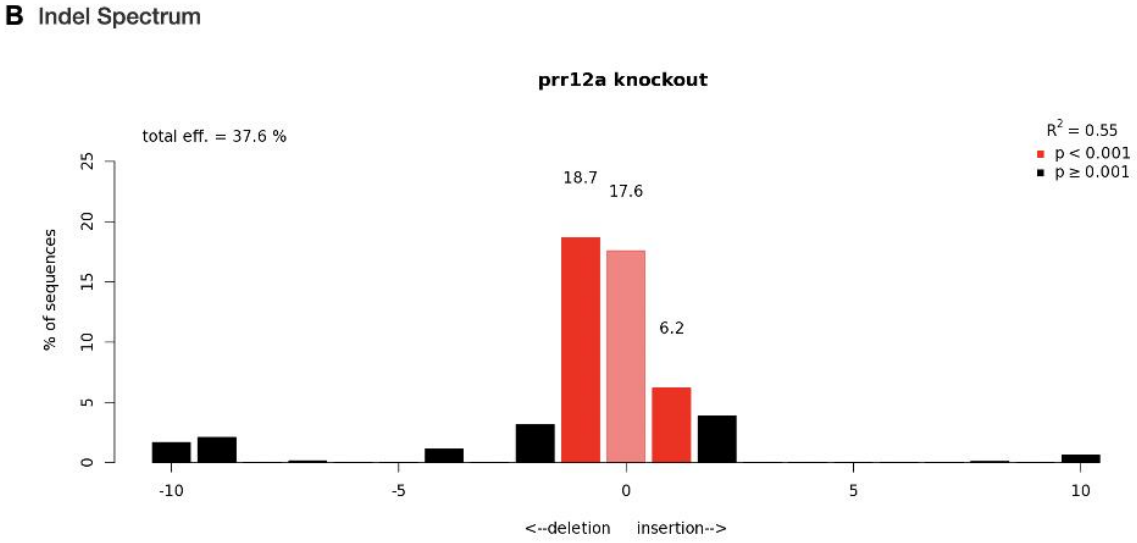

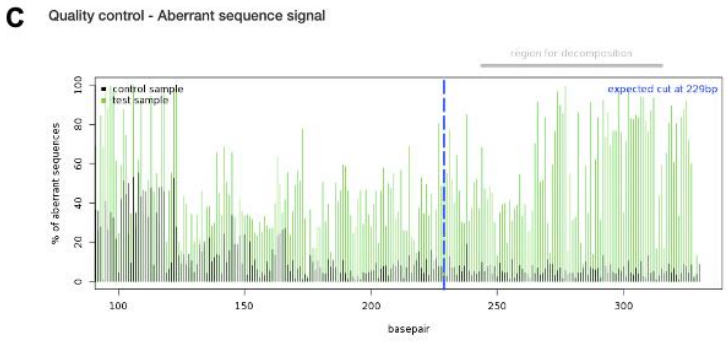

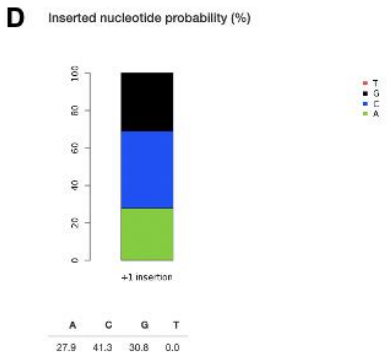

Figure 18. Preliminary analysis of *prr12a* genetic disruption. Sequence alignment analysis of control embryo and *prr12a* sgRNA microinjected embryo; DNA was extracted, processed for Sanger sequencing, and chromatograms were processed using Tracking of Indels by Decomposition (TIDE) analysis to determine indels (insertion/deletion). **A.** Control and *tyr* sgRNA microinjected embryos at 72 hpf. Red boxes show digitally enlarged images. **B.** Indel spectrum, yielding a range of indels and frequencies. Each bar represents the percentage of sequences recognized during analysis, with statistical significance indicated with a red bar. **C.** Visual representation of aberrant sequence signal before and after expected break site (vertical blue dashed line). Wildtype (control) sample signal indicated in black and *prr12a* sgRNA microinjected embryos (test) indicated in green. **D.** Percent probability score indicating inserted nucleotide: A (adenine), T (thymine), G, (guanine), and C (cytosine). Images and data analysis (**B**, **C** and **D**) obtained from TIDE analysis[241].

Curriculum Vitae

EDUCATION

Master of Science **2019-2022**
Biology
Collaborative Graduate Program in Developmental Biology
The University of Western Ontario, London, Ontario

Bachelor of Science **2015-2019**
Major: Biology, Pre-medical concentration
Minor: Biochemistry and Chemistry
Lake Superior State University, Sault Ste Marie, Michigan

RESEARCH EXPERIENCE

Graduate Research **2019-2022**
Dr. Gregory M. Kelly Laboratory
The University of Western Ontario, London, Ontario

Graduate Research **2021-2022**
Dr. Tugce B. Balci
London Health Sciences Center, London, Ontario

Undergraduate Research, Independent Study **2017-2019**
Dr. Britton Ranson-Olson
Lake Superior State University, Sault Ste Marie, Michigan

Undergraduate Research Assistant **2018**
Dr. Thu Nguyen-Mosey
Lake Superior State University, Sault Ste Marie, Michigan

Undergraduate Research Assistant **2016-2017**
Dr. Barbara Evans
Lake Superior State University, Sault Ste Marie, Michigan

RESEARCH WORK CONTRIBUTED

Biology Graduate Research Forum **November 2021**
London, Ontario
Characterization of the prr12 paralogues in zebrafish development: A Model for a Rare Human Disease (Platform Talk). **Resendes RJ**, Balci TB, Kelly GM. Department of Biology, Western University.

Child Health Research Day Meeting **May 2021**
London, Ontario

The role of prr12a and prr12b in Zebrafish: A Model for Rare Disease. (Platform Talk). **Resendes RJ**, Balci TB, Kelly GM. Department of Biology, Western University.

Western Research Forum 2021 **March 2021**
London, Ontario
Rare Disease Modelling of prr12a and prr12b in Zebrafish. (Platform Talk). **Resendes RJ**, Balci TB, Kelly GM. Department of Biology, Western University.

Child Health Research Day Meeting **May 2020**
London, Ontario
Rare Disease Modelling of prr12a and prr12b in Zebrafish. (Poster Presentation). **Resendes RJ**, Balci TB, Kelly GM. Department of Biology, Western University.

Biology Graduate Research Forum **October 2019**
London, Ontario
The effects of PFAs on the development and mitochondrial function in zebrafish embryos. (Platform Talk and Poster Presentation). **Resendes RJ**, Ranson-Olson B (Flash Talk). Department of Biology, Western University.

General Chemistry I&II Lab Manual First Edition. Nguyen TNT, Southwell BJ, **Resendes RJ**, Bauer TH, Harper JK. Xanedu. 2018. Print. School of Science and Medicine Department, Lake Superior State University, Xanedu. 2018. Print.

TEACHING EXPERIENCE

Advanced Cell Biology (Biology 3316), UWO, Teaching Assistant	**2020, 2021**
Scientific Methods in Biology (Biology 2290), UWO, Teaching Assistant	**2020, 2021**
First year Biology Laboratory (Biology 1001), UWO, Teaching Assistant	**2019, 2020**
First year Cells Biology (Biology 131), LSSU, Supplemental Instructor	**2017-2019**

CERTIFICATES AND AWARDS

Western Graduate Research Scholarship, UWO	**2019 -2021**
Zebrafish Husbandry Education Course Certificate, UAB	**2020**
Best Undergraduate Biology Research Poster, LSSU	**2019**
Ed and Jill Smith Scholarship, LSSU	**2018-2019**
Mary and Bill Thomsen Scholarship, LSSU	**2017-2019**
Undergraduate Research Fund Grant, LSSU	**2018**
Bud Cooper Scholarship, LSSU	**2017-2018**
Mary and Lou Lukenda Scholarship, LSSU	**2017-2018**
NCAA, GLIAC Student Athlete Award, USA	**2015, 2016, 2017**